Progress in Polymer Science 134 (2022) 101606

Contents lists available at ScienceDirect

Progress in Polymer Science

journal homepage: www.elsevier.com/locate/progpolymsci

Macrocyclic polymers: Synthesis, purification, properties and applications

Jordan Ochs[a,b], Carlo Andrea Pagnacco[a,b], Fabienne Barroso-Bujans[a,b,c,*]

[a] Donostia International Physics Center (DIPC), Paseo Manuel Lardizábal 4, 20018 Donostia–San Sebastián, Spain
[b] Centro de Física de Materiales, CSIC-UPV/EHU, Paseo Manuel Lardizábal 5, 20018 Donostia–San Sebastián, Spain
[c] IKERBASQUE, Basque Foundation for Science, María Díaz de Haro 3, E-48013 Bilbao, Spain

ARTICLE INFO

Article history:
Received 10 June 2022
Revised 5 August 2022
Accepted 1 September 2022
Available online 6 September 2022

Keywords:
Cyclic polymer
Ring polymer
Macrocycle
Synthesis
Ring closure
Ring expansion polymerization

ABSTRACT

Cyclic polymers present a topology that differ significantly from their linear counterparts due to their circular structure and therefore, the lack of chain ends. These simple characteristics are responsible for important unique properties (e.g. lower intrinsic and melt viscosity, lower hydrodynamic volumes, slower degradation profiles, increased blood circulation times and more selective bioaccumulation) thanks to which the cyclic polymers are today a vanguard in macromolecular chemistry. However, the preparation of cyclic polymers with high topological purity and in large quantities is challenging, therefore demanding the continuous development of synthetic methods. Advances in organic chemistry and the development of new catalytic systems has allowed the field of cyclic polymers to expand enormously in recent decades. In this review, ring closure and ring expansion polymerization strategies are described along the milestones that have characterized the evolution of cyclic (bio)polymer chemistry over the years. We also focus on very recent advances and state-of-the-art techniques for the synthesis and purification of cyclic polymers and provide an overview of properties and applications of cyclic polymers in different fields.

1. Introduction

The synthesis of well-defined macromolecular architectures has been the focus of much research in polymer chemistry. Both the physical and chemical properties of a material depend on its molecular characteristics, such as molecular weight, polydispersity, functional groups and macromolecular architecture. The development of synthetic routes that allow the control of molecular characteristics has led to the preparation of increasingly complex materials including polymeric brushes and stars, dendrimers, hyperbranched structures, networks and cyclic polymers. Extensive studies have been conducted to link physical properties (e.g. glass transition temperature, melt and crystallization temperatures, intrinsic

Abbreviations: DBA, *sym*-dibenzo-1,5-cyclooctadiene-3,7-diyne; DBN, 1,5-diazabicyclo[4.3.0]non-5-ene; DBU, 1,8-diazabicyclo[5.4.0]undec-7-ene; DMAP, *N*,*N*-dimethylaminopyridine; DMPO, 1,3-dimethyl-3-phospholene oxide; EDC, *N*-(3-dimethylaminopropyl)-*N*′-ethylcarbodiimide; GO, graphite oxide; IMes, 1,3-dimesitylimidazol-2-ylidene; Me_6TREN, tris[2-(dimethylamino)ethyl]amine; MeClPyI, 1-methyl-2-chloropyridinium iodide; MTBD, 7-methyl-1,5,7-triazabicyclo[4.4.0]dec-5-ene; NCA, *N*-substituted *N*-carboxylanhydrides; NHC, *N*-heterocyclic carbene; PMDETA, pentamethyldiethylenetriamine; PMP, 1,2,2,6,6-pentamethylpiperidine; TBD, 1,5,7-triazabicyclo[4.4.0]dec-5-ene; TSOH, p-toluenesulfonic acid; P2VP, poly(2-vinylpyridine); PBL, poly(β-butyrolactone); PBnGE, poly(benzyl glycidyl ether); PBO, poly(1,2-butylene oxide); PCEVE, poly(2-chloroethyl vinyl ether); PCL, polycaprolactone; PDMA, poly(*N*,*N*-dimethylacrylamide); PEG, poly(ethylene glycol); PEO, poly(ethylene oxide); PEOx, poly(2-ethyl-2-oxazoline); PnPropOx, poly(2-*n*-propyl-2-oxazoline); PnPropOzi, poly(2-*n*-propyl-2-oxazine); PGPE, poly(glycidyl phenyl ether); PLA, polylactide; PMA, poly(methyl acrylate); PMMA, poly(methyl methacrylate); PNIPAM, poly(*N*-isopropylacrylamide); PS, polystyrene; PtBA, poly(tert-butyl acrylate); PTHF, poly(tetrahydrofuran); PVBCZ, poly(4-vinylbenzyl-carbazole); PVL, poly(δ-valerolactone); PVO, poly(*N*-vinylpyrrolidone); RC, ring closure; REP, ring expansion polymerization; AREP, anionic ring expansion polymerization; CREP, cationic ring expansion polymerization; eZREP, electrophilic zwitterionic ring expansion polymerization; LP-ZREP, Lewis pair-mediated zwitterionic ring expansion polymerization; nZREP, nucleophilic zwitterionic ring expansion polymerization; REMP, ring expansion metathesis polymerization; RREP, radical ring expansion polymerization; ZREP, zwitterionic ring expansion polymerization; ATRC, atom transfer radical coupling; ATRP, atom transfer radical polymerization; CuAAC, copper-catalyzed azide alkyne cycloaddition; DSPAAC, double-strain-promoted azide-alkyne click reaction; ESA-CF, self-assembly and covalent fixation; FLP, frustrated Lewis pairs; RAFT, reversible addition-fragmentation chain transfer; ROCOP, ring-opening copolymerization; ROP, ring-opening polymerization; SPAAC, strain promoted azide-alkyne cycloaddition; SuFEx, sulfur(VI)-fluoride exchange; DNA, deoxyribonucleic acid; RNA, ribonucleic acid; BDS, broadband dielectric spectroscopy; DSC, differential scanning calorimetry; FTIR, Fourier transform infrared spectroscopy; GPC, gel permeation chromatography; HPLC, high-performance liquid chromatography; LCCC, liquid chromatography at the critical conditions; MALDI-ToF MS, matrix-assisted laser desorption/ionization time-of-flight mass spectrometry; NMR, nuclear magnetic resonance; SEC, size exclusion chromatography; STM, scanning tunneling microscopy.

* Corresponding author.
E-mail address: fbarroso@dipc.org (F. Barroso-Bujans).

https://doi.org/10.1016/j.progpolymsci.2022.101606
0079-6700/

and melt viscosities, thermo-responsiveness and rheological properties) and chemical properties (e.g. reactivity, chemical stability and solubility) to the covalent structure of a material.

The end groups of a polymer have a great influence on many of the aforementioned properties. Therefore, the absence of end groups makes the cyclic polymers unique. And not only that, the absence of end groups makes a cyclic polymer to have lower conformational degree of freedom and more compact coil conformation compared to their linear analogs. They are characterized by many unique physical properties such as reduced melt viscosity, reduced entanglement, increased T_g at medium-low molecular mass, and lower hydrodynamic volume [1,2]. A significant effort has been made to demonstrate their usefulness in medicine, nanotechnology and material science. In particular, the use of cyclic polymers in surface coating [3,4], crosslinked networks [5], and as platforms for drug and gene delivery [6] has been addressed. The difficulty in producing a large quantity of pure cyclic polymers has made these materials of little interest to industry, for the time being. However, great efforts are being made to improve synthetic techniques towards the production of high-purity cyclic polymers, as well as towards the implementation of new purification techniques [7,8].

Cyclic polymers have been prepared by different synthetic strategies. Ring-chain equilibration was the first reported method to synthesize cyclic polymers [9]. The formation of cyclic poly(decamethylene adipate) [10] in the polycondensation reaction of adipic acid with decamethylene glycol was used to validate previous theory developed by same authors, Jacobson and Stockmayer [11]. They included the formation of rings in the theories of distribution of molecular species in polycondensates and postulated that the fraction of rings increases with dilution and molecular weight [11]. The formation of cyclic oligo and poly(dimethyl siloxane) was also studied within the concepts of ring-chain equilibration [12,13]. Through the years, many excellent reviews and books have been published describing progress in the area of ring-chain equilibration [9,14–17], including some controversy around the Jacobson and Stockmayer theory [18] and new concepts [19].

The ring closure (RC) and ring expansion polymerization (REP) techniques are nowadays more attractive than the ring-chain equilibration for the synthesis of well-defined macrocyclic structures due to their versatility and purity of the obtained products. The RC strategy relies on intramolecular coupling of the end-groups of a previously synthesized linear precursor. The use of predesigned linear polymers as precursors for the preparation of cyclic polymers allows high control over the molecular characteristics of the obtained rings. REP allows the synthesis of “specific” cyclic polymers via the formation of an initial ring that expands upon the incorporation of monomer units through a weak labile bond (e.g. organometallic or electrostatic). At the end of the reaction, the catalyst is either retained or expelled from the macrocycle. We say “specific” because only the right combination of monomer and catalyst would produce the desired cyclic structure. Excellent reviews [7,20–30] and books [2,31–34] describe the most important aspects of both RC and REP methods, with special emphasis on catalytic and chemical processes, physical and chemical properties, and potential applications of cyclic polymers. However, the rise of cyclic polymers in the polymer community and the increasing literature in this area demand for constant updates. Therefore, we considered important to make an overview of the most recent advances in the design and synthesis of cyclic polymers by compiling already known concepts of RC and REP and recent synthesis examples.

2. Ring closure (RC) strategy

According to Laurent and Grayson [21], the RC can be divided into three different approaches: unimolecular homodifunctional coupling, unimolecular heterodifunctional coupling and bimolecular homodifunctional coupling (Fig. 1).

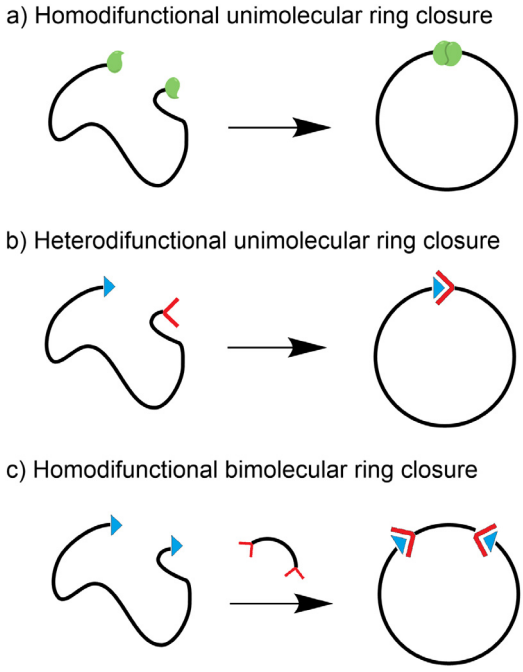

Fig. 1. Schematic representation of RC strategies.

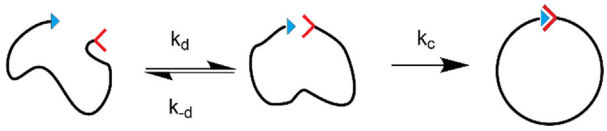

Fig. 2. Competition between diffusion and coupling in unimolecular RC.

2.1. Ring closure by unimolecular approach

The unimolecular strategy has the advantage of linking complementary end groups present in the same polymer chain. Stoichiometry between two reactants is not necessary, as it occurs in the bimolecular approach, eliminating a large source of impurities. Before the coupling reaction, the two reactive ends must diffuse within a capture volume. This step is characterized by a constant rate of diffusion, k_d (Fig. 2). Then, the coupling reaction can occur to form the cyclic chain. This is characterized by a constant rate of cyclization, k_c. If the coupling reaction does not occur, the chain ends diffuse away from each other with a constant rate k_{-d}. In the case of $k_c >> k_{-d}$ the ring closure reaction will be under diffusion control. In the inverse case, $k_c << k_{-d}$, the ring closure will be driven by its equilibrium kinetics.

The cyclization of a linear precursor *via* unimolecular RC is typically performed under high dilution and on small scales to avoid intermolecular coupling. Already in 1912, Paul Ruggli [35], and in 1933, Karl Ziegler [36], demonstrated that high dilution favored the intramolecular coupling of small organic molecules. The entropic penalty, associated to the localization of the two chain ends into a space small enough to promote intramolecular coupling, allows the cyclization of relatively low molecular weight chains (< 25 kg/mol) [11,32]. The probability of cyclization, can be described by the well-known Jacobson-Stockmayer equations [11].

$$P_c = \left(\frac{3}{2\pi}\right)^{3/2} \frac{v_s}{< r^2 >^{3/2}} \qquad \text{(Eq.1)}$$

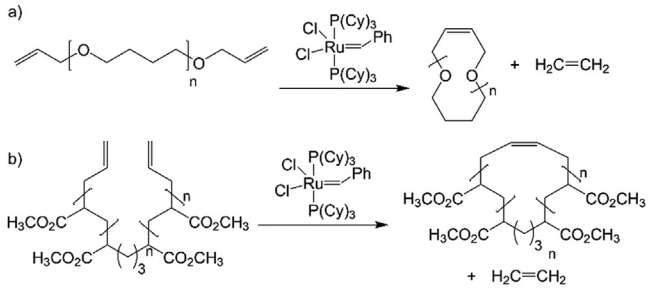

Fig. 3. Synthesis of a) cyclic PTHF [39] and b) cyclic poly(methyl acrylate) [40] by ring-closure metathesis.

$$P_l = 2N\,\frac{v_s}{V} = \frac{2N_A c}{M} v_s \qquad \text{(Eq.2)}$$

P_c is the probability of reaction when two ends of the same chain are within the capture volume, v_s; P_l is the probability of reaction when two ends from two different chains are within the capture volume; $\langle r^2 \rangle$ is the mean square of the end-to-end distance of a chain; N is the total number of molecules in a total volume V; N_A is the Avogadro number; M is the molecular weight of the polymer and c is the polymer concentration in g/mL.

The ratio P_c/P_l is defined as follows:

$$\frac{P_c}{P_l} = \left(\frac{3}{2\pi < r^2 >}\right)^{3/2} \frac{2000}{N_A[P]} \qquad \text{(Eq.3)}$$

[P] is the polymer concentration in mol/L.

The theoretical percentage of monocyclic chains can be calculated as follows:

$$\%_{cyclic} = \frac{P_c}{P_c + P_l} \times 100 \qquad \text{(Eq.4)}$$

From this set of equations, it is clear that a decrease in the concentration of the linear precursor [P] increases P_c/P_l, and therefore the probability of cyclization. Since the intramolecular coupling is a unimolecular process, it is not influenced by the dilution. Contrarily, the intermolecular coupling, which is a bimolecular process, is largely reduced upon dilution. Experimentally, it is possible to obtain a high percentage of cyclic chains by adding the previously synthesized linear precursor into a catalyst solution at a slow rate. In that way, the concentration of linear precursor is maintained as low as possible (pseudo-high-diluted conditions) and the active end-groups are consumed during intramolecular coupling [37,38]. The second important prediction of the Jacobson-Stockmayer theory is the decreasing probability of intramolecular coupling with the chain length. Indeed, the probability that the two ends of the same chain are within the capture volume decreases with the chain length. This is the reason why high molecular cyclic polymers cannot be achieved by RC. Despite this, RC remains the most versatile option for the generation of ring polymers.

2.1.1. Homodifunctional unimolecular ring closure

The homodifunctional unimolecular approach is motivated by the need to cyclize polymer chains that contain identical functional groups at both ends. Although the number of homocoupling reactions is limited in organic chemistry, successful cyclization reactions demonstrate the advantages of this technique.

In 2002, Tezuka et al. [39] demonstrated that the cyclization of a diallyl-terminated PTHF was possible via the metathesis condensation under high dilution using a Grubb's Ru-based catalyst (Fig. 3a). Concentration below 0.2 g/L was required to minimize intermolecular coupling. This ring closure methatesis (RCM) method was then extended and adapted to the synthesis of cyclic

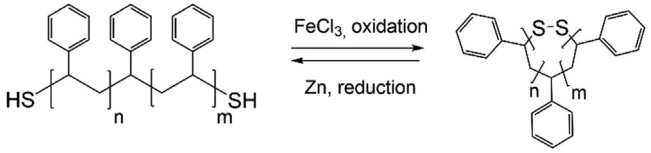

Fig. 4. Cyclization of polystyrene *via* the formation of disulfide bridges [44].

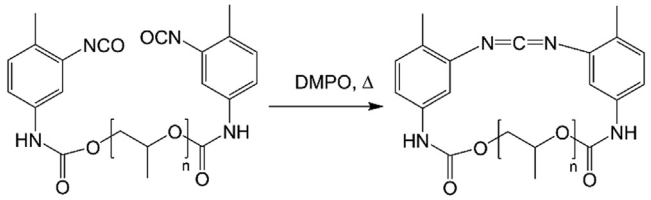

Fig. 5. Isocyanate coupling for the synthesis of cyclic poly(propylene oxide) [47].

poly(methyl acrylate) (Fig. 3b) [40], cyclic polystyrene [41], cyclic poly(ε-caprolactone) [42], and cyclic poly(phosphoesters) [43].

Disulfide bridges were first proposed by Monteiro et al. [44] in 2006 for the ring closure of polystyrene chains (Fig. 4). Polystyrene was generated by reversible addition-fragmentation chain transfer (RAFT) polymerization using a difunctional agent leading to dithioester terminated chains. By aminolysis followed by oxidation with $FeCl_3$ in diluted conditions, cyclic chains were generated. By reduction with zinc and acetic acid, the linear precursor is recovered. More recently the disulfide bridge strategy was used to the generation of cyclic (di-) triblock (co-) terpolymers containing styrene and acrylate monomers [45] and to the formation of cyclic poly(2-ethyl-2-oxazoline) [46].

The intramolecular reaction of diisocyanate-terminated poly(propylene oxide) was implemented by Dai et al. [47] in 2007 as a way to generate cyclic chains *via* the formation of a carbodiimide bond (Fig. 5). The cyclization reaction was carried at high dilution in the presence of 1,3-dimethyl-3-phospholene oxide (DMPO) under heating.

One of the earliest examples of oxidative homocoupling is the reaction between two alkynes to form a diyne bound, also known as Glaser coupling [48]. In 1869, Glaser reported the formation of diphenyldiacetylene when mixing phenylacetylene, copper (I) chloride and ammonium hydroxide in ethanol in air. Years later, Hay proposed a key modification by adding a nitrogen ligand such as N,N,N′,N′-tetramethyl ethylene diamine, allowing the reaction to occur under mild conditions [49]. It is now known that Glaser-Hay coupling is catalyzed by metal salts, copper (I) and copper (II), through a complex mechanism [50,51].

Cyclic poly(ethylene oxide) and cyclic polystyrene were synthesized from alkyne-terminated linear precursors *via* Glaser coupling in 2010 (Fig. 6a-b) [52]. A solution of the linear polymer dissolved in pyridine was slowly added to a Cu(I)Br / *N,N,N′,N″,N‴*-pentamethyldiethylenetriamine (PMDETA) catalyst solution to generate cyclic polymers in high yields >95 %. The reaction proceeded under air and at room temperature, demonstrating that the Glaser coupling was suitable for cyclization. In a more recent study the generation of cyclic poly(ethylene oxide) was optimized by using a microreactor [53]. The disappearance of alkyne groups and the formation of the diyne bound was confirmed by ^{1}H NMR and FTIR [52]. Additionally, the loss of two protons was confirmed by MALDI-ToF MS and the reduction of the hydrodynamic volume of the polymer chains was demonstrated by a clear shift toward higher retention times in SEC measurements. In our group, Glaser coupling technique was undertaken to cyclize two-arms poly(glycidyl phenyl ether) (PGPE) (Fig. 6c) synthesized by initiation with 1-*tert*-butyl-4,4,4-tris(dimethylamino)-

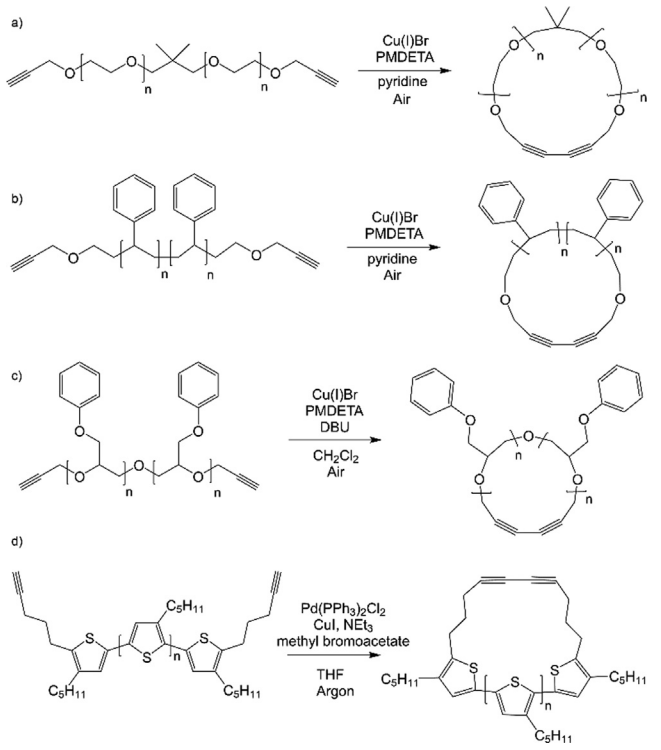

Fig. 6. Synthesis of cyclic polymers via Glaser coupling: a) poly(ethylene oxide) [52], b) poly(styrene) [52], c) poly(glycidyl phenyl ether) [54] and d) poly(3-hexylthiophene) [55].

2,2-bis[tris(dimethylamino)-phosphoranylidenamino]-2λ^5,4λ^5-catenadi(phosphazene) (*t*-BuP_4) and water [54]. In this case, pyridine was substituted by dichloromethane due to its lower toxicity and lower boiling point. Then, 1,8-diazabicyclo[5.4.0]undec-7-ene (DBU) was added to increase the reaction rate and reduce intermolecular coupling. We observed that the reaction conditions were critical to generate pure cycles and that purification by fractionation using a preparative GPC was needed in the majority of samples. Conjugated polymers such as poly(3-hexylthiophene) and poly(3-heptylselenophene) were also synthesized via Glaser coupling (Fig. 6d) [55]. The authors implemented a convenient purification method based on the reaction of unreacted linear chains to an alkyne-terminated poly(ethylene glycol) followed by separation in a chromatographic column. This strategy allowed the observation of the highly bended structures of pure cyclic chains by high-resolution scanning tunneling microscopy (STM).

The intramolecular coupling of radicals was first reported by Tillman et al. [56] in 2010 for the preparation of cyclic polystyrene. The reaction consisted in the formation of a dibrominated polystyrene and then the activation of the chain ends by metal-catalyzed, homolytic C-Br cleavage forming carbon-based radicals (Fig. 7). A highly active tris[2-(dimethylamino)ethyl]amine (Me_6TREN) ligand was used as activator. As a result, the intramolecular reaction *via* atom transfer radical coupling (ATRC) favored the formation of cyclic products in diluted conditions. Later, 2-methyl-2-nitrosopropane was incorporated during the activation of the C-Br bond in the presence of a milder PMDETA activator resulting in the formation of cyclic products via a radical trap-assisted ATRC [57]. ATRC method was applied for the generation of more complex bicyclic polystyrene containing a cleavable disulfide bond [58]. This labile bond allowed the formation of monocycles of different size upon disulfide cleavage.

In 2011, Schappacher and Deffieux generated cyclic polystyrene with a cyclization efficiency of 91 % by means of the coupling

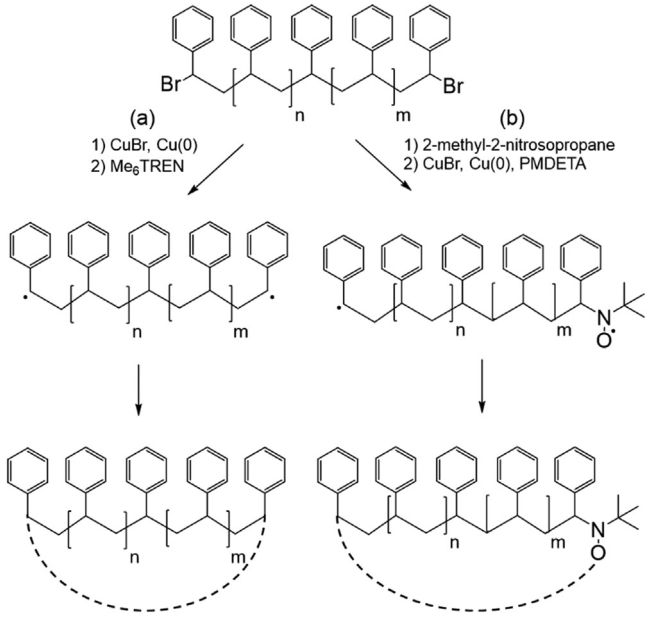

Fig. 7. Synthesis of cyclic polystyrene via a) ATRC [56] and b) radical trap-assisted ATRC [57].

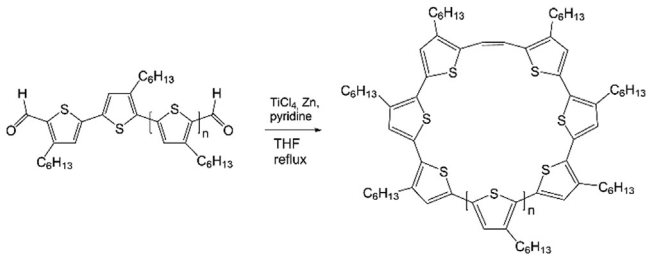

Fig. 8. Synthesis of cyclic poly(3-hexylthiophene) *via* McMurry coupling reaction of terminal aldehydes [60].

of iron(III) porphyrin moieties into a bis[iron(III) μ-oxoporphyrin] dimer [59]. This is a selective and rapid reaction that occurs in basic conditions. In acidic conditions, the closing unit opens to reversibly form iron(III) meso-tetraphenylporphyrin chloride end groups.

In 2017, Coulembier et al. [60] generated cyclic polythiophenes of molecular weights in the range of 4 to 10 kg/mol *via* an intramolecular McMurry coupling reaction (Fig. 8). The reaction occurs by coupling of two terminal aldehydes catalyzed by $TiCl_4$ and zinc, as a reduction agent.

In 2015, Jing et al. [61] utilized light to promote the intramolecular cycloaddition of naphthalene (or anthracene) end groups of poly(ethylene oxide) (PEO) chains assisted by cucurbit[8]uril (CB[8]) (Fig. 9). The addition of CB[8] was necessary to bring together the polycyclic aromatic hydrocarbons and stabilize them by π–π stacking. Then, upon UV-light irradiation covalent bonds between both end groups were formed leading to the formation of the cyclic PEO structures. Same year, Kim et al. [62] reported on the formation of cyclic poly(ε-caprolactone)s by UV-light assisted cycloaddition of α,ω-dianthracene-terminated linear poly(ε-caprolactone). They observed that by increasing the polymer concentration the ring size increased from di-, tri- to tetrameric cyclics. The formation of unimeric cyclic polymer was not found. By heating the cycles at 160 °C, the thermal dissociation of dimeric anthracene units and the formation of original linear telechelics occurred.

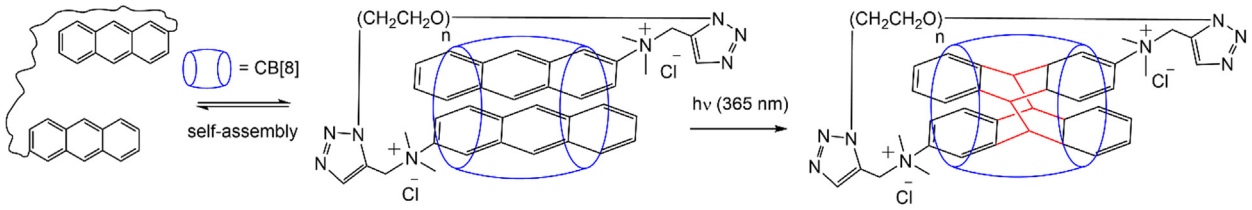

Fig. 9. Synthesis of cyclic PEO by means of CB[8]-assisted self-assembly and UV-light irradiation [61].

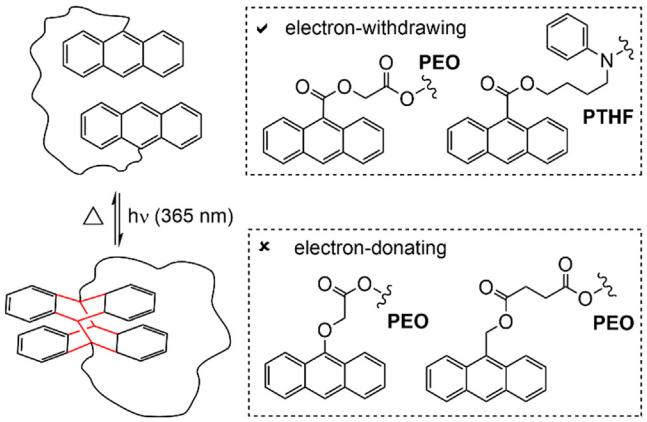

Fig. 10. Cyclic-linear topological conversion of PEO and PTHF by photodimerization of anthracene end groups and thermal dissociation, respectively. Effects of the substituent on the anthracene group [63].

In 2016, Tezuka et al. [63] reported on the reversible cyclic-linear topological conversion of poly(ethylene oxide) and poly(tetrahydrofuran) by means of the photodimerization reaction of anthracene end groups and thermal dissociation, respectively (Fig. 10). They demonstrated that by introducing an electron-withdrawing group to the anthracene moieties (anthracene-COO-PEO), the unimeric cyclization occurred efficiently in water and in organic solvents. However, by introducing electron-donating groups (anthracene-O-PEO and anthracene-CH_2-PEO), the anthryl groups oxidized to form anthraquinone upon irradiation at 365 nm. Moreover, upon heating at 150 °C, the linear precursor was reversible formed. This cyclization/de-cyclization experiment was performed 5 times with similar results. Similar synthetic strategy was later utilized by Hong et al. [64] in 2021 to synthesize the thermoresponsible cyclic poly(*N*-acryloylsarcosine methyl ester) from the anthracene-COO telechelic polymer and UV-irradiation in diluted water solution.

In 2022, a new approach based on the photo-induced cyclization of cyanostilbene-terminated telechelic poly(dimethyl siloxane) was reported by Wang et al. [65] This is based on the supramolecular stacking of cyanostilbenes, directed by hydrogen bonds, which allows the [2+2] photo-cycloaddition of active terminals upon 430 nm light irradiation. Multimeric cyclic chains are produced from concentrated polymer solution facilitating the formation of supramolecular crosslinked networks and gels.

2.1.2. Heterodifunctional unimolecular ring closure

The coupling of heterodifunctional polymers is the most efficient way to produce cyclic polymers [7]. Although the synthesis of α,ω-heterofunctional polymers is more challenging compared to α,ω-homofunctional polymers, the amounts of impurities generated during cyclization is notably reduced in heterodifunctional unimolecular ring closure reactions. This is because the rate of intermolecular coupling is reduced by a factor of two since the effective concentration of complimentary reactive groups is reduced by two [21].

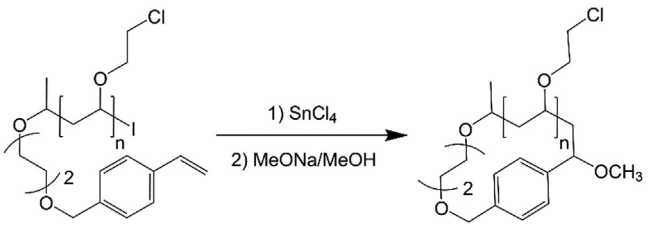

Fig. 11. Synthesis cyclic PCEVE *via* heterocoupling of α-styrenyl, ω-iodo PCEVE [66].

The first example of successful cyclization *via* the heterodifunctional unimolecular coupling was demonstrated by Deffieux et al. [66] in 1991. Cyclic poly(2-chloroethyl vinyl ether) (PCEVE) was generated from a well-defined linear precursor containing a iodo and a styrenyl groups at the chain ends (Fig. 11). In the reaction, the iodide was activated towards the terminal styrenyl group with $SnCl_4$ under high dilution. The reaction was quenched with sodium methoxide. Similar iodo-styrenyl activated reaction was used later by Deffieux et al. [67] for the synthesis of cyclic polystyrene with molecular weights of ~12000 Da and high cyclic purity (> 95 %). Table 1 summarizes these and subsequent reactions performed by introducing two distinct functional groups at the chain ends.

In 2001 the concept of "click" chemistry was introduced by Sharpless et al. [72]. In order to be qualified as "click" reaction, the reaction must be modular, very high yield and wide in scope. In the case of the formation of byproducts, they must be inoffensive and removable by non-chromatographic methods. Additionally, the reaction conditions must be simple (i.e. readily available reagents, easily removable solvent and purification by non-chromatographic methods). Finally, the product must be stable under physiological conditions. One of the most popular "click" reaction is the Huisgen dipolar cycloaddition [73] of an azide and an alkyne group, to form both 1,4 and 1,5-substituted [1,2,3]-triazole ring. Fokin, Sharpless et al. [74] and Meldal et al. [75] reported simultaneously the use of a copper (I) catalyst in the cycloaddition of azides and alkynes, allowing the reaction to proceed at room temperature and giving access to one specific regioisomer, the 1,4-substituted [1,2,3]-triazole. Since then, the copper-catalyzed azide alkyne cycloaddition (CuAAC) has been extensively used in polymer chemistry [76,77].

In 2006, Laurent and Grayson demonstrated that cyclic poly(styrene)s could be conveniently generated by means of CuAAC "click" reaction [37]. This use of "click" chemistry constituted a great breakthrough for the synthesis of cyclic polymers. Linear polystyrene chains were first synthesized by atom transfer radical polymerization (ATRP) with propargyl 2-bromoisobutyrate as initiator (Fig. 12). After modification of the terminal bromide into azide, a solution of the obtained polymer was added dropwise into a copper catalyst solution under inert atmosphere. The consumption of the two complementary end-groups to form triazole rings was confirmed by ^{1}H NMR and FTIR. The clear shift in retention time observed in SEC measurements demonstrated the formation

Table 1
Cyclic polymers generated from α, ω-heterodifunctional linear precursors via addition and condensation reactions.

α-group	ω-group	catalyst / activator	reaction	polymer	cyclic yield (%)	Ref.
iodide	Styrenyl	$SnCl_4$	addition	PCEVE	80	[66]
iodide	Styrenyl	$SnCl_4$	addition	PS	85-90	[67]
diethyl acetal	bis(hydroxyl methyl)	TSOH	cond.	PS	90	[68]
carboxyl	Amine	MeClPyI	cond.	PS	62, 64	[69,70]
hydroxyl	Carboxyl	MeClPyI	cond.	PS	95	[71]

p-toluenesulfonic acid = TSOH, 1-methyl-2-chloropyridinium iodide = MeClPyI, polystyrene = PS, condensation = cond.

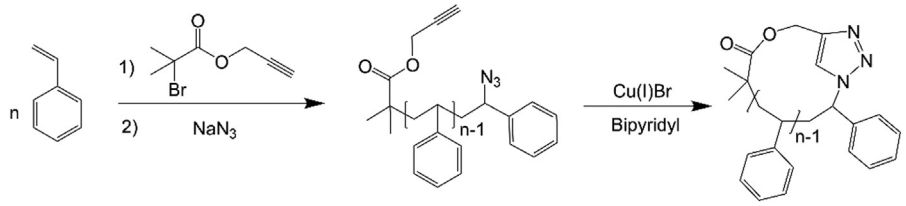

Fig. 12. Cyclization of poly(styrene) *via* CuAAC "click" reaction [37].

Table 2
Cyclic polymers generated from α-alkyne, ω-azide or α-azide, ω-alkyne linear precursors via CuAAC "click" reactions catalyzed by Cu(I).

polymerization	polymer	Cu salt	amine used in CuAAC	ref.
ATRP	PS	Cu(I)Br	2,2'-bipyridyl	[37]
	PNIPAM	Cu(I)Br	2,2'-bipyridyl	[78]
	PtBA	Cu(I)Br	triethylamine	[79]
	PVBCZ	Cu(I)Br	PMDETA	[80]
NMP	PS	Cu(I)Br	PMDETA	[81]
RAFT	PNIPAM	$CuSO_4$/sodium ascorbate	-	[82]
	PS	Cu(I)Br	2,2'-bipyridyl	[83]
	PS	Cu(I)Br	PMDETA	[84]
ROP	PCL	Cu(I)Br	PMDETA	[42,85,86]
	PVL	Cu(I)Br	2,2'-bipyridyl	[87]
	PBO, PBnGE	Cu(I)Br	2,2'-bipyridyl	[88]
	PEOx	Cu(I)Br	PMDETA	[89]
	PGPE	Cu(I)Br/sodium ascorbate	PMDETA	[90]
	PnPropOx, PnPropOzi	Cu(I)Br	PMDETA	[91]
Iterative convergent	PLA	Cu(I)Br	PMDETA	[92]

poly(*N*-isopropylacrylamide) = PNIPAM, poly(tert-butyl acrylate) = PtBA, poly(4-vinylbenzyl-carbazole) = PVBCZ, polycaprolactone = PCL, poly(δ-valerolactone) = PVL, poly(1,2-butylene oxide) = PBO, poly(benzyl glycidyl ether) = PBnGE, poly(2-ethyl-2-oxazoline) = PEOx, poly(glycidyl phenyl ether) = PGPE, poly(2-*n*-propyl-2-oxazoline) = PnPropOx, poly(2-*n*-propyl-2-oxazine) = PnPropOzi, polylactide = PLA.

of cyclic chains. In the following years, the same ATRP - CuAAC "click" strategy was employed for the synthesis of cyclic poly(*N*-isopropylacrylamide) [78], cyclic poly(tert-butyl acrylate) [79], and cyclic poly(4-vinylbenzyl-carbazole) [80]. Table 2 summarizes these and other reactions using the CuAAC "click" strategy to generate cyclic polymers.

Other polymerization techniques such as nitroxide-mediated radical polymerization (NMP) of styrene [81], RAFT of *N*-isopropylacrylamide [82] and styrene [83,84], ring-opening polymerization (ROP) of lactones [42,85–87] and epoxides [88,90], and iterative convergent synthesis of *rac*-lactide [92] have been reported in combination with CuAAC "click" chemistry to generate macrocycles. The cyclization efficiency of the latter was reported to decrease from 99% to 30% with increasing molecular weight from 3 to 37 kg/mol, as expected from the decreasing probability of the chain ends finding each other. The CuAAC "click" chemistry is clearly compatible for the preparation of cyclic block copolymers. Although they are not the main objective of this review, we can cite some of them such as cyclic poly(methyl methacrylate)-b-polystyrene [93], cyclic poly(2-(2-methoxyethoxy)ethyl methacrylate)-b-poly(oligo(ethylene glycol) methyl ether methacrylate) [94], cyclic polystyrene-b-polyisoprene [95], and cyclic poly(ethylene gylcol)-b-poly(caprolactone) [96].

In the effort to eliminate the use of copper-based catalyst in click reactions while retaining the high efficiency of the CuAAC reaction, the strain promoted azide-alkyne [3 + 2] cycloaddition (SPAAC) reaction was investigated by Zhang et al. [97] in the generation of cyclic polymers. SPAAC employs cyclooctynes that are activated by ring strain, and do not use the cytotoxic copper. In this initial study, α-cyclopropenone-masked dibenzocyclooctyne, ω-bromo polystyrene was synthesized by ATRP and the bromo group was modified into azide (Fig. 13). Finally, under UV-irradiation and high dilution the cyclopropenone-masked dibenzocyclooctyne was deprotected allowing the strained alkyne to react with the complementary azide and to yield the corresponding cyclic polymer. Interestingly, a batch procedure where three successive additions of the linear precursor (7 mg) into 30 mL of solvent followed by UV-irradiation for 5 h gave pure cyclic polymer in high amounts.

The Diels-Alder reaction, discovered in 1928 [98], is one of the simplest reactions forming carbon-carbon bonds. Heteroatom–heteroatom bonds are also plausible (hetero-Diels–Alder) [99]. One of the main advantages of Diels-Alder cycloaddition over the CuAAC "click" reaction is its catalyst-free aspect, and that its activation is easily done by heat or light [100]. In 2000, Mizawa et al. [101] prepared cyclic poly(methyl methacrylate) by Diels-Alder in-

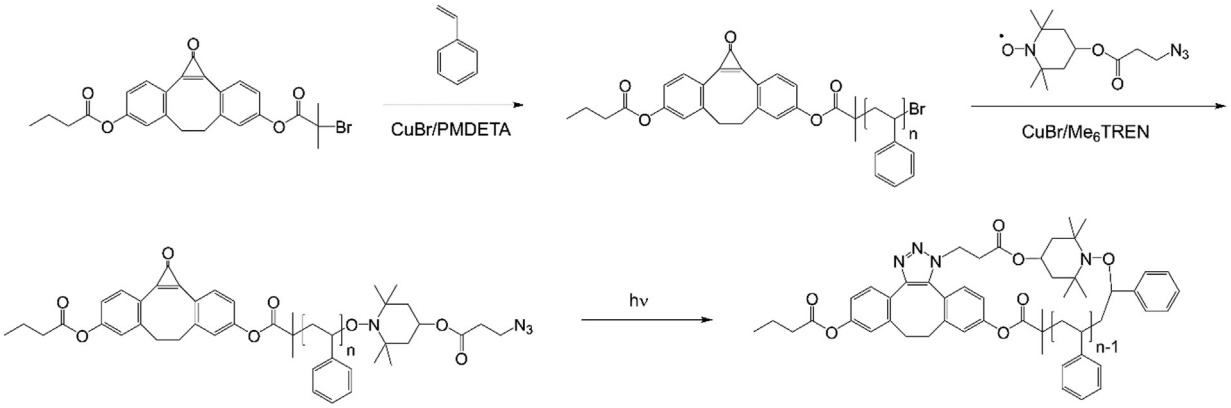

Fig. 13. UV-induced SPAAC reaction for the synthesis of cyclic polystyrene [97].

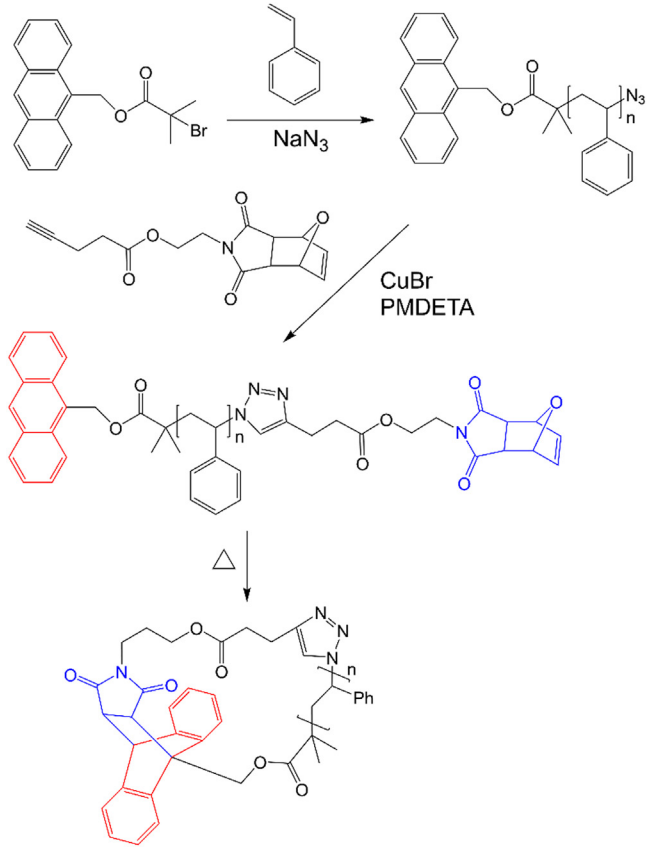

Fig. 14. ATRP and Diels-Alder [4 + 2] cycloaddition for the synthesis of cyclic polystyrene [102].

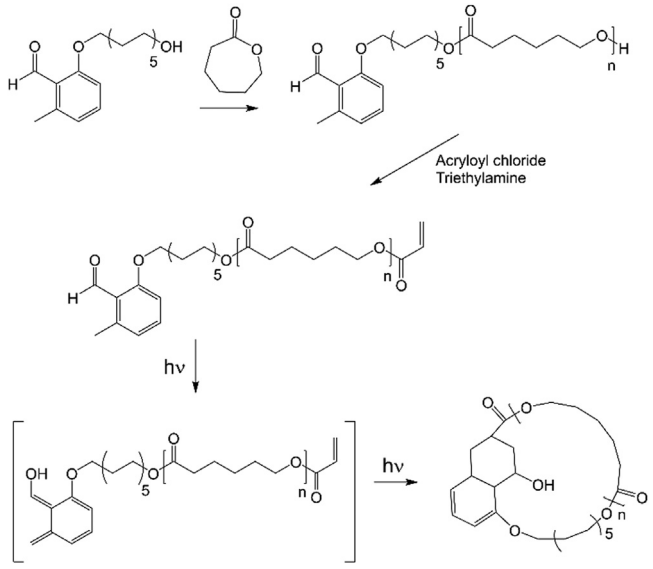

Fig. 15. ROP and photo-induced Diels-Alder [4 + 2] cycloaddition for the synthesis of cyclic poly(ε-caprolactone) [105].

tramolecular reaction of α-maleimide, ω-dienyl end-groups under reflux in THF. Ten years later, a more efficient procedure combining ATRP and Diels-Alder reaction was reported by Tunca et al. [102] (Fig. 14). They reacted intramolecularly an α-anthracene, ω-maleimide polystyrene by Diels-Alder [4 + 2] cycloaddition, a reaction that has been described as a click-type reaction [103]. The cyclization efficiency was 85% (M_n ~5 kg/mol) after 48 h of reflux. Cyclic block copolymers of styrene and *tert*-butyl acrylate, and styrene and ε-caprolactone of higher molecular weight (M_n ~10 kg/mol) were also prepared with a cyclization efficiency of 77%. Table 3 summarizes these and other reactions using the Diels-Alder reaction to generate cyclic polymers.

In 2011, Barner-Kowollik et al. [104] presented a Diels-Alder cyclization reaction that occurred much faster, in 6 h of reflux, and with a very high cyclic purity. They used a very efficient reaction between cyclopentadiene and maleimide end groups by synthesizing first α-furan-protected maleimide, ω-bromide functionalized poly(methyl methacrylate) and poly(tert-butyl acrylate) of M_n ~3 kg/mol via ATRP and then, the substitution of bromine by cyclopentadiene. Deprotection of maleimide end group occurred during reflux followed by the Diels-Alder [4 + 2] cycloaddition. Later, in 2014, Barner-Kowollik et al. [105] used light to activate the Diels-Alder [4 + 2] cycloaddition of α-*o*-methylbenzaldehyde, ω-acrylate functionalized poly(ε-caprolactone) (M_n ~ 3 kg/mol) and poly($_L$-lactide) (M_n ~ 4.5 kg/mol). This approach is based on the photoisomerization of the *o*-methylbenzaldehyde and the resulting *in situ* formation of a highly reactive diene, the hydroxy-*o*-quinodimethane (photoenol). The irradiation of a diluted polymer solution (25 mg/L) with UV-light (λ_{max} = 320 nm) for 12 h gave the corresponding cyclic polymer in very high yield (Fig. 15). A year later, Coulembier et al. [106] extended the use of this chemistry under sunlight irradiation.

Light induced activation has become an important method for synthesizing a variety of cyclic homopolymers and copolymers since the initial report of Barner-Kowollik et al. [105]. For

Table 3
Cyclic polymers generated *via* Diels-Alder reaction.

polymerization	Polymer	α-group	ω-group	activation	Ref.
Anionic	PMMA	maleimide	dienyl	Heat	[101]
ATRP	PS	anthracene	maleimide	Heat	[102]
ATRP	PMMA, PtBA	furan-protected maleimide	cyclopentadiene	Heat	[104]
ROP	PCL, PLA	*o*-methylbenzaldehyde	acrylate	UV light	[105]
	PCL, PLA	*o*-methylbenzaldehyde	acrylate	Sun light	[106]
RAFT	PS, PMMA, PtBA, PDMA, P2VP	*o*-methylbenzaldehyde	thiobenzoylthio	UV light	[107]

poly(methyl methacrylate) = PMMA, poly(*N,N*-dimethylacrylamide) = PDMA, P2VP = poly(2-vinylpyridine)

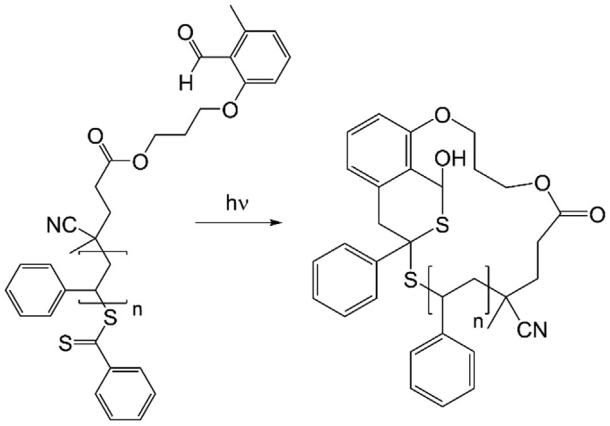

Fig. 16. Photo-induced Diels-Alder [4 + 2] cycloaddition for the synthesis of cyclic polystyrene [107].

instance, Zhang et al. [107] synthesized a series of vinyl homopolymers and copolymers via RAFT polymerization, by which the photosensitive moieties *o*-quinodimethane and dithioester end groups were introduced. As an example, Fig. 16 shows the Diels-Alder [4 + 2] cycloaddition of α-*o*-methylbenzaldehyde, ω-thiobenzoylthio polystyrene. This convenient synthetic route allows the generation of a variety of cyclic polymers with a high cyclization efficiency, either by using one-pot technique where the cyclic polymer is generated directly after polymerization without previous purification steps, or in batches by increasing the amounts of obtained products, in that case in the mg scale. Later, the use of a continuous flow technique demonstrated that the production of cyclic polystyrene could be conveniently scaled to the gram scale by using the previously described UV-induced Diels-Alder reaction [108]. This photo-induced Diels-Alder technique was also used by Zhao et al. [109] to generate cyclic poly(ionic liquids)s starting from the synthesis of cyclic poly(1-(4-vinylbenzyl)imidazole) and poly(2-pyridine) followed by the quaternization of nitrogen heterocylic side groups with bromoacetonitrile and counterion exchange with organic anions.

In 2013, Monteiro et al. [110] combined the RAFT polymerization with thiol-ene Michael addition for the synthesis of a number of cyclic polymers with a cyclization efficiency of 80 %. A test performed on the thio-bromo cyclization of polystyrene occurred in only 25 % demonstrating that the thiol-ene reaction was more efficient. Fig. 17 shows the involved reactions. A previously synthesized heterofunctional trithiocarbonate RAFT agent mediated the polymerization of styrene, tert-butyl acrylate, *N*-isopropylacrylamide and *N,N*-dimethylacrylamide. An activated acrylate function was introduced at one chain end via post polymerization modification. The cyclization was then performed in a one-pot reaction, via hexylamine-catalyzed cascade aminolysis and thiol-ene Michael addition sequence at 25 °C. Same year, Kim et al. [111] reported the synthesis of cyclic poly(*N*-isopropylacrylamide) by combining RAFF polymerization with the anthracene-thiol click reaction. Hydrazine hydrate was used as aminolysis agent to convert the dithioate group into a thiol group, and AIBN to promote the radical catalyzed anthracene–thiol click reaction. These and other reactions have been summarized in Table 4.

In 2019, Chen, Wu et al. [114] combined RAFT polymerization with sulfur(VI)-fluoride exchange (SuFEx) click reaction to synthesize cyclic poly(*N*-isopropylacrylamide) and cyclic poly(*N*-vinylpyrrolidone). RAFT polymerization was performed by using a predesigned RAFT agent containing both ether and sulfonyl fluoride moieties (Fig. 18). Then, the intramolecular cyclization reaction was catalyzed by TBD in air at room temperature. The SuFEx reaction is an extremely efficient click reaction, according to Sharpless et al. [117]. It has the advantages of being inert to UV light, insensitive to oxygen and water, and does not require a metal catalyst. Its fast reaction rates at room temperature, high yields, high tolerance toward various functional groups, and easy manipulation allow the fast intramolecular reaction typically needed for generating cyclic chains with low amounts of linear byproducts.

Also in 2019, Tezuka et al. [115] reported the synthesis of cyclic polystyrene and cyclic PTHF by means of electrostatic self-assembly and covalent fixation (ESA-CF), a technique developed in his group for years for the synthesis of complex architectures and cyclic topologies as described in next section. ESA-CF lies in the electrostatic self-assembly promoted by the attraction of ionic pairs and the balance of electric charges followed by the thermally induced transformation of ionic bonds to covalent bonds [118]. In the reaction, telechelic polymers containing a cyclic ammonium and a carboxylate end groups forming zwitterionic species were first diluted to preferentially form the intramolecular ionic pairs (Fig. 19). Then upon heating, selective reactions between end groups converted the ionic interactions into a permanent covalent group. High cyclic purity was obtained depending on the ammonium group [115].

In 2021, Tang et al. [116] reported an approach for the synthesis of cyclic polyesters based on the photo-induced intramolecular radical addition of an α-alkene, ω-O_2C-Co^{III}(salen) polymer precursor (Fig. 20). First, the α-alkene, ω-O-Co^{III}(salen) copolymer of propylene oxide and phthalic anhydride was generated by ring-opening copolymerization using a cobalt salen pentenoate complex as initiator, where the salen is the (R,R)-*N,N'*-bis(3,5-ditertbutylsalicylidene)-1,2-cyclohexanediamine. In the reaction, the insertion of CO triggered the transformation of α-alkene, ω-O-Co^{III}(salen) into the active α-alkene, ω-O_2C-Co^{III}(salen) copolymer. Finally, under the light of a white LED at high dilution the cyclization reaction took place.

2.2. Ring closure by bimolecular approach

The bimolecular ring closure approach relies on the coupling between a difunctional polymer chain and a difunctional coupling agent in dilute solution. The cyclization takes place in two distinct steps: first, the intermolecular coupling between the polymer chain end and the complementary functional group of the cou-

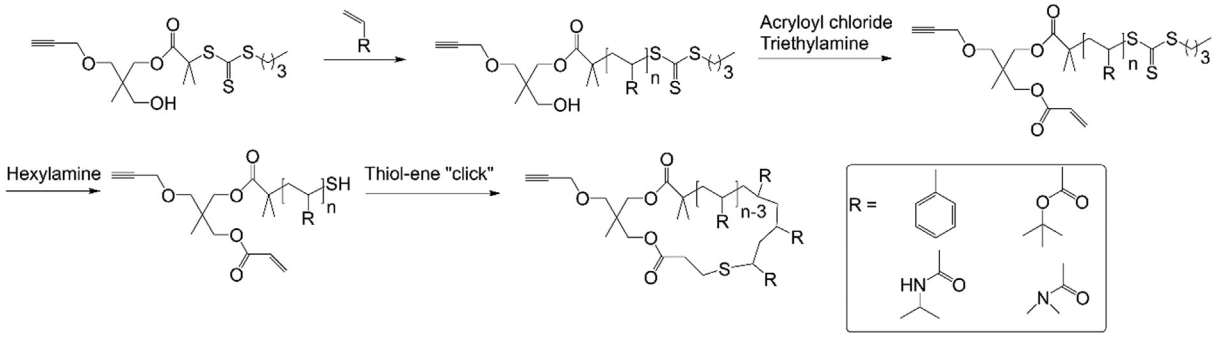

Fig. 17. RAFT polymerization combined with thiol-ene Michael addition for the synthesis of cyclic polymers [110].

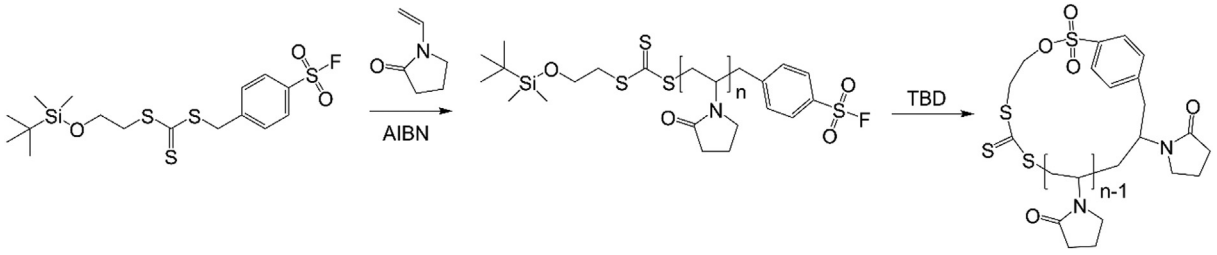

Fig. 18. RAFT polymerization and sulfur(VI)-fluoride exchange (SuFEx) click reaction for the synthesis of cyclic poly(*N*-vinylpyrrolidone) [114].

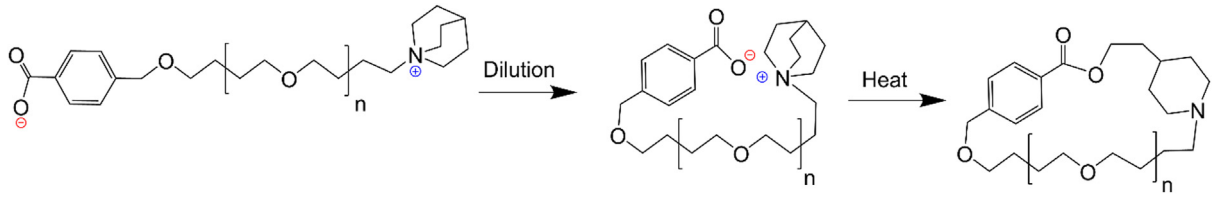

Fig. 19. Synthesis of cyclic poly(tetrahydrofuran) by unimolecular ESA-CF of linear precursor end-caped with quinuclidinium cation and benzyl carboxylate anion [115].

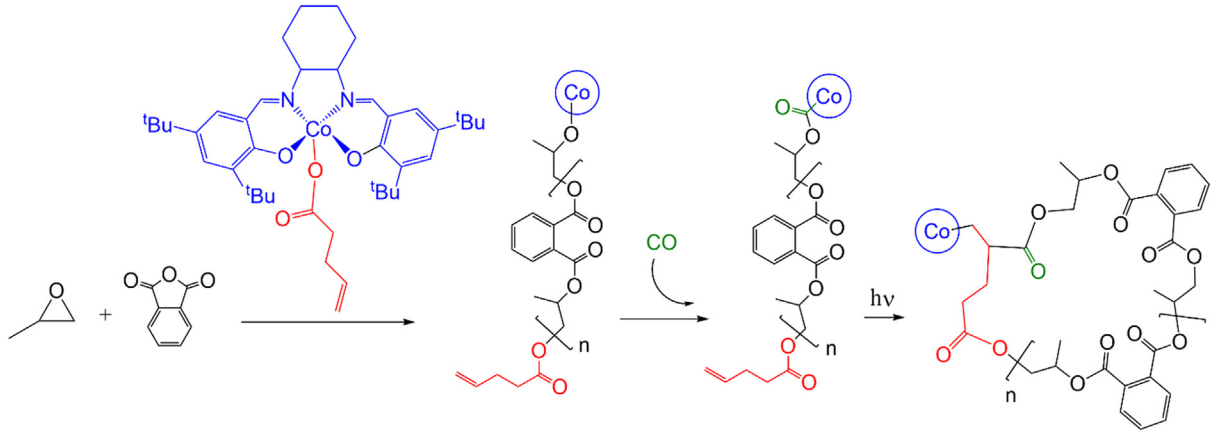

Fig. 20. Photo-induced radical cyclization of a copolyester of propylene oxide and phthalic anhydride mediated by a cobalt salen [116].

pling agent, and second, the intramolecular coupling between the remaining complementary functional groups of the polymer chain and the coupling agent. The stoichiometry between the polymer chain and the coupling agent must be respected to obtain a high percentage of cyclic product. If this condition is not fulfilled, linear byproducts will be obtained in large amounts. In the case of an excess of polymer over the coupling agent, the formation of polymer/coupling agent/polymer species will be favored. For an excess of coupling agent over the polymer, the formation coupling agent/polymer/coupling agent species will be then favored.

The second and major limitation of this approach is the combination of two steps that require opposite conditions. The first intermolecular reaction between the polymer chain and the coupling agent is favored by low dilution. However, high dilution favors the second intramolecular reaction to produce cyclic chains. Since the reaction is a one-pot process, the concentration of both components must be kept as low as possible to avoid the formation of linear byproducts. As a result, the intermolecular coupling occurring during the first step is very slow. To overcome the slow kinetics of the first step, highly efficient coupling reactions must

Table 4
Other cyclization reactions.

polymerization	polymer	α-group	ω-group	reaction	activation	cyclic yield (%)	Ref.
ATRP	PS	cyclopropenone-masked dibenzocyclooctyne	bromo	SPAAC	light	100	[97]
RAFT	PS, PtBA, PNIPAM, PDMA	acrylate	thiol	thiol-ene Michael addition	hexylamine*	80	[110]
	PNIPAM	anthracene	thiol	radical induced thiol-ene	AIBN	-	[111]
	PNIPAM, PDMA	Bromomaleimide	thiol	substitution	$NaBH_4$*	high	[112]
	PMMA	maleimide	thiol	thiol-Michael	$Na_2S_2O_3$*	80	[113]
	PNIPAM, PVP	*t*-butyldimethylsilyl ether	sulfonyl fluoride	SuFEx	TBD	-	[114]
Living anionic	PS	quinuclidinium or *N*-phenylpyrrolidinium	carboxylate	ESA-CF	heat	<88	[115]
Living cationic	PTHF	carboxylate	quinuclidinium or *N*-phenylpyrrolidinium	ESA-CF	heat	<88	[115]
ROCOP	Polyester of PO/PhA	alkene	O_2CCoIII-salen	photo-induced radical addition	light	-	[116]

*used to generate the thiol groups *in situ*. Poly(*N*-vinylpyrrolidone) = PVP, 1,5,7-triazabicyclo[4.4.0]dec-5-ene = TBD, poly(tetrahydrofuran) = PTHF, ring-opening copolymerization = ROCOP, propylene oxide = PO, phthalic anhydride = PhA

be used. However, in most cases cyclization via bimolecular ring closure is contaminated by non-cyclic byproducts.

2.2.1. Bimolecular homodifunctional coupling

In 1980, Geiser and Höcker [119], and Rempp et al. [120] reported simultaneously the first cyclic polystyrene with α,α'-dihalo-p-xylene as bifunctional coupling agent (Fig. 21). To generate a dianionic "living" chain, the anionic polymerization of styrene with sodium naphthalene was performed under argon atmosphere. A solution of the obtained polymer was then added simultaneously with an equimolar solution of the coupling agent into pure tetrahydropyran, where cyclization took place under high dilution. Cyclic polymers from 3 to 25 kDa with polydispersities below 1.2 were obtained, but with rather low yields of cyclization (< 50%). After the addition of one equivalent of coupling agent, the presence of styryl anion was still detected by means of colorimetry. The presence of unreacted anions is a sign of non-cyclic living chains. By adding an excess of coupling agent, linear chains with much greater molecular weight than the cyclic product were formed and could be efficiently separated by fractionation. A few years later, a similar method was used by Roovers and Toporowski to synthesize cyclic polystyrene of 450 kDa by replacing the α,α'-dihalo-p-xylene by dimethyldichlorosilane [121]. However, the yields of cyclization remained low. By using dianionic polymer precursors, a diversity of cyclic homopolymers have been synthesized including poly(butadiene) [122], poly(2-vinylpyridine) [123], and poly(isoprene) [124].

In 1996, Ishizu and Kanno implemented the interfacial reaction between the linear polymer precursor and the coupling agent as a method to reduce the problems associated to intermolecular coupling [125]. They first reacted the polystyryl dianion with a large excess of 1,4-dibromobutane to generate the dibromobutyl polystyrene (Fig. 22). Then, the polymer was dissolved in an organic phase (toluene/DMSO) and was reacted at the interphase with hexamethylene diamine dissolved in water/NaOH under stirring at 80°C. The authors demonstrated high yields of cyclization (80-90 %). Moreover, with this strategy the concentration of linear precursor was as high as 10^{-3} M, while other coupling strategies typically require much lower concentration (around 10^{-6} M) to avoid intermolecular coupling. Ishizu and Ichimura extended this strategy to the synthesis of polystyrene-b-poly(isoprene) copolymer [126].

The Williamson etherification reaction was implemented in the 90' by Booth et al. [127] to synthesize cyclic poly(ethylene oxide)s. They reacted α,ω-dihydroxy poly(ethylene glycol)s with dichloromethane in the presence of KOH, a technique that was later improved by adding poor solvents to the polymer solution to assure the ring closure by reducing the end-to-end distance of the linear polymer coil [128]. With this method, cyclization efficiencies as high as 93 % were reported. In a second approach, α,ω-dihydroxy poly(ethylene glycol)s was reacted with tosyl chloride in the presence of KOH [129]. The poor-solvent strategy was also used. Allgaier et al. [130] made important improvements of the purification method for obtaining multigram scale of the cyclic product obtained via tosyl chloride strategy. Hadjichristidis et al. [131] reported the synthesis of gram scale of cyclic polystyrene and cyclic poly(ethylene oxide) by means of the Williamson etherification reaction of α,ω-dihydroxy polymer precursors and dibromo coupling agents: 1,4-bis(bromomethyl) benzene and 2,6-bis(bromomethyl)pyridine.

In 2000, Tezuka et al. [132] reported the first examples of cyclic and multicyclic architectures of poly(tetrahydrofuran) synthesized via ESA-CF. Telechelic poly(tetrahydrofuran)s end-capped with moderately strained cyclic *N*-phenylpyrrolidinium salt groups, carrying a plurifunctional carboxylate counteranion, were prepared as polymer precursors (Fig. 23). At high dilution, the polymer

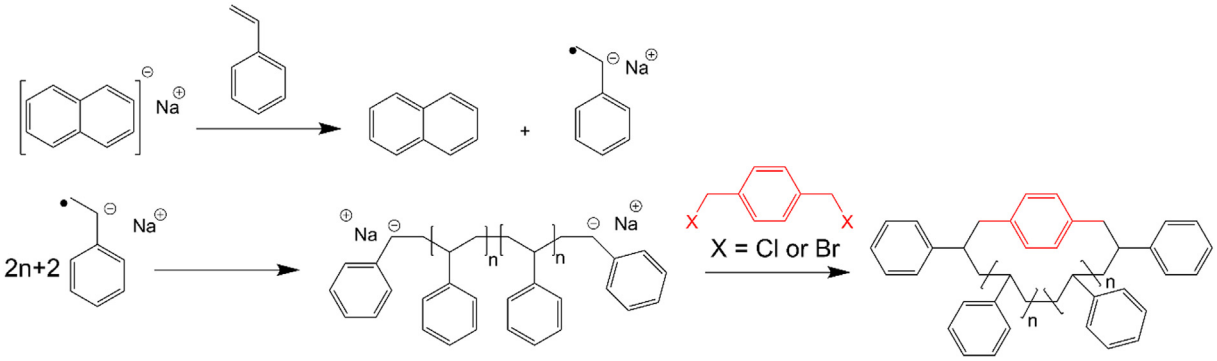

Fig. 21. Synthesis of the first cyclic polystyrene via bimolecular ring closure using α,α'-dihalo-p-xylene as bifunctional coupling agent [119,120].

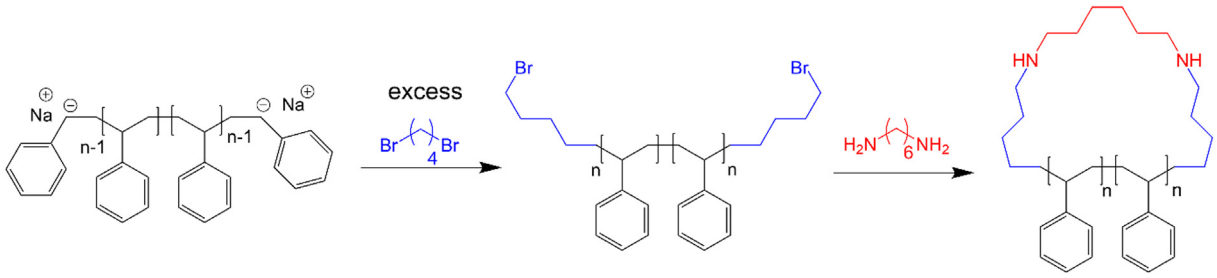

Fig. 22. Cyclization of polystyrene using interfacial condensation (last step) [125].

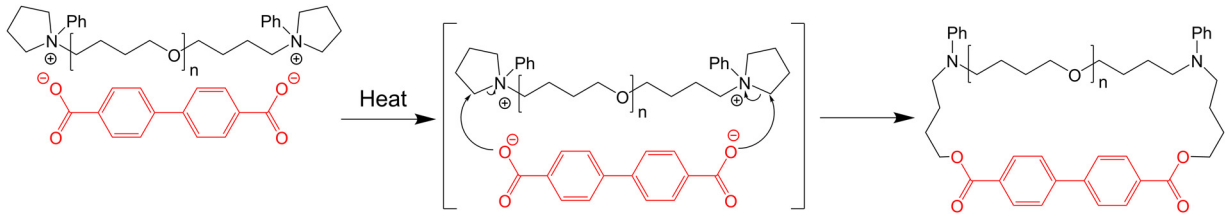

Fig. 23. Example of cyclization of poly(tetrahydrofuran) via electrostatic self-assembly covalent fixation (ESA-CF) [132].

formed cyclic assemblies. Then, upon heating, the attack of the carboxylate anion to the pyrrolidinium end-group was triggered, forming the neutral diester cyclic product. The authors extended this method to other cyclic polymers such as cyclic polystyrene [133], cyclic poly(ethylene oxide) [134], and a collection of many other cyclic and multicyclic architectures [135].

In 2010, the use of the extremely fast thiol-ene "click" reaction, specifically the Michael addition of thiols to maleimides, was first reported by Dove et al. [136] for the preparation of cyclic poly(lactide). They reacted α,ω-maleimido-functionalized poly(lactide) with 1,2-ethanedithiol in the presence of triethylamine and sodium metabisulfite (to suppress thiol reduction), obtaining a high yield of cyclization (>95 %). An advantage of using the thiol-ene "click" reaction is the absence of copper catalyst and the mild conditions that are compatible with sensitive polymer backbones containing ester functions.

In 2017, Zhang et al. [137] implemented the self-accelerating double-strain-promoted azide-alkyne click reaction (DSPAAC) for the synthesis of cyclic polystyrene (Fig. 24). The reaction of α,ω-diazide polystyrene and α,ω-diazide poly(ethylene oxide) with *sym*-dibenzo-1,5-cyclooctadiene-3,7-diyne (DBA) as coupling agent conducted to the formation of pure cyclic polymers in mild conditions. This reaction is self-accelerating: the cycloaddition of the first alkyne with azide increases the DBA ring strain and activates the second alkyne, which reacts with a second azide much faster than the original DBA alkyne group. Given this self-accelerating property, the requirement of 1:1 stoichiometry between the complimentary reactive groups is no longer needed, allowing to increase the rate of intermolecular reaction by using an excess of the coupling agent (first reaction step). Furthermore, the formation of multicyclic structures is also possible by using multifunctional polymer precursors.

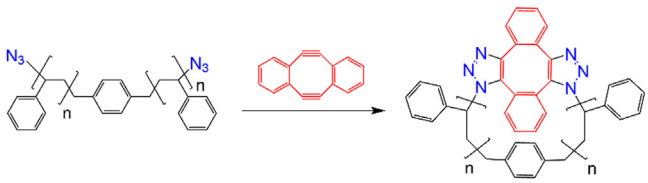

Fig. 24. Cyclization of polystyrene *via* double-strain-promoted azide–alkyne click reaction [137].

Given the enormous advantages of the DSPAAC for the synthesis of cyclic and multicyclic structures with a high topological purity, this strategy was rapidly extended to the synthesis of other cyclic polymers including the poly(L-lactide) [138], polynorbornenes [139], poly(*N*,*N*-dimethylacrylamide) [140], poly(tert-butyl acrylate) [140], poly(vinyl acetate) [141], poly(*N*-vinylcarbazole) [141,142], and complex architectures [143].

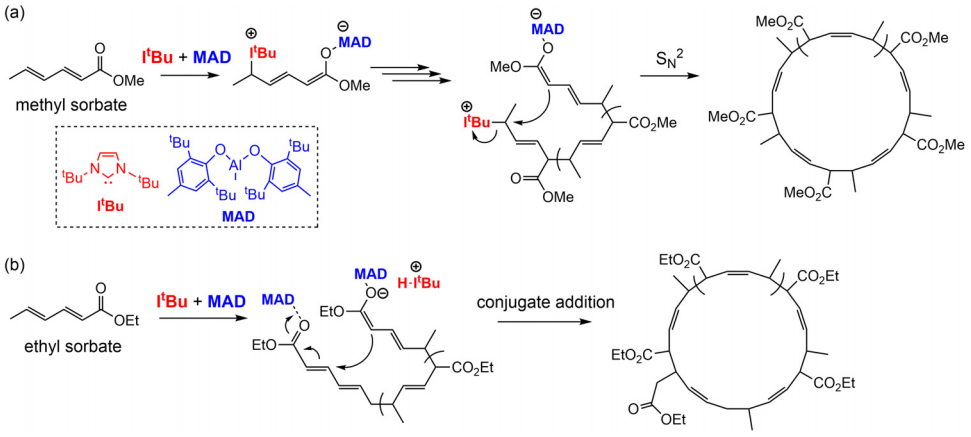

Fig. 25. LPP mechanism for the synthesis of cyclic polysorbates by (a) Takasu et al. [144] and (b) Chen et al. [146].

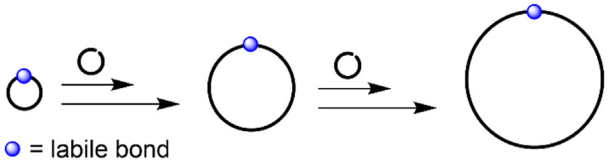

Fig. 26. Schematic representation of the ring expansion polymerization.

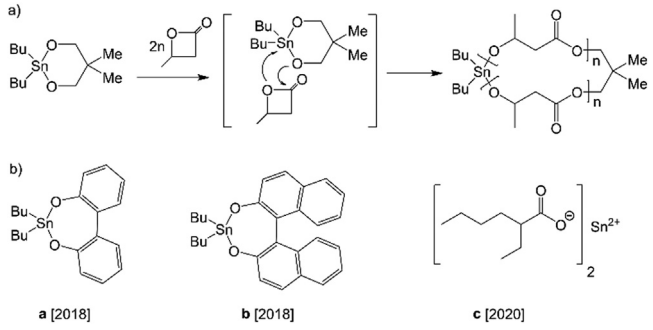

Fig. 27. a) First synthesis of cyclic polylactones by REP in 1995 [148]. b) Novel Sn (IV) [156] and Sn (II) [157] catalysts used for REP of cyclic poly(L-lactide).

2.3. Lewis pair polymerization (LPP)

Cyclization by LPP relies on a ring closure process occurring after all the monomer has been consumed during polymerization and at specific site in the chain. In this way, purification steps, post-functionalization reactions and the addition of exogenous reagents are avoided, thus simplifying the synthesis of cyclic polymers and improving chemical purity. In 2017, Takasu et al. [144] synthesized diene-based cyclic polymer with M_n of 23 kDa (Đ =1.17) *via* anionic polymerization of methyl sorbate (MS) with an N-heterocyclic carbene (NHC), 1,3-bis(tert-butyl)imidazole-2-ylidene (I^{t}Bu), in the presence of a bulky aluminum Lewis acid, methylaluminum bis(2,6-di-tertbutyl-4-methylphenoxide) (MAD) (Fig. 25a). Similar mechanism was used to later synthesize cyclic PMMA initiated by a 1:1 adduct of MAD:I^{t}Bu, a reaction that does not need diluted conditions [145]. They proposed that ring-closure occurred by a nucleophilic attack of the anionic propagating center into the adjacent carbon of the imidazolium cationic α-terminus. Recently, Chen et al. [146] proposed an alternative mechanism, where cyclization occurs via conjugate addition (Fig. 25b). In that work, a review of the mechanism of cyclic PMMA is also proposed [146].

3. Ring expansion polymerization (REP)

In REP the monomer is incorporated into a preformed cyclic structure that held together by a relatively labile bond (e.g. organometallic or electrostatic) (Fig. 26). The cyclic structure is maintained throughout the chain growth. Therefore, this process does not suffer from entropic penalties associated to the reaction between two terminal groups as it occurs in the ring closure method. High molecular weights can be accessed and the reaction can be scaled to obtain large amounts of cyclic product. Some drawbacks are that the number of cyclic polymers obtained by REP is limited because their synthesis depends on that specific monomer and catalyst pairs are chemically allowed to follow such mechanism. High polydispersity can be obtained because the formation of stable ring polymers depends on the rates of polymerization, depolymerization and backbiting. And finally, the removal of the catalyst can be challenging.

3.1. REP with metal-based catalysts to cyclic polyesters

The development of REP techniques using tin-based initiators for the generation of cyclic polyesters has been pioneered by Kricheldorf [147]. In 1995, Kricheldorf and Lee prepared macrocycles of different (thio)lactones using tin heterocyclic initiators such as 2,2-dibutyl-1,3-dioxa-2-stannates generated from dibutyltin oxide and aliphatic diols [148,149]. The monomer units are inserted into the Sn-O bond of the initiator leading to the propagation of macrocyclic esters (Fig. 27a). Molecular weights up to 32 kg/mol were obtained with a Đ value of 1.7. The cyclic structure was confirmed by SEC and ^{1}H NMR analysis. The condensation of α,ω-dihydroxy polymers such as poly(ethylene glycol) [150], poly(tetrahydrofuran) [151], and poly(siloxane) [152] with $Bu_2Sn(OMe)_2$ was later confirmed to conduct to the formation of macrocycles containing the tin catalyst. After the insertion of two γ-thiobutyrolactones into the macrocycle by formation of Sn-S bonds, the macrocycles were used as REP initiators of ε-caprolactone leading to the formation of macrocyclic block copoly(ether-esters). By removal of the Bu_2Sn group, hydroxyl-terminated polymers can be generated. The use of tin-based initiators were expanded to synthesize cyclic polyesters based on lactide monomers [153,154]. The replacement of the Bu_2Sn groups from the macrocycles was demonstrated by using cyclic bis(thiophthalates) [155]. A ring-exchange process allowed the formation of a more stable macrocycle without an intermediate ring-opening reaction.

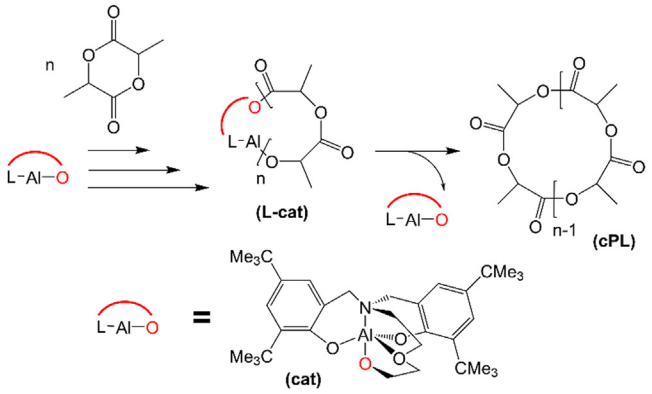

Fig. 28. Aluminum-based catalyst (alumatrane type) for the REP of lactide [159].

Continuous effort in Kricheldorf's group for the synthesis of cyclic polyesters have conducted to the exploration of novel Sn-based catalysts as for example those depicted in Fig. 27b. In 2018, Sn(IV)-based catalyst containing aromatic alkoxide groups (catalysts a and b) showed fast polymerization of L-lactide in bulk at temperatures between 160 and 180°C without observing racemization [156]. Molecular weight of about 30 kg/mol were obtained but with high Đ values from 3 to 6. In a novel approach, industry-standard Sn(II) 2-ethylhexanoate (catalyst c) showed M_n values as high as 160 kg/mol (Đ ~ 2) of cyclic poly(L-lactide) in the bulk polymerization at 160 °C [157]. To explain the formation of cyclic chains the authors invoked a ROP mechanism, where initiation occurs by a coordination–insertion mechanism yielding a tin alkoxide end group, and the simultaneous occurrence of polycondensation and end-to-end cyclization. More information on the polymerization mechanisms with tin catalysts can be found in a recent review of Kricheldorf and Weidner [158].

In 2012, Getzler et al. [159] reported on the use of a novel alumatrane catalyst [*N,N*-bis(3,5-di-tert-butyl-2-benzyloxy)-2-(2-aminoethoxy)ethoxy)aluminum] (cat) to generate cyclic poly(lactic acid) (cPL) by REP of lactide (Fig. 28). The polymerization occurs in solution and in melt, which is in line with many REP polymerizations. cPLs of M_n up to 39 kDa were obtained with relatively low Đ values. The proposed mechanism of polymerization is based on a coordination–insertion mechanism generating the macrometallacycle L-cat. At certain time and conditions, L-cat undergoes an intramolecular chain transfer to liberate cPL and regenerate free catalyst. This hypothesis was later confirmed by kinetics studies, where first order in catalyst and zero order in monomer were found supporting the intramolecular catalyst rearrangement [160].

In 2015, Phomphrai et al. [161] reported on the use of salicylaldiminato tin (II) catalysts containing different alkoxy side chains to catalyze the REP of L-lactide and ε-caprolactone (Fig. 29). The tin complex having the shorter alkoxy chain (complex a) conducted to the formation of cyclic PLA, whereas that having the longer chain (complex c) conducted only to linear PLA. The length of the side chain determines the distance between the tin atom and the growing polymer chain. The intramolecular transesterification is responsible for the formation of cyclic polymer chains but only when occurring near the metal atom. A further development of guanidinate tin (II) catalytic complexes by Phomphrai et al. [162] in 2020 corroborated the ability of these catalysts to synthesize cyclic polyesters of $_L$-lactide and ε-caprolactone.

In 2015, Bonnet et al. [163] synthesized cyclic PLA by means of bulk polymerization and reactive extrusion polymerization of L-lactide using alkaline-earth and lanthanide borohydride complexes as catalyst: $Mg(BH_4)_2$, $Ca(BH_4)_2(THF)_2$ and $Ln(BH_4)_3(THF)_3$ with Ln = Nd, Sm and La. They observed that the cyclic product was obtained in all the polymerization systems. The higher activity of the lanthanides complexes made it possible for the reaction to proceed at 130 °C (typically 185 °C), providing molecular weights of up to 30 kg/mol. This technique has a great potential for industrial-scale synthesis of cyclic polyesters.

In 2018, Chen et al. [164] proposed a modified version of non-polymerizable γ-butyrolactone (GBL), the 3,4-trans six-membered ring–fused GBL (3,4-T6GBL), which polymerized at room temperature under solvent-free conditions yielding high-molecular weight products. Moreover, by using a coordination-insertion ROP catalyst and commercially available $La[N(SiMe_3)_2]_3$ at low loadings (1 to 0.05 mol % catalyst) they found that cyclic polymers were generating at high monomer conversions (79-84 %), achieving molecular weights in the range of 73.0-85.5 kDa and Đ of 1.34-1.48 (Fig. 30). Previous to this work, Hong and Chen [165], had found that the $La[N(SiMe_3)_2]_3$ catalyst was able to polymerize the GBL at subzero temperatures to produce mixtures of linear and cyclic poly(GBL) structures. The latter are believed to be produced by back-biting reactions. Moreover, by finely tuning the reaction conditions (solvent, monomer concentration, and nature of added alcohol) a control over the topology was achieved. More information on the production of recyclable polyesters by using this $La[N(SiMe_3)_2]_3$ and other catalysts can be found in a recent review by Tang and Chen [166].

In 2020, Milione et al. [167] reported the use of a new [OSSO]-type iron (III) catalyst for the synthesis cyclic PLA, poly(ε-caprolactone) and poly(β-butyrolactone). Although the catalyst was moderately active (initial turnover frequency up to 2718 h^{-1}), the molecular weight achieved with this new catalyst were relatively low (~5 kg/mol).

In 2022, Guillaume, Carpentier et al. [168] found that an yttrium amido complex, supported by a diamino-bis(phenolate) ligand bearing sterically bulky ^{t}Bu substituents, conducted to the formation of cyclic poly(3-thiobutyrate) (P3TB) with M_n up to 10 kDa (Đ ~ 1.5) by ROP of racemic mixtures of 3-thiobutyrolactone (*rac*-TBL) (Fig. 31). The reaction proceeded with the catalyst alone or in the presence of co-initiators (^{i}PrOH, ^{i}PrSH or BnSH). The reaction in toluene occurred very rapidly at room temperature, and turnover frequencies above 3000 h^{-1}. Cyclization is believed to occur *via* transthioesterification and not by a back-bitting mechanism, as that proposed by Chen et al. [165] in the ROP of GBL. By varying the nature of the different substituents in the yttrium complex, a control over the stereoselectivity was achieved with turnover frequencies in the range of 2400 and 12 000 h^{-1}.

3.2. REP with non-metal catalysts

In 1997, Shea et al. [169], discovered a borane initiated/mediated C1 living polymerization of dimethylsulfoxonium methylide, which was called polyhomologation. This C1 polymerization occurs through rapid methylene insertion (one by one) from dimethylsulfoxonium methylide into a weak carbon-boron bond of an initiator, i.e. a REP mechanism (Fig. 32). Using this strategy, the authors demonstrated that 3-arm polymethylene stars can be generated from trialkyl boranes and macrocyclic polymethylenes from boracyles [170]. The mechanism involves the formation of an organoboron "ate" complex (zwitterionic intermediate) formed by the attack of the nucleophilic dimethylsulfoxonium methylide (monomer) on the Lewis acidic borane (initiator) followed by migration/insertion of $-CH_2-$ into the initiator. M_n up to 2 kDa and Đ ~ 1.6 were generated.

The synthesis of cyclic polysulfides from thiiranes initiated by cyclic thioester derivatives started in 2005 by Kudo, Nishikubo et al. [171]. They demonstrated that 3-phenoxypropylene sulfide (PPS) is inserted into a cyclic dithioester in the presence of tetrabutylammonium chloride (TBAC) to generate cyclic

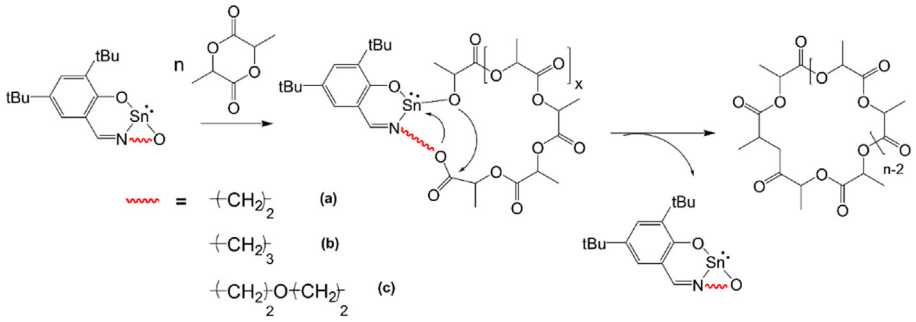

Fig. 29. Tin (II)-based catalyst containing an alkoxy side chain for the REP of lactide [161].

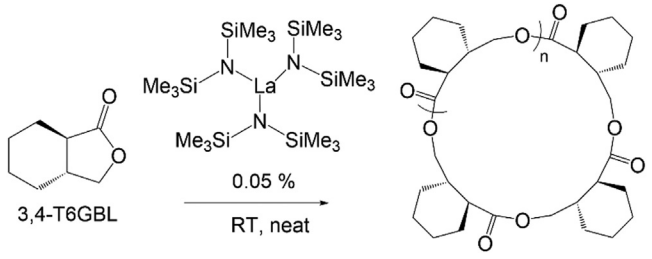

Fig. 30. Synthesis of cyclic poly(3,4-T6GBL) with a coordination-insertion ROP catalyst, La[N(SiMe$_3$)$_2$]$_3$ [164].

polysulfides with narrow dispersity and $M_n = 8$ kDa (Fig. 33a). Then, a cyclic thiourethane, thiazolidine-2,4-dione (TZD), proved to be efficient in the insertion of PSS to give the corresponding polymers with M_n up to 10 kDa and low dispersities (Fig. 33b) [172]. Recently, Kameyama et al. found that a cyclic thiourethane, 3H-benzothiazol-2-one [173], and a dithiocarbamate, 3H-benzothiazol-2-thione (BTT) [174] are able to initiate different thiirane monomers conducting to the formation of the cyclic polysulfides with narrow dispersities (Fig. 33c). The mechanism involves the formation of a thiolate anion intermediate that facilitates the ring opening of thiirane monomers. Propagation occurs through a thioacyl-transfer mechanism by expanding the cyclic structure. The living character of this system is proved by chain extension and the generation of block copolymers [173,174].

The continuous efforts in the development of new catalysts, metallic and non-metallic, have opened up new possibilities for the synthesis of a variety of cyclic polymers. Given the concepts established behind the use of these catalysts in distinct types of polymerizations, subsequent subsections have been divided into mechanisms of REP.

3.3. Ring expansion metathesis polymerization (REMP)

In 2002, Grubbs et al. [175] demonstrated the great potential of REMP to generate high molecular weight cyclic polybutadiene from *cis*-cyclooctene using a Ru-based catalyst (Fig. 34). The catalyst contains an unsaturated backbone in the *N*-heterocyclic carbene (NHC) and 7 carbons tethered between the Ru center and NHC ligand (UC-7 catalyst). REMP relies on the olefin metathesis (metal-catalyzed redistribution of carbon−carbon double bonds) where the cyclic olefin coordinate to the REMP catalyst from both ends and add into the growing polymer. During the final step, the macrocyclic ruthenium complex undergoes an intramolecular cross-metathesis to regenerate the ruthenium catalyst and yield the cyclic polybutadiene. This work established the first route to extremely high molecular weight cyclic polybutadiene, >1000 kDa. Upon hydrogenation, cyclic polyethylene was obtained. A year later, same authors extended this approach to the REMP of 1,5-cyclooctadiene (COD) [176]. Linear byproducts were formed by polymerization of 4-vinylcyclohexane (4VC), an impurity contained in COD. The formation of those linear chains were suppressed when 1,5,9-trans-cis-trans-cyclododecatriene was used as a monomer, since it was free of 4VC and formed the same cyclic polybutadiene by REMP.

In 2021, Golder et al. [177] designed a Ru-benzylidene initiator (CB6) that showed an excellent molecular weight control for the synthesis of high molecular weight cyclic poly(norbornene)s (up to M_n = 400 kg/mol) (Fig. 35). The performance of this new catalyst was compared with a catalyst similar to UC-7 but that contained 5 carbons anchored between the Ru center and NHC ligand (UC-5). The authors found that CB6 was more stable and presented much faster reaction kinetics, and better molecular weight control by generating polymer chains with values closer to theoretical masses.

In the context of REMP, Veige and co-workers have made significant advances in the development of tungsten catalysts [178–182], and, recently, of a molybdenum-based catalyst [183], for the synthesis of cyclic polyenes (Fig. 36 and Table 5). In 2016, they reported the first catalyst based on tungsten promoting stereocontrolled REMP to yield *cis*-syndiotactic cyclic polynorbornene (catalyst A) [178]. The catalyst was produced by the reaction of a trianionic pincer-supported tungsten alkylidyne complex (catalyst B) with CO_2 generating an active tungsten-oxo alkylidene catalyst (catalyst A). The obtained cyclic polymers showed great control over their structures, *cis*-selectivity and syndiotacticity over 98%,

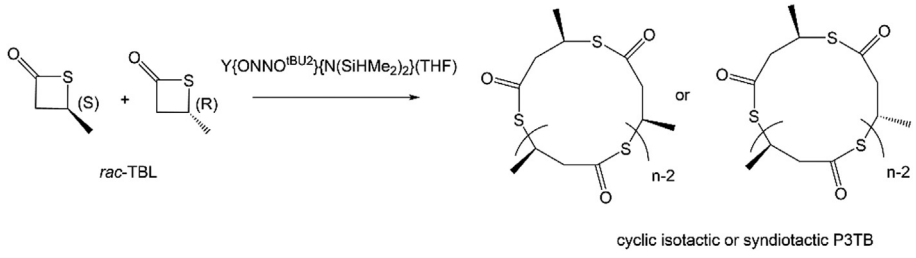

Fig. 31. Synthesis of cyclic poly(3-thiobutyrate) by ROP of 3-thiobutyrolactone with an yttrium amido complex [168].

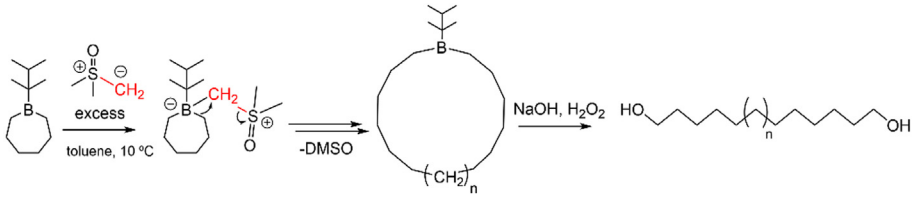

Fig. 32. Polyhomologation reaction producing macrocyclic polymethylene. Verification of REP to boromacrocycle was conducted by oxidation to α,ω-dihydroxy polymethylene [170].

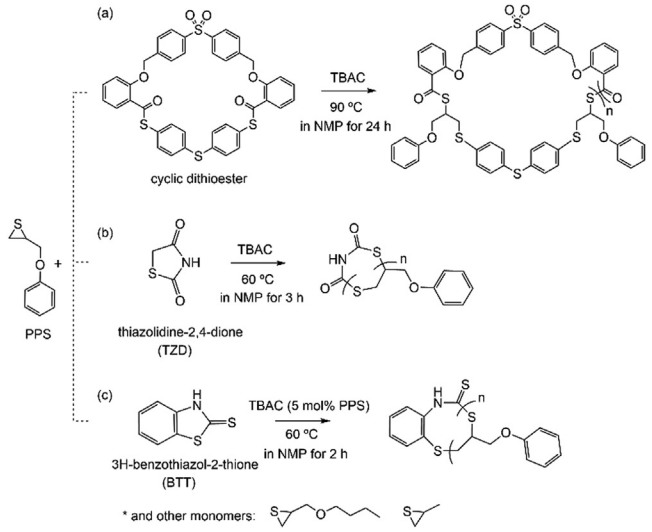

Fig. 33. REP of thiiranes initiated with (a) cyclic dithioester [171], (b) cyclic thiourethane [172] and (c) dithiocarbamate [174].

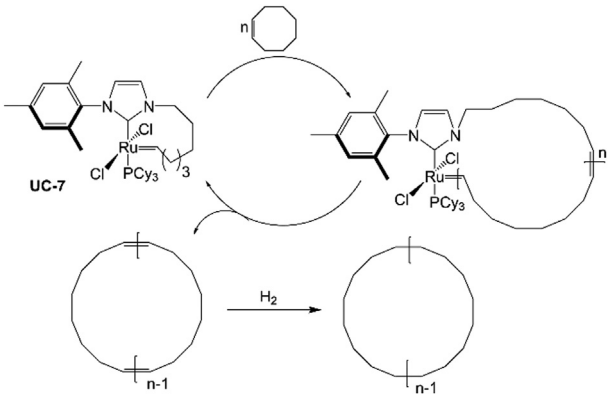

Fig. 34. REMP of *cis*-cyclooctene using a Ru-based catalyst (UC-7) generating cyclic polyolefin that upon hydrogenation produces cyclic polyethylene [175].

Table 5
Cyclic polyenes synthesized by REMP with the catalysts of Fig. 36 and their post-modified cyclic compounds.

Catalyst	Cyclic polymer generated	Post modification	Ref.
A	polynorbornene	-	[178]
B	polynorbornene	-	[179]
B	poly(cyclic alkenes)	polyacetylene	[188]
C	poly(phenylacetylene)	polystyrene	[180]
C	polyacetylene	bottlbrush (PS side chains)	[181]
C	poly(4-ethynylanisole)	poly(4-ethynylphenol)	[184]
C	poly(4-methyl-1-pentene)	-	[185]
C	polypropyne	polypropylene	[186]
D, E	polynorbornene	-	[182]
F	polynorbornene	-	[183]

and molecular weights up to 578 kDa with relatively low Đ (~1.2). The insertion of the monomer unit into the highly hindered metal complex is believed to provide *cis* selectivity, whereas the change of configuration of the metal center after each monomer addition provides syndiotacticity. Same group demonstrated that catalyst B was able to undergo ynene metathesis producing highly cis and syndiotactic cyclic polynorbornene and therefore, that the reaction of catalyst B with CO_2 was not mandatory to generate a REMP catalyst [179]. Also in 2016, catalyst C was generated from the reaction of catalyst B with 3,3-dimethyl-1-butyne, demonstrating to be very active in the REMP of cyclic phenylacetylene [180]. This catalyst was further used in the synthesis of a number of cyclic polyenes [184–186] including cyclic polyacetylene (c-PA) [181]. These polyenes are postmodifiable to new cyclic polymers and architectures (see Table 5). For instance cyclic bottlebrushes with side chains of polystyrene and poly(butyl acrylate) were generated from cyclic polyacetylenes, allowing the clear visualization of the cyclic structures by AFM [181,187]. Catalyst E was found as an isolable intermediate during the synthesis of D [182]. Interestingly, catalyst E was more active and stereoselective than D, finding values as high as >99% *cis* and syndiotactic selectivity, for the synthesis of cyclic polynorbornene.

With the aim of generating soluble precursors of cyclic polyacetylene, catalyst B was employed for the REMP of cyclic alkenes

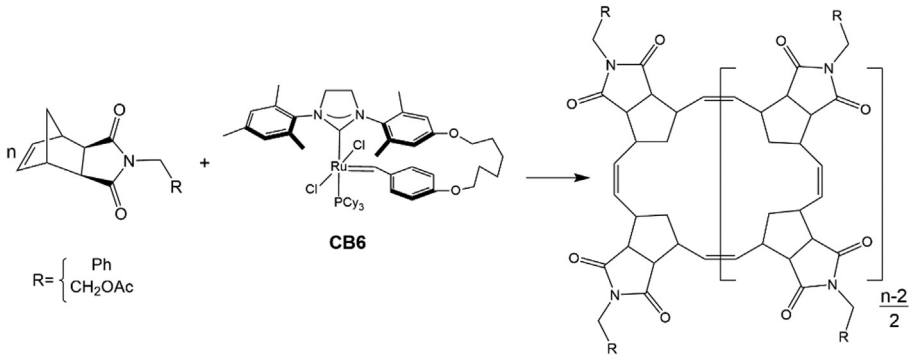

Fig. 35. REMP of norbornene-imide monomers using a Ru-benzylidene initiator (CB6) producing cyclic poly(norbornene)s [177].

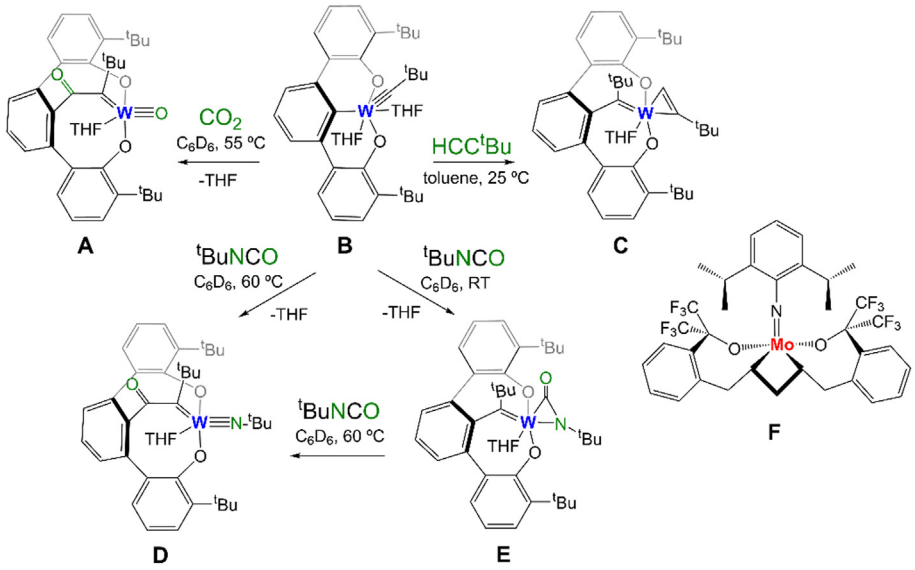

Fig. 36. Scheme of some catalysts developed in Veige's group used in REMP.

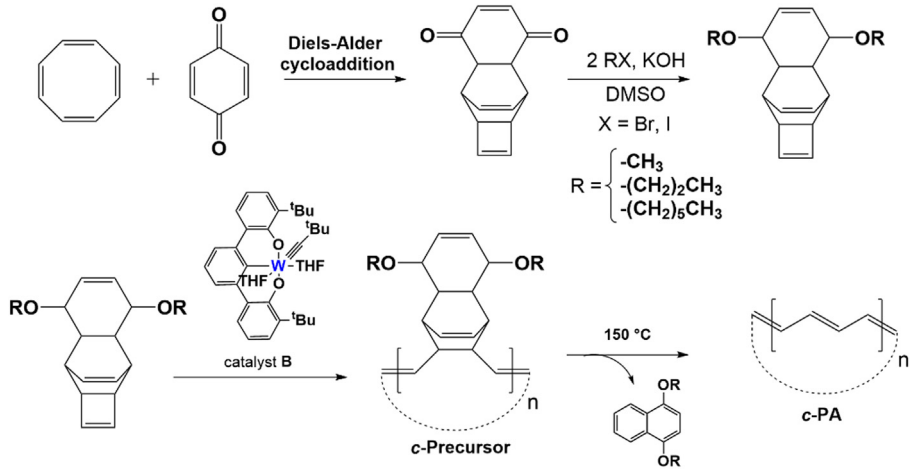

Fig. 37. Synthesis of cyclic polyacetylene by heating soluble cyclic precursors generated by REMP of cyclic alkenes with catalyst B of Fig. 36 [188].

prepared by Diels-Alder cycloaddition between cyclooctatetraene and benzoquinone and subsequent incorporation of different R moieties (Fig. 37) [188]. The generated cyclic polymers presented different solubility in organic solvents. The one containing 6 carbon atoms in R was soluble in benzene and in THF allowing NMR characterization, GPC verification of cyclic structure and preparation of films by solvent-casting. Finally, c-PA was generated by temperature-triggered retro Diels-Alder reaction of soluble polymer precursors in which naphthalene derivatives are eliminated.

In 2021, Maeda et al. [189] found that *cis*-stereoregular cyclic-poly(diphenylacetylene)s were produced by revisiting the polymerization reaction of diphenylacetylene with $TaCl_5$ and different co-catalysts such as nBu_4Sn, Et_3SiH, Ph4Sn and 3,6-bis(trimethylsilyl)-1,4-cyclohexadiene. They proposed a mechanism different from the metathesis polymerization accepted in this system for years by suggesting that the cyclic formation proceeded *via* an insertion ring expansion polymerization mechanism mediated by low-valent tantalum species, which are produced *in situ* by reaction of $TaCl_5$ with the cocatalyst.

More information on the olefin metathesis for generating cyclic polymers and the distinct existing catalysts can be found in other recent reviews by Grubbs [30], Golder [22,190], Veige [191] and co-workers.

3.4. Zwitterionic ring expansion polymerization (ZREP)

"*When the counterion is covalently bound to the chain, the polymerization is termed macrozwitterionic*" [192]. In fact, the charge cancellation in the macrozwitterionic polymerization conducts to the formation of cyclic structures, as already suggested by Szwarc in 1960 [193], by Johnston in 1982 [192], and confirmed by Waymouth et al. [194] in 2007 in the ZREP of lactide with *N*-heterocyclic carbenes (NHCs), also found in the literature as zwitterionic ring-opening polymerization (ZROP).

3.4.1. Nucleophilic zwitterionic ring expansion polymerization (nZREP)

Waymouth pioneered the nZREP technique for the synthesis of cyclic polyesters by using nuleophilic organocatalysts. The polymerization of lactide using 1,3-dimesitylimidazol-2-ylidene (IMes) provided a new route to synthesize metal-free cyclic polyesters of moderate molecular weight (M_n < 25 kg/mol) and narrow polydispersity (Đ < 1.4) (Fig. 38) [194]. The attack of the NHC to the carbonyl of lactide forms an initial zwitterionic intermediate, which upon the addition of more monomer forms a macrozwitterion. The cyclic structure is retained due to the electrostatic interactions that keep together the chain ends. Then, at certain re-

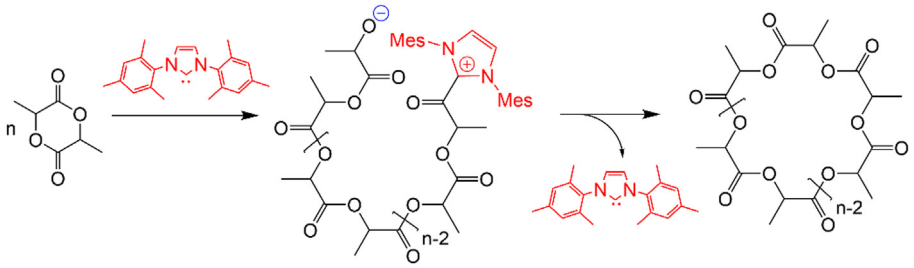

Fig. 38. First synthesis of cyclic PLA by nZREP with 1,3-dimesitylimidazol-2-ylidene in 2007 [194].

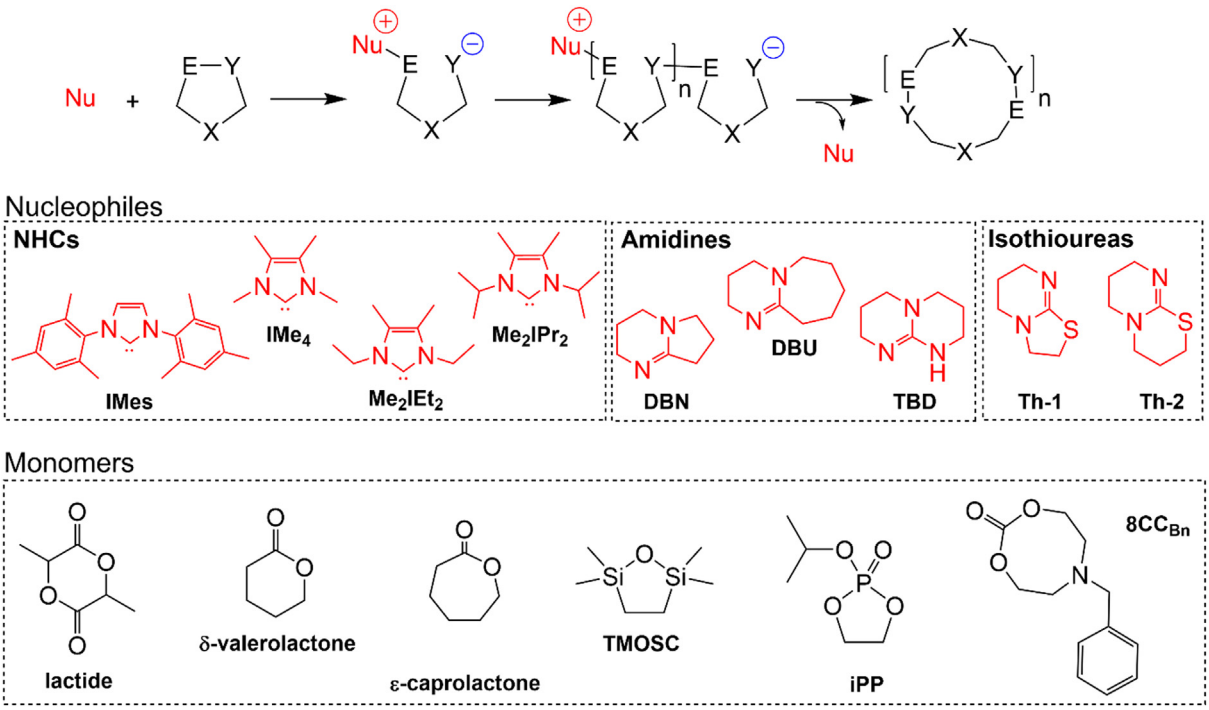

Fig. 39. General mechanism of nZREP. Nucleophiles and monomers used in nZREP.

action time, the catalyst is expelled from the growing chain by generating the macrocycles. This reaction is extremely rapid, reaching complete conversion within minutes. Kinetic investigations on the nZREP of lactide with IMes found that initiation is slower than propagation and that cyclization is slower than propagation [195]. This favor the formation of large rings due to rapid consumption of the monomer from few initiation sites and that cyclization occurs when almost all the monomer has been consumed. Chain growth does not conform to $[M_0]/[I_0]$ making control over molecular weight difficult. However, optimization of the reaction conditions (solvent, temperature, and monomer concentration) are possible to attain desired molecular weights.

The nZREP strategy provided access to a number of cyclic polymers by making the right combination of monomer and catalyst. Waymouth's group demonstrated that this is possible by studying the polymerization of lactide, lactones, cyclic carbonates, cyclic phosphates, and cyclic siloxanes with different nucleophiles such as NHCs, amidines and isothioureas (Fig. 39, Table 6). The general mechanism of nZREP depicts the formation of zwitterionic active species and their cyclization upon the release of the catalyst. Further information on the mechanisms and scope of nZREP can be found in previous reviews of 2013 and 2017 from Waymouth et al. [25,27].

In 2021, Arnold et al. [205] reported the synthesis of high molecular weight cyclic PLA with Cerium (III) – NHC complexes containing three NHC ligands (catalysts I and II, Fig. 40). The polymerization rates of *rac*-lactide were extremely rapid, in the order of few seconds, and the obtained molecular weights were in the range of 60-250 kg/mol, indicating that the catalyst is very active, efficient and topologically selective (> 95 % of cycles). The proposed mechanism of cyclization resembles that proposed by Waymouth in that one NHC ligand is able to open the lactide by forming zwitterionic active species. The negative charge of the anionic chain is stabilized by coordination to Ce (III). The polymerization of L-lactide with catalyst I yielded cyclic poly(L-lactide) with M_n up to 400 kg/mol without observing racemization, and that of ε-caprolactone yielded a M_n of 39 kg/mol. The polymerization rates in both cases were slower than with *rac*-lactide, but are still quite fast, in the scale of few minutes.

3.4.2. Electrophilic zwitterionic ring expansion polymerization (eZREP)

As opposed to nZREP, in eZREP an electrophile attacks the monomer forming zwitterionic cyclic species capable of growing and undergoing cyclization. In 2014, Barroso-Bujans et al. [206] reported the synthesis of cyclic polyethers by reaction of monosubstituted epoxides (e.g., GPE, glycidol and glycidyl octafluoropentylether) with $B(C_6F_5)_3$ at room temperature. The best represented example was the synthesis of cyclic PGPE, where molecular weights up to 12 kg/mol were obtained (Fig. 41). Bulk poly-

Table 6
Cyclic polymers generated by nZREP.

Catalyst	Monomer	M_n (kg/mol)[a]	Ref.
IMes	lactide	< 31	[194,195]
Me_2IEt_2	δ-valerolactone + ε-caprolactone	46-77[b]	[196]
IMes, IMe_4, Me_2IEt_2, Me_2IPr_2	ε-caprolactone	< 114	[197,198]
DBU, DBN	lactide	< 56	[199]
IMes, IMe_4, Me_2IPr_2	TMOSC	< 942	[200]
IMe_4, Me_2IPr_2	δ-valerolactone	< 39	[201]
IMes, IMe_4, Me_2IPr_2	iPP	< 202	[202]
Th-1, Th-2	lactide	< 66	[203]
Me_2IPr_2	$8CC_{Bn}$	< 96	[204]

[a] Number average molecular weight determined by GPC with polystyrene calibration. [b]Copolymers of different monomer composition.

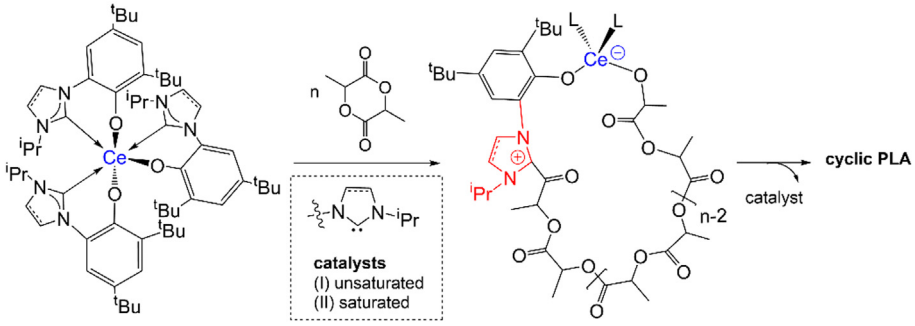

Fig. 40. Synthesis of cyclic PLA with Ce(III) – NHC complexes [205].

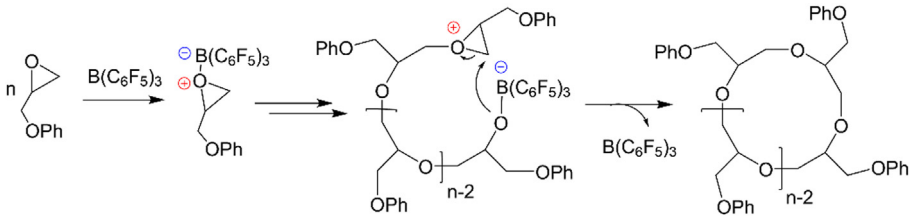

Fig. 41. eZREP of glycidyl phenyl ether catalyzed by $B(C_6F_5)_3$ [206].

merization afforded higher molecular weights than solution polymerization likely due to the release of $B(C_6F_5)_3$ in the termination step is hampered by the high viscosity of the polymerization system. Similarly as in nZROP, the molecular weight does not conform to $[M_0]/[I_0]$, making control over molecular weight difficult. Changes in the solvent polarity had no important effects on the molecular weight, and when using THF or dioxane as a solvent, copolymers of these with GPE were generated. Further study on the copolymerization of GPE with THF showed that copolymers generated with low THF fraction conducted to the formation of cyclic chains whereas, the opposite led to high molecular weight linear copolymers of M_n up to 333 kg/mol [207]. Moreover, studies of eZREP with optically pure (S)-GPE showed that this polymerization conducts to regio-irregular, atactic, and amorphous cyclic PGPE demonstrating that enchainment occurs by attack at both the methine and methylene carbons of the epoxide ring as in many carbocationic polymerizations [208].

The major advantage of eZREP is the gram amount of cyclic product that can be obtained in a single easy step of reaction, as it occurs in nZREP. However, one disadvantage of eZREP is that non cyclic impurities are unavoidably produced in all the reactions investigated [209,210]. These side reactions are in part originated from the reaction of $B(C_6F_5)_3$ with the oxygen in the glycidyl ether moiety causing the termination of the growing chains with undesired terminal groups [209]. Other side reactions come from the termination with adventitious water [206]. Despite this, highly pure cyclic polyether can be obtained by removal of hydroxyl-terminated non-cyclic impurities by using click scavenging techniques [210].

By following previous eZREP mechanism, branched cyclic polyglycidol (bcPG) was recently synthesized by Lee et al. [211] by reaction of glycidol with $B(C_6F_5)_3$ in solution. In nonpolar solvents, bcPG precipitates during the course of the polymerization due to a change in solubility. In these conditions, part of the initial $B(C_6F_5)_3$ remains in solution maintaining its catalytic activity and enabling the reinitiation of subsequent polymerization reactions. This study demonstrated that the catalyst can be recycled for n^{th} times without needing purification protocols. M_n up to 2.5 kg/mol was obtained. Recent kinetic investigation in our group [212] on the eZREP of glycidol in the absence of solvent points to the formation of low molecular weight chains at the initial stages of the polymerization followed by ring fusion events. These events, together with branching reactions promoted by the hydroxyl groups in the polyglycidol chains, would explain the sudden increase of the molecular weight at high conversions, where M_n up to 8 kg/mol ($Đ \sim 2$) were obtained (Fig. 42). Initiation occurs by the reaction of boron with both glycidol oxygens leading to the formation of oxonium ions, which are prone to be attacked by a second glycidol monomer. The ring opening occurs competitively by attack of epoxide groups (active chain-end mechanism, ACEM) and hydroxyls (activated monomer mechanism, AMM) leading to the formation of $L_{1,3}$ and $L_{1,4}$ units, respectively, as previously described by Dworak, Penczek, et al. in the cationic polymerization of glycidol with Lewis acids [213] and described in the work of Leet

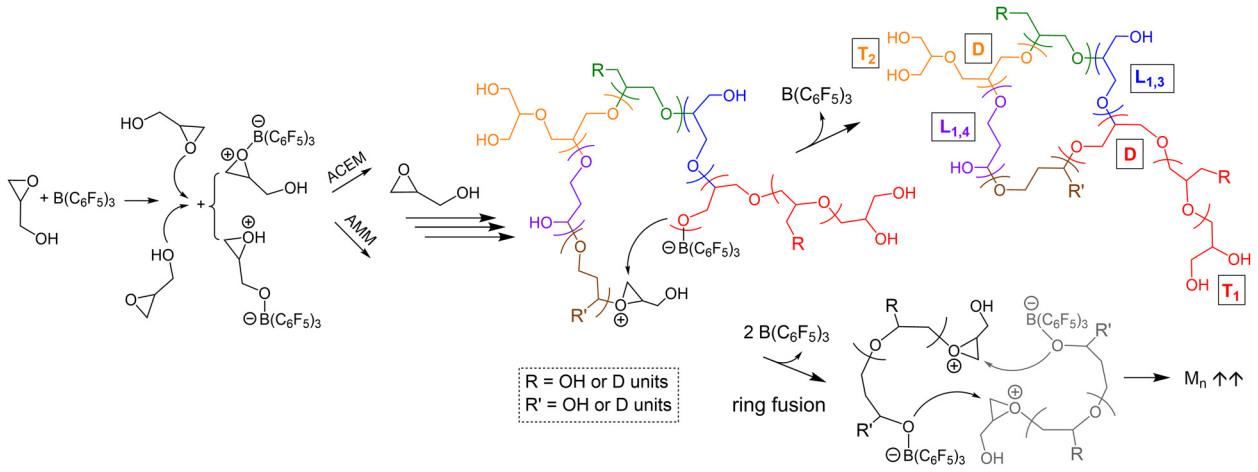

Fig. 42. eZREP of glycidol with $B(C_6F_5)_3$ exhibiting ring fusion events [212].

et al. [211]. Finally, termination occurs by an intramolecular attack of the oxygen next to borane on the electron-deficient α-carbon of the oxonium ion, as proposed in our previous study [206]. Inspired on the work of Sawamoto, Ouchi et al.[214,215], and Engler and Kohl [216] on the cationic REP mechanisms (explained below), we added a second termination mechanism, the intermolecular chain fusion. As a result of the different reactions occurring in the polymerization of glycidol, the resulting structures are formed by linear ($L_{1,3}$ and $L_{1,4}$), dendritic (D) and terminal units (T_1 and T_2) (Fig. 42).

3.4.3. Lewis pair-mediated zwitterionic ring expansion polymerization (LP-ZREP)

The use of acid/base Lewis pairs for the polymerization of epoxides [217], lactones [218], and acrylates [219,220] has already been well documented in the literature. In 2013, Bourissou et al. [221] combined the Lewis acid, $Zn(C_6F_5)_2$, with organic bases (amines or phosphines) to catalyze the ROP of lactide and ε-caprolactone and generate cyclic structures. The bases were 1,2,2,6,6-pentamethylpiperidine (PMP), *N,N*-dimethylaminopyridine (DMAP), $P(n\text{-}Bu)_3$ and PPh_3. By monitoring the polymerization of lactide with PMP, they found that the molecular weight increased linearly with monomer conversion indicating controlled polymerization. M_n were moderately high, generating chains up to 50 kg/mol and $Đ \sim 1.5$. Moreover, chain extension was possible by addition of a second batch of monomer at high conversion in contrast to nZROP of lactones with NHCs, where reinitiation occurred instead of chain extension. Finally, the ability of this Lewis pair to promote chain extension was used to synthesize block copolymers of lactide and ε-caprolactone.

Mechanistic investigations on the polymerization of lactide by $Zn(C_6F_5)_2$/organic base Lewis pairs was reported by Li et al. [222] in 2016. They used $P(n\text{-}Bu)_3$, DBU, 7-Methyl-1,5,7-triazabicyclo[4.4.0]dec-5-ene (MTBD) and IMes as a base, finding that DBU, MTBD and IMes formed frustrated Lewis pairs (FLP) whereas DMAP formed a classical acid-base adduct. The most sterically hindered base, MTBD, exhibited the highest catalytic activity towards the polymerization of lactide. IMes and DBU showed moderate activity and DMAP the lowest one. The effect of temperature and solvent were also investigated finding that initiation rates increased with increasing temperature and with increasing solvent polarity as a result of the weakening of acid-base interactions. M_n up to 29 kg/mol and $Đ \sim 1.2$ were obtained. A plausible polymerization mechanism was proposed based on the monomer activation by the Lewis acid/base pair and the propagation of a zwitterionic active chain that expands upon the addition of monomer (Fig. 43).

In 2017, Verpoort et al. [223] found that a zeolitic imidazole framework ZIF-8 produced cyclic PLA in the absence of solvent at 160 °C. The authors proposed a LP-ZREP mechanism where the Lewis acid (Zn) coordinates with the monomer to generate a zinc alkoxide, and the basic nitrogen functions as nucleophilic initiator. The incorporation of monomer leads to a growing chain that contains Zn-O and N-O linkages at both chain ends. Intramolecular transesterification conducts to the formation of cyclic PLA and the release of the ZIF-8 catalyst. Interestingly, after washing the catalyst with plenty of solvent, it was reused in at least three other runs without losing catalytic activity.

In 2019, Du et al. [224] synthesized cyclic poly(β-butyrolactone) (PBL) by using amido-oxazolinate zinc complexes as LP-ZREP catalyst (Fig. 44). In the figure only one of the studied zinc complexes is represented, the one that conducted to the highest molecular weight of the series (M_n = 197 kg/mol and $Đ \sim 2$). The authors demonstrated that the Zn-N(imine) bond forms a loose pair with increasing temperature that favors the coordination of Zn with β-butyrolactone and the attack of imine nitrogen to carbonyl group. Then, they postulated a zwitterionic ring expansion mechanism, where zwitterionic active species allowed the incorporation of monomer units. By adding alcohols as cocatalysts, linear PBLs were formed.

In 2022, Lee et al. [225] investigated on the LP-ZREP of glycidol catalyzed by $B(C_6F_5)_3$ and organic bases (tributylamine and pyridine). The polymerization of glycidol with $B(C_6F_5)_3$ alone conducts to the formation of cyclic branched polyglycidol structures according to an eZREP mechanism (Fig. 42) [211,212]. By the addition of organic bases to this polymerization system, the eZREP mechanism changes to become LP-ZREP (Fig. 45) [225]. The $B(C_6F_5)_3$ forms frustrated Lewis pairs with tributylamine and pyridine. With increasing temperature, loose or dissociated Lewis pairs are formed. The $B(C_6F_5)_3$ recovers its acidity and forms zwitterionic intermediates with glycidol by interaction with the epoxide group. The hydroxyl group of glycidol interacts by hydrogen bonding with the organic base further activating the hydroxyl towards the activated monomer mechanism that leads to the formation of $L_{1,4}$ units (Fig. 45). Cyclic branches structures were generated by using the less steric hindered pyridine as a base, whereas the more steric hindered tributylamine, yielded hyperbranched non-cyclic structures. These results were attributed to differences in the stability of zwitterionic intermediates caused by steric effects of the Lewis bases. M_n of the obtained polymers were relatively low, of the order of 2 kg/mol.

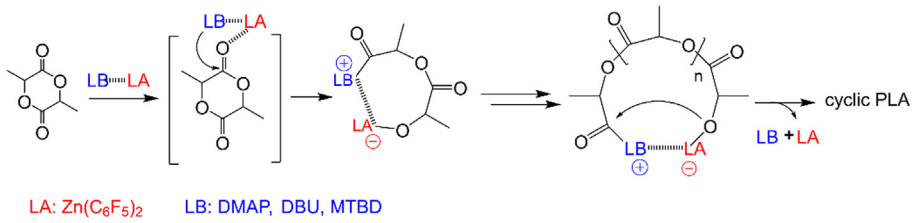

Fig. 43. LP-ZREP of lactide catalyzed by $Zn(C_6F_5)_2$/organic base Lewis pairs [222].

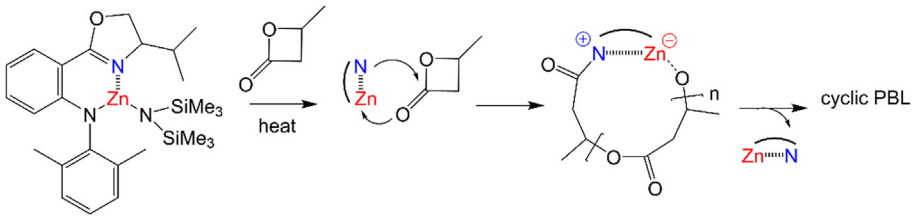

Fig. 44. Amido-oxazolinate zinc catalyst for LP-ZREP of β-butyrolactone [224].

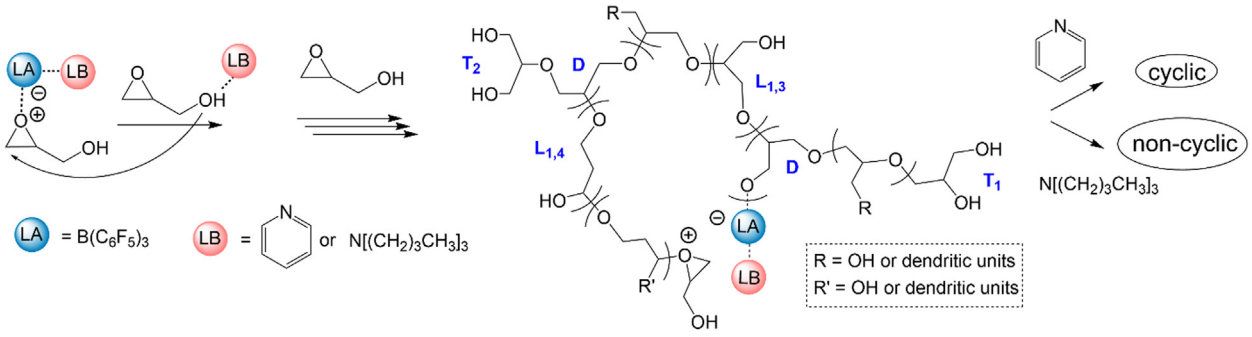

Fig. 45. LP-ZREP of glycidol catalyzed by the Lewis pair $B(C_6F_5)_3$ / tributylamine and $B(C_6F_5)_3$ / pyridine [225].

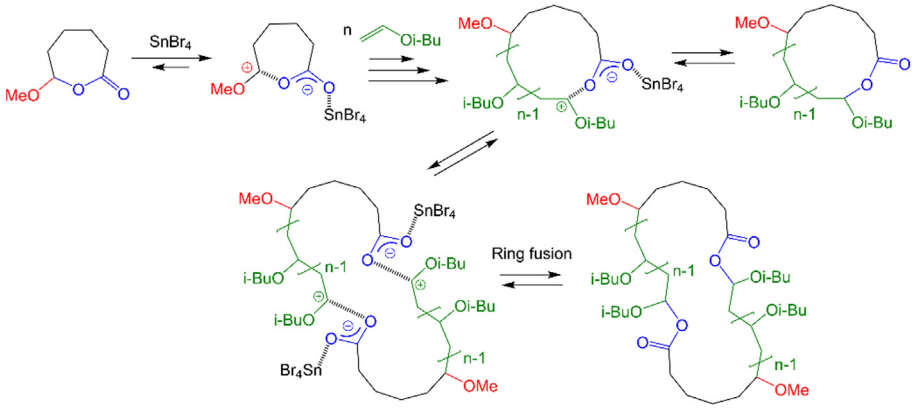

Fig. 46. Lewis acid-assisted ring-expansion cationic polymerization of poly(isobutyl vinyl ether) showing the ring fusion that causes molecular weight increase and multimodal molecular weight distribution [214].

3.5. Cationic ring expansion polymerization (CREP)

In 2013, Sawamoto, Ouchi et al. [214] implemented the Lewis acid-assisted ring-expansion living cationic polymerization initiated by a seven-member cyclic hemiacetal initiator to generate cyclic poly(isobutyl vinyl ether) (Fig. 46). Although this polymerization system shares many characteristics of ZREP, we decided to keep the CREP name as it was originally published by their inventors [214]. In these studies, $SnBr_4$ is best suited as a Lewis acid catalyst to control the reaction by retaining the cyclic structure during propagation and quenching termination. The living character of the polymerization was demonstrated by two main features of the polymerization reaction, the multimodal molecular weight distribution associated to the ring fusion of two or more cyclic living polymers, and the increase of molecular weight and monomer consumption after the addition of fresh monomer at 95% of conversion. The use of cyclic hemiacetals was key in this mechanism, as it allows a controlled initiation and propagation under reversible activation of hemiacetal bond assisted by the Lewis acid. The occurrence of ring fusion was verified by acidolysis, a reaction that cleaves all the hemiacetal units and generates linear chains with monomodal molecular weight distribution. Efforts were made to reduce the ring fusion events, finding that decreasing the initiator concentration [226] and diluting the reaction [215] greatly reduced

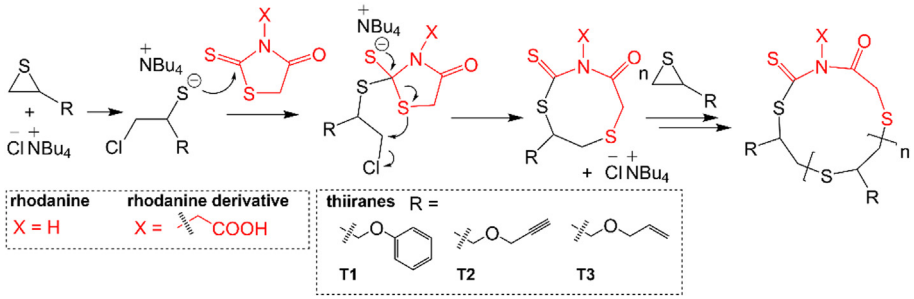

Fig. 47. Rhodanine-mediated AREP of thiiranes catalyzed by tetrabutylammonium chloride [229].

them. Further studies demonstrated that $MgBr_2$ is also suited as a Lewis acid for the generation of cyclic poly(isobutyl vinyl ether) initiated not only by the seven-membered cyclic hemiacetal used in previous studies but by other cyclic hemiacetals that do not work with $SnBr_4$ [227]. A minireview on the CREP of vinyl ethers can be found in reference [28].

Also in 2013, Moore et al. [228] found that the cationic polymerization of *o*-phtalaldehyde with BF_3OEt_2 and other cationic initiators such as triethyloxonium tetrafluoroborate and tin (IV) chloride conducted to the formation of cyclic poly(phthalaldehyde) in high yields and M_n up to 109 kg/mol. Due to the low ceiling temperature of *o*-phtalaldehyde, chain scrambling reactions occur during polymerization leading to high cyclic purity. The linear chains are able to depolymerize whereas the cyclic chains remain stable. A REP model was suggested to explain the kinetic characteristics of this polymerization system and the sudden increase of the molecular weight observed at high conversion, where a ring fusion mechanism was also invoked [216].

3.6. Anionic ring expansion polymerization (AREP)

In 2020, You et al. [229] incorporated new synthetic route to produce cyclic polythioethers based on rhodanine chemistry and AREP. A quaternary onium salt (in this case tetrabutylammonium chloride) catalyzes the ring opening of a thiirane monomer by opening the ring and forming a thiolate (Fig. 47). This anion then attacks the rhodanine forming a cyclic thioester that is able to expand and incorporate more thiirane monomer. This route give the possibility to produce cyclic homopolythioethers and copolythioethers containing reactive functional groups as for example alkynes that are further functionalized to form brush cyclic copolymer. These structures with diameters of about 50 nm were clearly detected by TEM and AFM. Furthermore, the authors demonstrated that thanks to the reaction of rhodanine with aldehydes via Knoevenagel condensation showing nearly quantitative conversion (~99 %), the AREP route allowed the formation of multicyclic structures, either with cyclic units in the backbone or with side cyclic chains.

3.7. Radical ring expansion polymerization (RREP)

Radical polymerization involves a reversible homolytic bond cleavage, propagation and radical recombination. In 2003, Pan et al. [230] used the ability of weak C-S to undergo homolytic cleavage upon ^{60}Co irradiation from a cyclic RAFT initiator containing two dithioesters, which triggers the polymerization of methyl acrylate via RREP mechanism (Fig. 48). Benzyl radical initiates the vinyl polymerization upon irradiation. Then, the generated radical propagating chains terminate by coupling with initial sulfur radical to form a macrocyclic structure. The obtained molecular weights were relatively low, up to 6 kg/mol and $Đ \sim 1.3$. Low temperatures were required to avoid rapid radical diffusion and recombination with other active radicals that could form linear byproducts. By using the generated cyclic poly(methyl acrylate) (PMA) as a macroinitiator, a triblock cyclic copolymer of NIPAAM-b-PMA-NIPAAM was synthesized demonstrating the versatility of this method. In 2014 Advincula et al. [231] designed and synthesized a cyclic dixanthate containing a phenanthroline moiety to be used as RAFT initiator. Then, cyclic poly(*N*-vinylcarbazole)s with M_n up to 33 kg/mol and $Đ \sim 2$ were generated via thermally activated RREP. The authors attributed the broad molecular weight distribution to chain transfer caused by the high temperature used (60 °C in this case).

In 2010, Narumi et al. [232] reported the synthesis of cyclic polystyrene by using a cyclic NMP initiator. They synthesized a cyclic alkoxyamine derivative as NMP initiator that produces active radicals by homolysis of a C-ON bond upon heating. This initiator, however, had solubility problems causing that the polymerization reaction were carried out in uncommon fluoroalcohol solvents. In a second report [233], same group synthesized a more soluble cyclic NMP initiator containing a flexible tetra(oxyethylene) unit for the synthesis of cyclic polystyrene via RREP. These ring structures were visualized by AFM identifying not only the formation of macrocycles but also the generation of linear chains and multimers by ring fusion processes [234].

4. Applications of REP and RC in the synthesis of cyclic biomacromolecules

4.1. Cyclic polypeptides and polypeptoids

Kricherldorf et al. [235] showed in 2006 that initiation of *N*-substituted *N*-carboxylanhydrides (NCA) by amines (pyridine, tertiary amines) conducted to the formation of cyclic polypeptoids. They found that the polymerization of sarcosine *N*-carboxyanhydride with pyridine occurred by forming a zwitterion in the initiation step followed by chain growth via ZROP (Fig. 49) [235]. A large number of studies in this group include the polymerization of *N*-substituted and *N*-unsubstituted NCA, as well as the use of different amines and solvents [236]. A recent review by Kricherldorf and Weidner addresses the details of this and similar polymerization systems [19].

Zhang et al. synthesized cyclic poly(α-peptoid)s by means of NHC- and amidine-mediated ROP of *N*-substituted NCAs (R-NCA, R = butyl and methyl) [237,238]. The first report dates from 2009 [237], where polymerization of butyl-NCA and methyl-NCA with 1,3-bis(2,6-diisopropylphenyl)imidazol-2-ylidene yielded cyclic poly(*N*-substituted glycine)s with M_n up to 27 kg/mol and narrow polydispersity. Mechanistic investigations on butyl-NCA indicated that polymerization occurs through zwitterionic propagating intermediates (Fig. 50), where the solvent and the NHC significantly influence the polymerization rate and the polymer MW control [239].

The propagating species undergo intramolecular rearrangement releasing CO_2 irreversibly. Prior to monomer addition, the zwitteri-

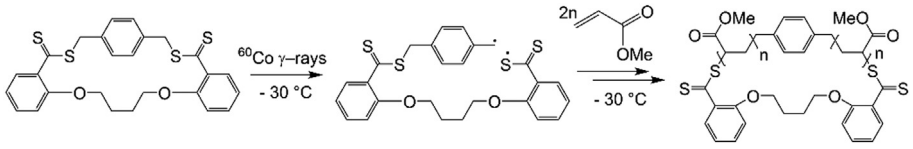

Fig. 48. RAFT-RREP of methyl acrylate initiated by ^{60}Co irradiation [230].

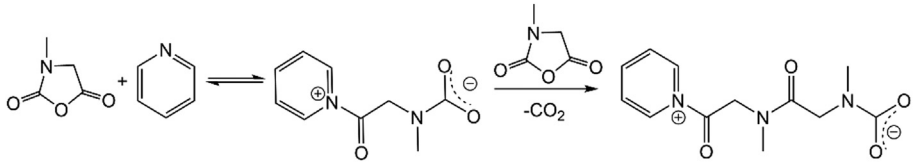

Fig. 49. Zwitterions formed in the polymerization of sarcosine *N*-carboxyanhydride with pyridine [235].

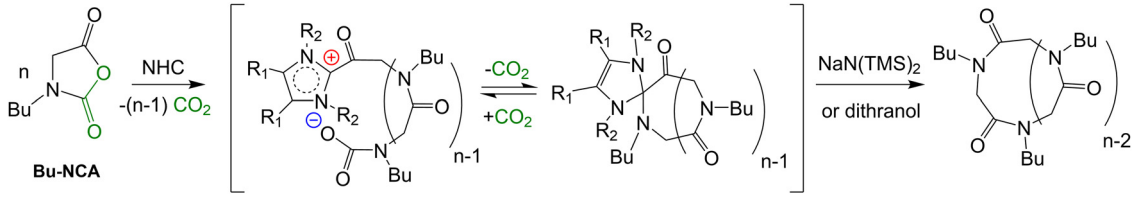

Fig. 50. Synthesis of cyclic poly(α-peptoid)s by NHC-mediated ROP of *N*-substituted *N*-carboxylanhydride (R-NCA) [239].

onic propagating species establish rapid equilibria with the spirocyclic propagating species via reversible decarboxylation. To release the NHC moiety from the polymer chain and generate NHC-free cyclic poly(α-peptoid)s, the polymer has to be treated with $NaN(TMS)_2$ or dithranol [237,239]. In 2016, DBU was investigated as an initiator of butyl-NCA, yielding cyclic poly(*N*-butylglycine) of M_n up to 32 kg/mol [238]. Other cyclic structures based on cyclic poly(α-peptoid)s were generated such as amphiphilic diblock copolymers[240] and brush polymers and copolymers [241]. In 2020, Bonduelle et al. [242] synthesized cyclic poly(α-peptoid)s of M_w up to 8 kg/mol by ZREP of R-NCA (R = methyl, benzyl and carbobenzyloxy-aminobutyl) with lithium bis(trimethylsilyl)amide (LiHMDS). Initiation is assumed to occur by hydrogen abstraction from the R-NCA monomer promoted by the LiHMDS base and subsequent reaction with a second monomer molecule to form active zwitterionic species.

The polymerization of *N*-unsubstituted NCAs with imidazolium hydrogen carbonate (a precursor of a highly reactive NHC upon the release of H_2CO_3 at room temperature [243]) was demonstrated to form cyclic polypeptides with M_n up to 42.5 kg/mol and Đ ~ 1.2 in a controlled manner when the polymerization is performed in the absence of amines [244]. In the presence of amines, linear polypeptides are obtained. The authors attributed to hydrogen bond interactions of amines with NHC to the formation of propagating chains terminated in ω-amino groups that react with further NHC molecules and lead to ROP of the *N*-unsubstituted NCA. In the absence of amines, the free NHC acts as initiator by generating the imidazolium carbamate zwitterionic growing chain. Then, by intramolecular decarboxylation the cyclic polypeptide is finally generated.

RC strategies have been of the great importance in the synthesis of cyclic polypeptides due to the advantage of this method to access to a variety of cyclic structures. As in all RC strategies, the success or failure of this method relies on the ability of the end groups of a linear precursor to become in close proximity before cyclization. Various strategies for directing macrocyclization have been developed and reviewed [245]. Those include internal conformational elements, where chemical modification of the peptide chain is introduced to favor the end proximity (e.g. the introduction of turn-inducing elements into the chain), and external conformational elements (eg. the use of molecular scaffolds). The RC strategies include condensation reactions (e.g. amide bond formation), CuAAC "click" reactions, Ruthenium-based alkene metathesis, and a variety of organic reactions, catalyzed by transition-metals [246], that can be chemoselective [247], and which have been revised in excellent reviews [245,246,248,249].

4.2. Cyclic oligonucleotides

Cyclic RNAs and DNAs are generated by RC of linear precursors *via* chemical and enzymatic protocols. It is usually found in the literature the term "ligation" to refer to the chemical or enzymatic type of reaction in which the two RNA(DNA) ends react. Chemical reactions frequently involve the intramolecular formation of a 3′, 5′-phosphodiester bond, requiring close proximity of the 3′- and 5′-terminus of the linear precursor (Fig. 51a). The reaction catalyzed by BrCN or *N*-(3-dimethylaminopropyl)-N′-ethylcarbodiimide (EDC) leading to a condensation reaction and subsequent formation of a 3'-5' phosphodiester bond is commonly used to form cyclic RNA(DNA) [250,251]. Other methods consist on the modification of the 3′- or 5′-native terminus into amines, azides or alkynes to make use of other chemical reactions such as amidation [252], phosphoramidation [251] and CuAAC "click" reaction [253,254] (Fig. 51b-c).

The particularities in the synthesis of these complex systems, which in many cases involve the protection and deprotection of functional groups, their properties and functions can be found in thematic reviews for cyclic RNAs [9,255–261] and cyclic DNAs [9,259,261,262].

5. Purification methods of macrocycles

Most of the synthetic routes to produce cyclic polymers generates linear byproducts [21,263,264]. Tadpoles can also be formed [209,210]. For that reason, removal of non-cyclic impurities is a key concern for synthetic polymer samples. However, separation of cyclic chains from non-cyclic byproducts is not always a simple task. The most common and practical technique for separat-

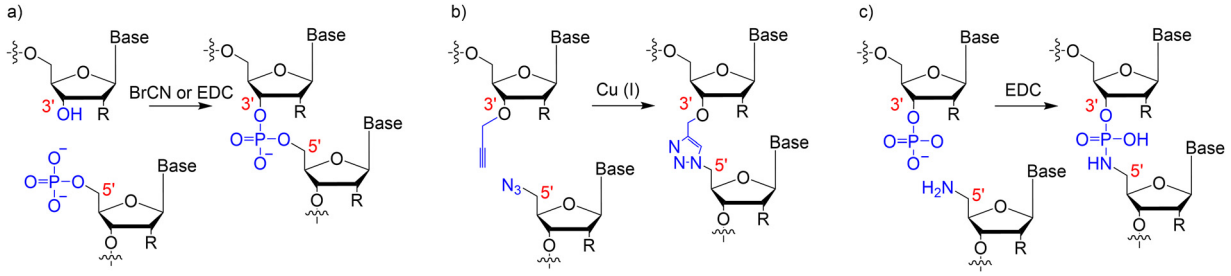

Fig. 51. The formation of (a) phosphodiester, (b) triazole and (c) phosphoramidate bonds by 3'-5' backbone reactions to generate cyclic oligonucleotides.

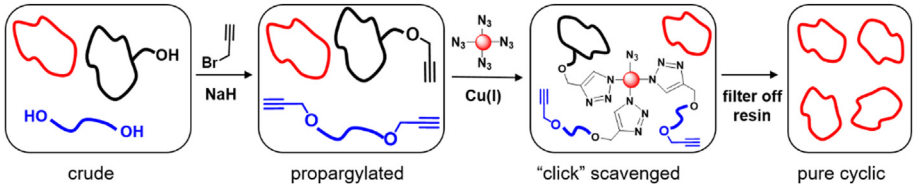

Fig. 52. Purification protocol via "click-scavenging" of cyclic PGPE synthesized by eZREP [210].

ing cyclic from non-cyclic impurities is the preparative GPC, where samples can be fractionated based on the retention times. If the cyclic chains elute at retention times that are long enough compared to the linear ones, a good separation can be achieved. However, in most cases the chromatographic peaks of linear and cyclic chains overlap making difficult the separation and compromising the cyclic purity. In this sense, a recycling preparative GPC, where the sample is reinserted in the columns n^{th} times mimicking a longer separation column, could help in improving separation and therefore in generating samples of high topological purity [54,265,266].

The liquid chromatography at the critical conditions (LCCC) has demonstrated to be a very efficient method to purify macrocycles [267]. Under critical conditions, polymers with the same chemical composition will elute at the same time independently of their molecular weight, whereas polymer chains with the same degree of polymerization but with different chemical compositions (e.g., end-group chemistry) will be separated. However, the determination of the experimental conditions that efficiently separate the distinct topologies can be very tedious since the efficient separation for each polymer type depends on a combination of parameters such as the stationary phase, the mobile phase (usually a solvent mixture) and temperature.

The use of purification methods different from HPLC techniques are also possible and indeed convenient when preparative GPC or LCCC are not available. For example, a multigram-scale method of purification was reported for cyclic PEG of M_n from 2 to 20 kg/mol [130]. This method is based on the oxidation of PEG hydroxyl end groups of linear impurities to carboxyl groups and their further sequestering by using basic ion-exchange resin. Cyclodextrins were also proved to be useful for purifying cyclic PEG chains of M_n of 600 and 900 g/mol from their linear precursors and chain-extended byproducts by using multistep purification protocols [268]. This method is based on the ability of cyclodextrins to form insoluble inclusion complexes with linear PEG chains, which can be separated by centrifugation.

The click "scavenging" is a facile technique that allows the removal of azide- or alkyne- functionalized impurities by click reaction with a solid support followed by filtration [269]. The potential of this technique is that it can be used to purify not only macrocycles generated via CuAAC-ring closure methods but by other cyclization techniques like eZREP. Haque et al. [210] used this technique to eliminate the byproducts generated by eZREP of glycidyl

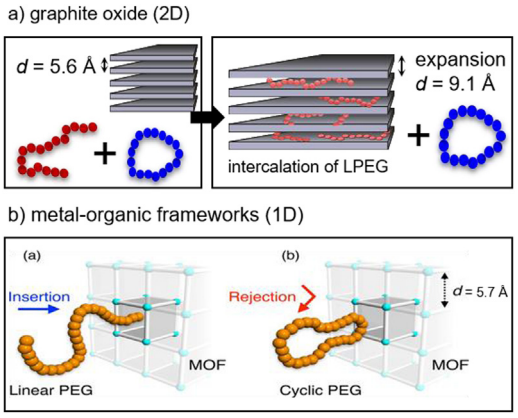

Fig. 53. Separation by selective intercalation of linear PEG into (a) graphite oxide [270,271] and (b) MOFs. Adapted with permission from [274]. Copyright 2021 John Wiley and Sons.

phenyl ether with $B(C_6F_5)_3$ (Fig. 52). In that study, linear and tadpole impurities terminated in hydroxyl groups were functionalized with propargyl bromide to generate alkyne terminated chains. Then, the alkyne-functionalized non-cyclic impurities were CuAAC-click reacted with an azide-modified resin. Finally, the cyclic product was recovered by filtration.

Common silica gel column chromatography has been used in the purification of cyclic polystyrene generated by intramolecular cyclization of α-carboxyl, ω-amino linear precursors [70]. The unreacted material and chain extended byproducts terminated in amine and carboxyl functionalities are able to interact with silica gel and being retained while the cyclic product elutes with a relatively low polar solvent used as mobile phase.

The use of different porous materials to selectively separate cyclic from linear architectures has also been investigated (Fig. 53). In particular, graphite oxide (GO), a layered 2D material, was used in our group as a host to separate linear and cyclic oligomers of PEG [270,271]. The advantages of using GO in architecture-based separation lie on the simplicity of the method and its scalability to the multigram scale. The selectivity is based on the slower rate of intercalation of cyclic oligomers in the interlayer space of graphite oxide (typically of about 5.6 Å in Brodie GO) compared to their linear analogs. This slower intercalation kinetics was also ex-

hibited by larger molecular weight cyclic PEO (with M_n up to 20 g/mol) suggesting that this method, that was initially proved for oligomers, can be extended to higher molecular weight polymers [272]. Upon intercalation of the linear chains, the GO interlayer is expanded to a value of approximately 9.1 Å, where polymers of large molecular weights are irreversibly trapped due to strong H-bonding interactions within the interlayer [273]. Uemura, Hosono, et al. demonstrated that metal-organic frameworks (MOFs) can be used as a filler of preparative liquid chromatographic columns to separate cyclic from linear PEG chains in gram scale yielding high cyclic purity based on the same principle of slower insertion rates of cyclic polymers in porous materials compared to the linear ones [274]. The used MOFs had regular one-dimensional nano-channels with an aperture of $d = 5.7$ Å along the c-axis.

6. Properties of macrocycles

6.1. Physical properties

Due to their unique topology, macrocyclic polymers differ from their linear analogs in terms of physical properties in solution and in the bulk phase. There are excellent reviews that address the structure and dynamics of ring polymers, where comparison between literature data from experiments and simulations can be found [1,275].

Ring polymers present higher T_g values compared to their linear analogs in the medium-low molecular weight range as a consequence of the absence of plasticizing end-groups. This effect disappears at high molecular weights, where the T_g becomes independent of both the molecular weight and the topology as the contribution of the end groups vanishes. The molecular weight dependence of the T_g for rings has been found to decrease or increase with decreasing molecular weight, depending on the polymer type and the ring purity. For instance, macrocyclic poly(dimethylsiloxane) showed increasing T_g values with decreasing molecular weight [276], in agreement with the theoretical model of Di Marzio and Guttman [277]. On the contrary, macrocycles of polystyrene [278], poly(2-vinylpyridine) [278], poly(α-methylstyrene) [278], poly (2-vinylnaphthalene) [278], poly(phenylmethylsiloxanes) [279], and poly(glycidyl phenyl ether) [280] exhibited decreasing T_g values with decreasing molecular weight. It is also known that, for instance, linear impurities decreases the T_g of macrocyclic polystyrene, resulting in a much higher molecular weight dependence of the T_g respect to that in highly pure macrocyclic polystyrene [281]. The presence of salts has been also demonstrated to affect the molecular weight dependence of the T_g as in the case of macrocyclic poly(2-vinylpyridine) where in a first study an increase of the T_g with decreasing molecular weight was found, but latter, by reducing the amounts of LiBr in the sample, the opposite effect was discovered [282].

The melt viscosity of ring polymers is lower than that of linear analogs of identical molecular weights at iso-frictional conditions (at the same distance from the glass transition temperature, T_g). For unentangled chains, the rings exhibit approximately the half of the melt viscosity of linear chains in a range of low molecular weights ($\eta_{linear}/\eta_{rings} \sim 2$) (Fig. 54) [283]. With the appearance of entanglements, the ratio between the melt viscosity of linear chains and rings becomes dependent on the molecular weight, with a possible universal behavior showing a dependence of $\eta_{linear}/\eta_{rings} \sim Z^{1.2}$. The continuous and dashed blue lines of Fig. 54 exhibit predicted slopes according to the pure reptation model of linear and loopy globule model of rings (slope 1.3) and tube length fluctuations model of linear melts and lattice animal model for melts of rings, respectively (slope 1.9) [283]. These discrepancies remain as an open question [1,284].

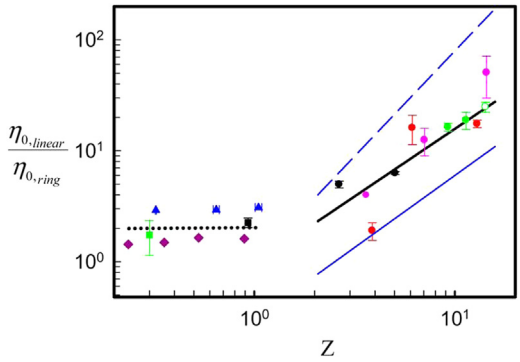

Fig. 54. Ratio of the zero shear viscosities of linear and ring polymers as a function of the number of entanglements (Z). The black dotted horizontal line sets the theoretical value of 2 in the low-Z region. The black continuous line is the best fit of the experimental data (slope of 1.2 ± 0.3). The continuous and dashed blue lines have slopes of 1.3 and 1.9, respectively (see text for details). Black circles: PEO experimental data [283]. Red circles: PI experimental data [283]. Green open circle: PS experimental data point [283]. Green filled circles: PS experimental data [284]. Black square: PEO experimental data point [285]. Green square: PS experimental data point [283,286]. Purple diamonds: PEO experimental data [287]. Blue triangles: polyethylene (PE) atomistic simulations [288]. Pink circles: MD simulations on coarse-grained bead–spring chains [289]. Adapted with permission from [283]. Copyright 2013 American Chemical Society.

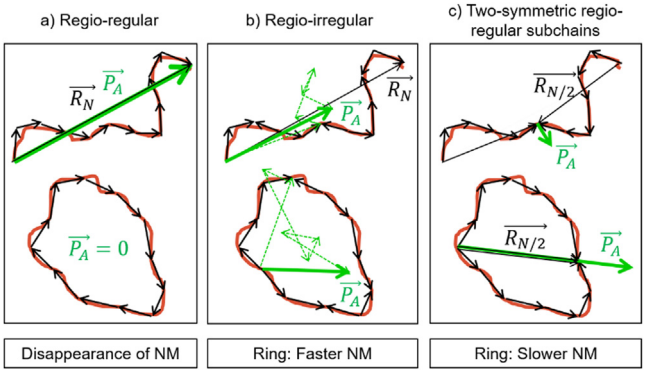

Fig. 55. Dipolar microstructures of polymer chains with different topologies and regicities [54,90,280,290].

The dipolar microstructure is a property related to the orientation of dipole moments along a polymer chain, which is dependent on how asymmetric monomers are oriented (i.e., regio-order). The control over the dipolar microstructure offers the possibility to monitor single-chain behavior in an electric field thus providing important structural and dynamical information. Broadband dielectric spectroscopy (BDS) is a suitable technique for these purposes [290]. According to the classification of Stockmayer [291], type-A polymers are those that present fix dipolar moments of the monomeric unit (μ_p) parallel to the main chain backbone. In this case, there is a dipolar moment associated to the main chain $\vec{P_A} = \mu_p \vec{R_N}$, where $\vec{R_N}$ is the "end-to-end" vector of the chain (Fig. 55). Thus, the end-to-end vector fluctuations results in a dielectric relaxation usually referred to as normal mode (NM) relaxation. Cyclic polymers containing all monomers oriented in the same direction (i.e., regio-regular chains) present a zero dipole moment associated to the main chain ($\vec{P_A} = 0$), whereas cyclic chains composed by regio-irregular monomer units, or two regio-regular subchains, will exhibit a non-zero resultant dipole moment ($\vec{P_A} \neq 0$) (Fig. 55). Cyclic polymers characterized by $\vec{P_A} = 0$ do not present NM. The NM relaxation is found in linear polymer chains. Therefore, the cancellation of the dielectric NM mode in a cyclic polymer synthesized from a linear precursor can be used as a signa-

ture of cyclization and cyclic purity. This hypothesis was proved in a BDS study in our group of cyclic poly(glycidyl phenyl ether) samples synthesized by CuAAC ring-closure of linear regio-regular precursors terminated in azide and alkyne groups [90]. In a further study, cyclic poly(glycidyl phenyl ether) samples were generated *via* Glaser-coupling ring-closure of linear precursors terminated in two alkyne groups, where the chain was composed of two symmetric regio-regular subchains with an opposite dipole moment orientation [54]. The macrocycles displayed a dielectric NM relaxation that reflected the fluctuations of the ring diameter. This important characteristic allowed us to evaluate the macrocyclic chain dynamics by BDS resulting in a dipole relaxation of the ring diameter 1.6 times slower compared to the analogous relaxation in the inverted-dipole linear precursor.

The crystallization kinetics and the morphology of crystals are notably affected by the topology. Tezuka et al. [292] found that cyclic PTHF of M_n = 5.1 kg/mol presented slower spherulitic growth rates than the linear analog by polarized light optical microscopy (PLOM). They also reported that the melting temperature of cyclic PTHF was lower than its linear counterpart and a distinct spherulite morphology. They attributed those findings to differences in the conformational entropy of the chains in the molten state, an adsorption mechanism of the crystal growth front during the secondary nucleation process, or differences in chain folding surface energy. Later, Müller et al. [293] found by PLOM that cyclic PCLs of 2-7 kg/mol generated by an RC strategy exhibited much faster spherulitic growth rates than linear analogs, contrarily to previous results. They also found by isothermal DSC that the overall crystallization rate, which includes contributions from both primary nucleation and crystal growth, was faster for cyclic PCL, which also required higher crystallization temperatures to crystallize. These results were also confirmed in cyclic PCLs with molecular weights above 75 kg/mol generated by nZREP [197]. The faster crystallization exhibited by cyclic PCLs were explained on the basis of their lower melt viscosity, which causes a greater molecular diffusion with respect to that in the linear chains [293]. Threading effects introduced by the presence of linear chains in cyclic polymer samples have demonstrated that reduce even more the isothermal crystallization rates in cyclic PLCs, reduce the crystallization and melting temperatures and the degree of crystallinity due to an increase of entanglement density and reduction of molecular diffusion [294]. Floudas et al. [295] studied the crystallization kinetics of cyclic PEO within the M_n range between 2 and 20 kg/mol. They found faster spherulitic growth rates for the cyclic chains compared to the linear ones, as expected from their faster diffusion and more compact structure, and a distinct lamellar thickening process by doubling of the long period.

Thermostability of bulk cyclic polymers is higher than that of their respective lineal analogues, with some data reported in the literature [164,165,168,228]. The differences in the maximum decomposition temperature (found in the 1st derivative of TGA curves) can be up to the order of hundred degrees, as in the case of poly(γ-butyrolactone)s synthesized with $La[N(SiMe_3)_2]_3$ [165]. Interestingly, samples containing mixtures of the cyclic and linear products exhibited two degradation steps with maximum peaks of the 1st derivative curves at the corresponding degradation temperatures of topologically pure cyclic and linear polymers.

6.2. Biological properties

Synthetic cyclic polymers have been tested in relation to their blood circulation time and biodistribution in mice. Szoka et al. demonstrated that cyclic PEGylated PCL and cyclic PEGylated PAA comb polymers with molecular weights above the renal filtration threshold exhibited longer circulation times than their linear analogues [296,297]. The explanation to these results seem to be related to the differences in the reptation mechanism through the nanopores between the cyclic and linear chains. Snake-like motions are possible for the diffusion of linear chains but not for cyclic chains [1,298]. Instead, cyclic chains must diffuse by amoeba-like motions. These appealing results provide a window of opportunity for cyclic polymers as drug carriers or imaging agents.

Biological functions of cyclic oligonucleotides have been studied extensively over the years, mainly after the first imaging observations of cyclic DNA strands [299–302]. To cite some of these functions: cyclic oligonucleotides can act as efficient hosts for molecular recognition; circular DNA oligomers can bind strongly and sequence specifically to single strands of DNA and RNA by forming triple helical complexes; cyclic RNAs are less prone to degradation in cells than linear RNAs since they are protected from exoribonuclease activity; and cyclic RNAs can function as a sponge for a particular miniRNA altering gene expression [303].

7. Applications of macrocycles

The use of macrocyclic polymers in industrial applications is mainly limited by the amounts of product that can be generated. However, lab-scale experiments have demonstrated the great potential of cyclic polymers in the fields of biomedicine [302] and advanced (bio)materials [3,6,20,23]. Other less explored fields for cyclic polymers are packaging [304], semiconductors [305,306], dielectric capacitors [307], circularly-polarized luminescence [308]and artificial light harvesting materials [309]. Micelles formed from cyclic block copolymers containing hydrophilic and hydrophobic blocks have been explored as drug carriers due to their topology-enhanced performance (micelle stability, drug load capacity and degradation rate). Their structure-property relationship has been reviewed elsewhere [6,20,23,310]. Other cyclic structures such as the “sunflower” copolymers composed by a macrocycle core decorated with brushes or “petals” have also been applied for targeted drug delivery systems [311].

Surface modification with ring polymers is a recent attractive subject given the possibilities of the rings to lubricate the surfaces and prevent the adhesion of proteins more efficiently than linear polymers [312–318]. In this field, the work developed by Benettiś group has been crucial in demonstrating the superior surface properties of macrocyclic poly(2-alkyl-2-oxazoline)s (C-PAOx)s grafted onto metal oxide surfaces (TiO_2 and Fe_3O_4) [313–317], cartilage [312] and poly(glycidyl methacrylate) [318] compared to linear analogs. The enhanced properties of C-PAOx-grafted surfaces, which include friction, lubrication and antifouling when exposed to full human serum, fibrinogen and albumin, are correlated with the absence of chain ends preventing interchain entanglements and increased grafting density compared to linear brushes. Fig. 56a-c show an example of superlubrication properties of a TiO_2 surface modified with cyclic poly(2-ethyl-2-oxazoline) (C-PEOXA).

In our group, we have studied the behavior of flat gold surfaces and gold nanoparticles (AuNPs) chemically grafted with cyclic PEO (CPEO) brushes (Fig. 56d-e). The surface wettability presented clear topological effects exhibiting higher contact angles the surfaces modified with CPEO than with the linear analog (LPEO), a result that is likely attributed to the lack of chain ends migrating to the surface [175] and the more rigid structure of the loops compared to the linear ones [319]. Moreover, we demonstrated that CPEO can be used as an alternative of classical LPEG ligands for AuNP stabilization showing different colloidal behavior when subjected to external stimuli like temperature and salt in aqueous solutions [4]. The differences found between CPEO brushes and their linear analogs can be attributed to the fact that cyclic brushes have to accommodate in less space near the surface than the linear chains, thus, causing increased concentration of polymer segments near the surface. As a result, the cyclic chains are forced

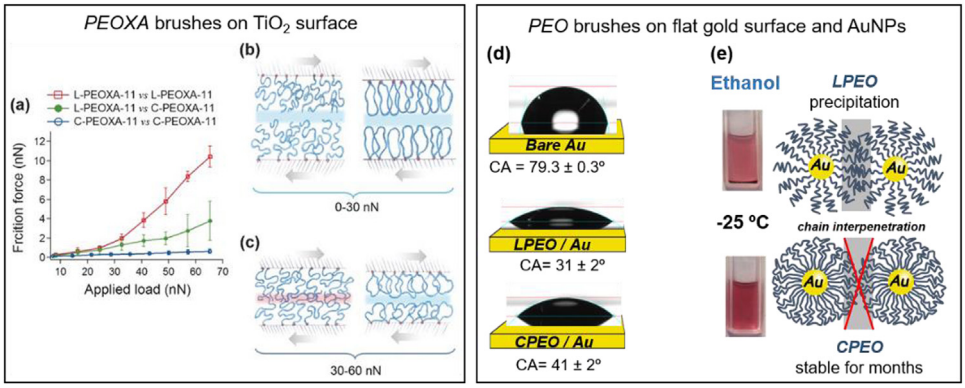

Fig. 56. Left: (a) Friction-*vs*.-applied load (FL) profiles recorded by colloidal-probe lateral force microscopy shearing PEOXA brush-functionalized colloids against PEOXA brushes on flat substrates. (b) At relatively low applied loads both linear-versus-linear and cyclic-versus-cyclic brush tribo-pairs show low friction; (c) above 30 nN of applied force, interdigitation between two linear brush-bearing surfaces causes a steady increase of friction, whereas cyclic brushes do not interact due to the absence of chain ends and maintain low friction. Adapted with permission from [314]. Copyright 2016 John Wiley and Sons. Right: (d) Contact angle (CA) measurements with water droplets of flat gold surface modified with LPEO and CPEO. (e) Colloidal stability at -25 °C in ethanol of AuNPs modified with LPEO and CPEO.

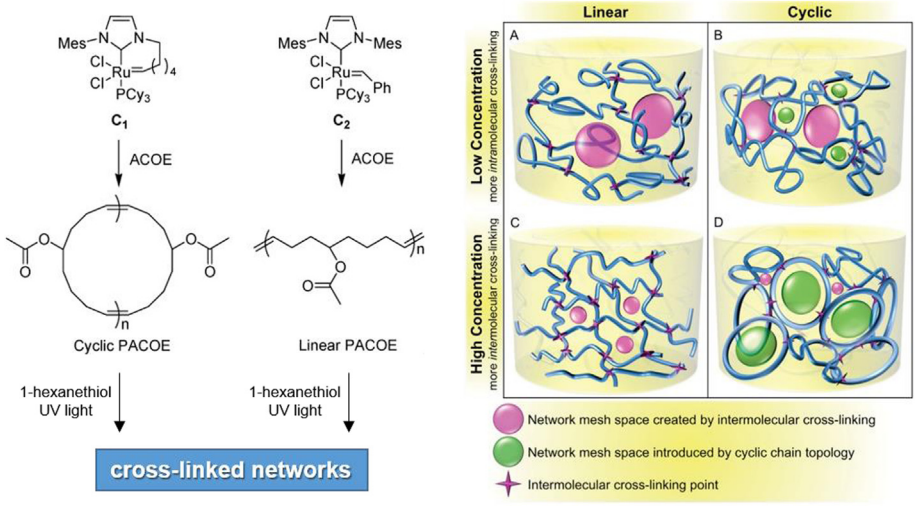

Fig. 57. Left: Synthesis of cyclic and linear PACOE to form cross-linked networks upon the addition of 1-hexanediol and UV irradiation. Right: Ideal network structural units are shown to highlight the most important features in each system. The top two systems correspond to low C_0 for linear PACOE (A) and cyclic PACOE (B), whereas the bottom two panels correspond to high C_0 for linear PACOE (C) and cyclic PACOE (D).Adapted with permission from [5]. Copyright 2011 American Chemical Society.

to stretch more than the linear chains. In ethanol, AuNPs modified with LPEO suffer from reversible phase separation upon temperature drop over the course of few hours [320]. However, the use of a polymer brush with cyclic topology as stabilizer prevents sedimentation, ensuring the colloidal stability in ethanol at -25 °C for, at least, several months. We postulated that temperature-driven collapse of chain brushes promotes the interpenetration of linear chains, causing progressive AuNPs sedimentation, a process that is unfavorable for cyclic polymer brushes whose topology prevents chain interpenetration.

A study on CPEO chains physisorbed on AuNPs (containing original sodium citrate) also demonstrated different stability compared with physisorbed and chemisorbed linear PEO (LPEO) against heating, freezing and salt addition [321]. In those cases, the cyclic topology provided higher colloidal stability, likely due to a stronger surface adsorption of cycles, as suggested by the authors [321], based on previous works on the adsorption of cyclic PEO on silica nanoparticles of 25 nm of diameter [322] and other experimental and computational studies.

Polymer networks based on cyclic polymers are another class of materials with potential applications in drug delivery systems and smart materials [323]. These were first developed in 2011 by Tew et al. [5], who synthesized cyclic poly(5-acetoxy-1-cyclooctene) (C-PACOE) with M_n >200 kg/mol using REMP (Fig. 57). The double bonds of the chain were subsequently crosslinked with 1-hexanethiol under UV irradiation. With increasing initial polymer concentration (C_0), the gel fraction, swelling ratio and modulus increased simultaneously for cyclic polymer-based gels in contrast to linear analogs, which showed an inverse relationship of gel fraction and modulus (increasing values) with the swelling ratio (decreasing value). These differences can be associated to dissimilarities in the intermolecular and intramolecular crosslinks between the cyclic and linear topologies at low and high C_0. The mesh size of a crosslinked network formed by linear chains is classically reduced at higher C_0 due to an increase of the intermolecular reactions. However, the mesh size of the cyclic polymers remains higher at higher C_0 since the intermolecular reactions favors the expansion of the ring introducing more space in the network. The increased modulus in cyclic polymer-based gels respect to the linear analog was further confirmed in physically crosslinked networks based on cyclic diblock copolypeptoids composed by poly(*N*-methyl-glycine)-b-poly(*N*-decyl-glycine) [324]. The gels consist of a thermo-reversible network formed by crystalline fibrils cross-linked by dynamic entanglements. Other example of cyclic polymer-based networks with increased modulus is that generated by cyclic chains containing azobenzene moieties

with M_n of 10-22 kg/mol chemically crosslinked by using boronic acid/diol chemistry [325].

Cyclic peptides have been found important applications as therapeutic agents with antimicrobial, anti-inflammatory, antitumor, antiviral, and antifungal activities [248]. Some examples of cyclic peptide antiobiotics include the gramicidin S, daptomycin, cyclosporine, teixobactin, and malacidin [248]. Non-peptidic main-chain formed by a flexible thioether backbone was found to display antimicrobial activity [326]. The macrocyclic oligothioetheramides (oligoTEAs) were synthesized by an acid-catalyzed cascade reaction allowing the incorporation of guanidinum functionalities as pendant groups. The antimicrobial activity was studied on Gram-negative (*Escherichia coli*) and Gram-positive (*Bacillus subtilis*) bacteria finding higher activity against the latter. In general, the macrocycles with smaller ring sized performed better than their larger-ring analogues. Moreover, by substituting specific groups in the backbone (more hydrophilic or more hydrophobic) a better control over the selectivity was achieved. A comparison of antimicrobial activity between a medium-sized macrocycle and its linear analog found higher activity in the macrocycle but similar selectivity and activity in small sized macrocycles. These results highlight the importance of the overall macromolecular structure (backbone and side chain composition, topology and sequence) to achieve desired results in biological activity as well as highlight the difficulties encountered in design/synthesis/property relationships.

8. Conclusions

Today, there exist a vast collection of synthetic methods for producing a variety of cyclic polymers. This collection has been expanded over the years, in part associated with the evolution of innovative advances in organic synthesis and catalysis, creating a variety of pathways to cyclization of preformed chains through ring-closure strategies and ring-expansion polymerization of various monomers. The advent of "click" chemistry and the sophistication of coupling techniques greatly increased the possibility of ring formation by reaction of a wide variety of functional groups. In particular, metal-free and light-assisted techniques have provided significant advantages in this field. However, the progress of cyclic polymers is still limited by some milestones that continue to be the most complicated to address in the synthesis of these structures. These are large-scale production, molecular weight scalability and topological purity. The potential utility of cyclic polymers in the biomedical and pharmacological fields, surface chemistry, and plastic and electronic industry, represents an opportunity to design, develop and implement synthesis and purification protocols that overcome these problems. Undoubtedly, future efforts should focus on simple production methods, capable of producing well-defined cyclic polymers with high mass recovery.

Data availability

No data was used for the research described in the article.

Declaration of Competing Interest

The authors declare that they have no known competing financial interests or personal relationships that could have appeared to influence the work reported in this paper.

Acknowledgments

We gratefully acknowledge the grants PID2021-123438NB-I00, funded by MCIN/AEI/10.13039/501100011033 and “ERDF A way of making Europe”; IT-1566-22 and PIBA 2021_1_0034, funded by the Basque Government; and RED 2021:ID44, funded by Diputación Foral de Guipúzcoa.

References

[1] Richter D, Gooßen S, Wischnewski A. Celebrating soft matter's 10th anniversary: topology matters: structure and dynamics of ring polymers. Soft Matter 2015;11:8535–49.
[2] Tezuka Y. Topological polymer chemistry. In: Progress of Cyclic Polymers in Syntheses, Properties and Functions. Word Scientific Publishing Co. Pte. Ltd.; 2013. p. 352.
[3] Romio M, Trachsel L, Morgese G, Ramakrishna SN, Spencer ND, Benetti EM. Topological polymer chemistry enters materials science: expanding the applicability of cyclic polymers. ACS Macro Lett 2020;9:1024–33.
[4] Aboudzadeh MA, Iturrospe A, Arbe A, Grzelczak M, Barroso-Bujans F. Cyclic polyethylene glycol as nanoparticle surface ligand. ACS Macro Lett 2020;9:1604–10.
[5] Zhang K, Lackey MA, Cui J, Tew GN. Gels based on cyclic polymers. J Am Chem Soc 2011;133:4140–8.
[6] Golba B, Benetti EM, De Geest BG. Biomaterials applications of cyclic polymers. Biomaterials 2021;267:120468.
[7] Josse T, De Winter J, Gerbaux P, Coulembier O. Cyclic polymers by ring-closure strategies. Angew Chem Int Ed 2016;55:13944–58.
[8] Beckham HW. Ring polymers: effective isolation and unique properties. In: Complex Macromolecular Architectures. John Wiley & Sons (Asia) Pte Ltd; 2011. p. 791–821.
[9] Semlyen JA. Cyclic Polymers. New York, Boston, Dordrecht, London, Moscow: Kluwer Academic Publishers; 2002. p. 790.
[10] Jacobson H, Beckmann CO, Stockmayer WH. Intramolecular reaction in polycondensations. II. Ring-chain equilibrium in polydecamethylene adipate. J Chem Phys 1950;18:1607–12.
[11] Jacobson H, Stockmayer WH. Intramolecular reaction in polycondensations. I. The theory of linear systems. J Chem Phys 1950;18:1600–6.
[12] Brown JF, Slusarczuk GMJ. Macrocyclic polydimethylsiloxanes. J Am Chem Soc 1965;87:931–2.
[13] Dodgson K, Semlyen JA. Studies of cyclic and linear poly(dimethyl siloxanes): 1. Limiting viscosity number-molecular weight relationships. Polymer 1977;18:1265–8.
[14] Kricheldorf HR. Macrocycles. 21. Role of ring−ring equilibria in thermodynamically controlled polycondensations. Macromolecules 2003;36:2302–8.
[15] Kricheldorf HR. Cyclic polymers: Synthetic strategies and physical properties. J Polym Sci A: Polym Chem 2010;48:251–84.
[16] Kricheldorf H. The role of cyclization and a new theory of polycondensation. In: Polycondensation: History and New Results. Berlin, Heidelberg: Springer Berlin Heidelberg; 2014. p. 95–116.
[17] Lang M, Kumar KS. Simple and general approach for reversible condensation polymerization with cyclization. Macromolecules 2021;54:7021–35.
[18] MorattiComment on “Macrocycles 21. Role of ring−ring equilibria in thermodynamically controlled polycondensations. Macromolecules 2005;38:1520–2.
[19] Kricheldorf HR, Weidner SM. The ring-opening polymerization–polycondensation (ROPPOC) approach to cyclic polymers. Macromol Rapid Commun 2020;41:2000152.
[20] Haque FM, Grayson SM. The synthesis, properties and potential applications of cyclic polymers. Nat Chem 2020;12:433–44.
[21] Laurent BA, Grayson SM. Synthetic approaches for the preparation of cyclic polymers. Chem Soc Rev 2009;38:2202–13.
[22] Wang T-W, Golder MR. Advancing macromolecular hoop construction: recent developments in synthetic cyclic polymer chemistry. Polym Chem 2021;12:958–69.
[23] Liénard R, De Winter J, Coulembier O. Cyclic polymers: advances in their synthesis, properties, and biomedical applications. J Polym Sci 2020;58:1481–502.
[24] Jia Z, Monteiro MJ. Cyclic polymers: methods and strategies. J Polym Sci A: Polym Chem 2012;50:2085–97.
[25] Brown HA, Waymouth RM. Zwitterionic ring-opening polymerization for the synthesis of high molecular weight cyclic polymers. Acc Chem Res 2013;46:2585–96.
[26] Tu X-Y, Liu M-Z, Wei H. Recent progress on cyclic polymers: synthesis, bioproperties, and biomedical applications. J Polym Sci A: Polym Chem 2016;54:1447–58.
[27] Chang YA, Waymouth RM. Recent progress on the synthesis of cyclic polymers via ring-expansion strategies. J Polym Sci A: Polym Chem 2017;55:2892–902.
[28] Ouchi M, Kammiyada H, Sawamoto M. Ring-expansion cationic polymerization of vinyl ethers. Polym Chem 2017;8:4970–7.
[29] Yang PB, Davidson MG, Edler KJ, Brown S. Synthesis, properties, and applications of bio-based cyclic aliphatic polyesters. Biomacromolecules 2021;22:3649–67.
[30] Edwards JP, Wolf WJ, Grubbs RH. The synthesis of cyclic polymers by olefin metathesis: achievements and challenges. J Polym Sci A: Polym Chem 2019;57:228–42.
[31] Grayson SM, Getzler Y, Zhang D. Special issue ‘cyclic polymers: new developments. React Funct Polym 2014;80:1–108.
[32] Jia Z, Monteiro MJ. Synthesis of cyclic polymers via ring closure. In: Percec V, editor. Hierarchical Macromolecular Structures: 60 Years after the Staudinger Nobel Prize II. Cham: Springer International Publishing; 2013. p. 295–327.
[33] Deffieux A, Schappacher M. 6.02 - Synthesis and properties of macrocyclic polymers. In: Matyjaszewski K, Möller M, editors. Polymer Science: A Comprehensive Reference. Amsterdam: Elsevier; 2012. p. 5–28.

[34] Tezuka Y. Topological Polymer Chemistry: Concepts and Practices. Springer SingaporeXI; 2022. p. 436.
[35] Ruggli P. Über einen Ring mit dreifacher Bindung. Justus Liebigs Annalen der Chemie 1912;392:92–100.
[36] Ziegler K, Eberle H, Ohlinger H. Über vielgliedrige Ringsysteme. I. Die präparativ ergiebige Synthese der Polymethylenketone mit mehr als 6 Ringgliedern. Justus Liebigs Annalen der Chemie 1933;504:94–130.
[37] Laurent BA, Grayson SM. An efficient route to well-defined macrocyclic polymers via "click" cyclization. J Am Chem Soc 2006;128:4238–9.
[38] Lonsdale DE, Bell CA, Monteiro MJ. Strategy for rapid and high-purity monocyclic polymers by CuAAC "click" reactions. Macromolecules 2010;43:3331–9.
[39] Tezuka Y, Komiya R. Metathesis polymer cyclization with telechelic poly(THF) having allyl groups. Macromolecules 2002;35:8667–9.
[40] Shotaro H, Kaoru A, Yasuyuki T. An efficient route to cyclic polymers by ATRP–RCM process. Chem Lett 2007;36:982–3.
[41] Quirk RP, Wang S-F, Foster MD, Wesdemiotis C, Yol AM. Synthesis of cyclic polystyrenes using living anionic polymerization and metathesis ring-closure. Macromolecules 2011;44:7538–45.
[42] Xie M, Shi J, Ding L, Li J, Han H, Zhang Y. Cyclic poly(ε-caprolactone) synthesized by combination of ring-opening polymerization with ring-closing metathesis, ring closing enyne metathesis, or "click" reaction. J Polym Sci A: Polym Chem 2009;47:3022–33.
[43] Ding L, Lu R, An J, Zheng X, Qiu J. Cyclic polyphosphoesters synthesized by acyclic diene metathesis polymerization and ring closing metathesis. React Funct Polym 2013;73:1242–8.
[44] Whittaker MR, Goh Y-K, Gemici H, Legge TM, Perrier S, Monteiro MJ. Synthesis of monocyclic and linear polystyrene using the reversible coupling/cleavage of thiol/disulfide groups. Macromolecules 2006;39:9028–34.
[45] Hakobyan K, McErlean CSP, Müllner M. RAFT without an "R-Group": from asymmetric homo-telechelics to multiblock step-growth and cyclic block copolymers. Macromolecules 2021;54:7732–42.
[46] Ali MW, Muhammad Z, Jia Q, Li L, Saleem M, Siddiq M, et al. Synthesis of cyclic poly(2-ethyl-2-oxazoline) with a degradable disulfide bond. Polym Chem 2020;11:4164–71.
[47] Chen C-W, Cheng C-C, Dai SA. Reactive macrocyclic ether−urethane carbodiimide (MC−CDI): synthesis, reaction, and ring-opening polymerization (ROP). Macromolecules 2007;40:8139–41.
[48] Glaser C. Beiträge zur Kenntniss des Acetenylbenzols. Berichte der deutschen chemischen Gesellschaft 1869;2:422–4.
[49] Hay AS. Oxidative coupling of acetylenes. II1. J Org Chem 1962;27:3320–1.
[50] Jover J, Spuhler P, Zhao L, McArdle C, Maseras F. Toward a mechanistic understanding of oxidative homocoupling: the Glaser–Hay reaction. Catal Sci Technol 2014;4:4200–9.
[51] Leophairatana P, Samanta S, De Silva CC, Koberstein JT. Preventing alkyne–alkyne (i.e., glaser) coupling associated with the ATRP synthesis of alkyne-functional polymers/macromonomers and for alkynes under click (i.e., CuAAC) reaction conditions. J Am Chem Soc 2017;139:3756–66.
[52] Zhang Y, Wang G, Huang J. Synthesis of macrocyclic poly(ethylene oxide) and polystyrene via glaser coupling reaction. Macromolecules 2010;43:10343–7.
[53] Shen H, Wang G. A versatile flash cyclization technique assisted by microreactor. Polym Chem 2017;8:5554–60.
[54] Ochs J, Alegría A, González de San Román E, Grayson SM, Barroso-Bujans F. Synthesis of macrocyclic poly(glycidyl phenyl ether) with an inverted-dipole microstructure via ring closure of two-arm linear precursors obtained by initiation with t-BuP4/Water. Macromolecules 2020;53:10005–14.
[55] McKeown GR, Fang Y, Obhi NK, Manion JG, Perepichka DF, Seferos DS. Synthesis of macrocyclic poly(3-hexylthiophene) and poly(3-heptylselenophene) by alkyne homocoupling. ACS Macro Lett 2016;5:1075–9.
[56] Voter AF, Tillman ES. An easy and efficient route to macrocyclic polymers via intramolecular radical−radical coupling of chain ends. Macromolecules 2010;43:10304–10.
[57] Voter AF, Tillman ES, Findeis PM, Radzinski SC. Synthesis of macrocyclic polymers formed via intramolecular radical trap-assisted atom transfer radical coupling. ACS Macro Lett 2012;1:1066–70.
[58] Wang S, Zhang K, Chen Y, Xi F. Isomeric dicyclic polymers via atom transfer radical polymerization and atom transfer radical coupling cyclization. Macromolecules 2014;47:1993–8.
[59] Schappacher M, Deffieux A. Reversible switching between linear and ring polystyrenes bearing porphyrin end groups. J Am Chem Soc 2011;133:1630–3.
[60] Delbosc N, De Winter J, Moins S, Persoons A, Dubois P, Coulembier O. Macrocyclic P3HT obtained by intramolecular McMurry coupling of linear bis-aldehyde polymer: a direct comparison with linear homologue. Macromolecules 2017;50:1939–49.
[61] Ji Z, Li Y, Ding Y, Chen G, Jiang M. A fixable supramolecular cyclic polymer based on the cucurbit[8]uril-stabilized π–π interaction. Polym Chem 2015;6:6880–4.
[62] Wang H, Zhang L, Liu B, Han B, Duan Z, Qi C, et al. Synthesis of high molecular weight cyclic poly(ε-caprolactone)s of variable ring size based on a light-induced ring-closure approach. Macromol Rapid Commun 2015;36:1646–50.
[63] Yamamoto T, Yagyu S, Tezuka Y. Light- and heat-triggered reversible linear–cyclic topological conversion of telechelic polymers with anthryl end groups. J Am Chem Soc 2016;138:3904–11.
[64] Wu Z, Zhang H, Liu C, Hong C. Phototunable cloud point temperatures stemming from cyclic topology: synthesis and thermal phase transition behavior of cyclic poly(N-acryloylsarcosine methyl ester). Macromol Rapid Commun 2021;42:2100136.
[65] Xue Y, Jiang S, Zhong H, Chen Z, Wang F. Photo-induced polymer cyclization via supramolecular confinement of cyanostilbenes. Angew Chem Int Ed 2022;61:e202110766.
[66] Schappacher M, Deffieux A. Synthesis of macrocyclic poly(2-chloroethyl vinyl ether)s. Makromol Chem, Rapid Commun 1991;12:447–53.
[67] Rique-Lurbet L, Schappacher M, Deffieux A. A new strategy for the synthesis of cyclic polystyrenes: principle and application. Macromolecules 1994;27:6318–24.
[68] Schappacher M, Deffieux A. α-Acetal-ω-bis(hydroxymethyl) heterodifunctional polystyrene: synthesis, characterization, and investigation of intramolecular end-to-end ring closure. Macromolecules 2001;34:5827–32.
[69] Kubo M, Hayashi T, Kobayashi H, Tsuboi K, Itoh T. Synthesis of α-carboxyl, ω-amino heterodifunctional polystyrene and its intramolecular cyclization. Macromolecules 1997;30:2805–7.
[70] Kubo M, Takeuchi H, Ohara T, Itoh T, Nagahata R. Synthesis of a well-defined cyclic polystyrene via α-carboxyl, ω-amino heterodifunctional polystyrene. J Polym Sci A: Polym Chem 1999;37:2027–33.
[71] Lepoittevin B, Perrot X, Masure M, Hemery P. New route to synthesis of cyclic polystyrenes using controlled free radical polymerization. Macromolecules 2001;34:425–9.
[72] Kolb HC, Finn MG, Sharpless KB. Click chemistry: diverse chemical function from a few good reactions. Angew Chem Int Ed 2001;40:2004–21.
[73] Huisgen R. 1,3-Dipolar cycloadditions. Past and future. Angew Chem Int Ed 1963;2:565–98.
[74] Rostovtsev VV, Green LG, Fokin VV, Sharpless KB. A stepwise huisgen cycloaddition process: copper(I)-catalyzed regioselective "ligation" of azides and terminal alkynes. Angew Chem Int Ed 2002;41:2596–9.
[75] Tornøe CW, Christensen C, Meldal M. Peptidotriazoles on solid phase: [1,2,3]-triazoles by regiospecific copper(I)-catalyzed 1,3-dipolar cycloadditions of terminal alkynes to azides. J Org Chem 2002;67:3057–64.
[76] Neumann S, Biewend M, Rana S, Binder WH. The CuAAC: principles, homogeneous and heterogeneous catalysts, and novel developments and applications. Macromol Rapid Commun 2020;41:1900359.
[77] Binder WH, Sachsenhofer R. 'Click' chemistry in polymer and material science: an update. Macromol Rapid Commun 2008;29:952–81.
[78] Xu J, Ye J, Liu S. Synthesis of well-defined cyclic poly(N-isopropylacrylamide) via click chemistry and its unique thermal phase transition behavior. Macromolecules 2007;40:9103–10.
[79] Chen F, Liu G, Zhang G. Synthesis of cyclic polyelectrolyte via direct copper(I)-catalyzed click cyclization. J Polym Sci A: Polym Chem 2012;50:831–5.
[80] Zhu X, Zhou N, Zhang Z, Sun B, Yang Y, Zhu J, et al. Cyclic polymers with pendent carbazole units: enhanced fluorescence and redox behavior. Angew Chem Int Ed 2011;50:6615–18.
[81] O'Bryan G, Ningnuek N, Braslau R. Cyclization of α, ω heterotelechelic polystyrene prepared by nitroxide-mediated radical polymerization. Polymer 2008;49:5241–8.
[82] Qiu X-P, Tanaka F, Winnik FM. Temperature-induced phase transition of well-defined cyclic poly(N-isopropylacrylamide)s in aqueous solution. Macromolecules 2007;40:7069–71.
[83] Goldmann AS, Quémener D, Millard P-E, Davis TP, Stenzel MH, Barner-Kowollik C, et al. Access to cyclic polystyrenes via a combination of reversible addition fragmentation chain transfer (RAFT) polymerization and click chemistry. Polymer 2008;49:2274–81.
[84] Hossain MD, Valade D, Jia Z, Monteiro MJ. Cyclic polystyrene topologies via RAFT and CuAAC. Polym Chem 2012;3:2986–95.
[85] Josse T, De Winter J, Dubois P, Coulembier O, Gerbaux P, Memboeuf A. A tandem mass spectrometry-based method to assess the architectural purity of synthetic polymers: a case of a cyclic polylactide obtained by click chemistry. Polym Chem 2015;6:64–9.
[86] Hoskins JN, Grayson SM. Synthesis and degradation behavior of cyclic poly(ε-caprolactone). Macromolecules 2009;42:6406–13.
[87] Misaka H, Kakuchi R, Zhang C, Sakai R, Satoh T, Kakuchi T. Synthesis of well-defined macrocyclic poly(δ-valerolactone) by "click cyclization. Macromolecules 2009;42:5091–6.
[88] Misaka H, Tamura E, Makiguchi K, Kamoshida K, Sakai R, Satoh T, et al. Synthesis of end-functionalized polyethers by phosphazene base-catalyzed ring-opening polymerization of 1,2-butylene oxide and glycidyl ether. J Polym Sci A: Polym Chem 2012;50:1941–52.
[89] Cortez MA, Godbey WT, Fang Y, Payne ME, Cafferty BJ, Kosakowska KA, et al. The synthesis of cyclic poly(ethylene imine) and exact linear analogues: an evaluation of gene delivery comparing polymer architectures. J Am Chem Soc 2015;137:6541–9.
[90] Ochs J, Veloso A, Martínez-Tong DE, Alegria A, Barroso-Bujans F. An insight into the anionic ring-opening polymerization with tetrabutylammonium azide for the generation of pure cyclic poly(glycidyl phenyl ether). Macromolecules 2018;51:2447–55.
[91] Huettner N, Goldmann AS, Hoogenboom R, Dargaville TR. Macrocyclization efficiency for poly(2-oxazoline)s and poly(2-oxazine)s. Polym Chem 2022;13:3975–80.
[92] Koo MB, Lee SW, Lee JM, Kim KT. Iterative convergent synthesis of large cyclic polymers and block copolymers with discrete molecular weights. J Am Chem Soc 2020;142:14028–32.

[93] Eugene DM, Grayson SM. Efficient preparation of cyclic poly(methyl acrylate)-block-poly(styrene) by combination of atom transfer radical polymerization and click cyclization. Macromolecules 2008;41:5082–4.
[94] Ge Z, Zhou Y, Xu J, Liu H, Chen D, Liu S. High-efficiency preparation of macrocyclic diblock copolymers via selective click reaction in micellar media. J Am Chem Soc 2009;131:1628–9.
[95] Touris A, Hadjichristidis N. Cyclic and multiblock polystyrene-block-polyisoprene copolymers by combining anionic polymerization and azide/alkyne "click" chemistry. Macromolecules 2011;44:1969–76.
[96] Zhang B, Zhang H, Li Y, Hoskins JN, Grayson SM. Exploring the effect of amphiphilic polymer architecture: synthesis, characterization, and self-assembly of both cyclic and linear poly(ethylene gylcol)-b-polycaprolactone. ACS Macro Lett 2013;2:845–8.
[97] Sun P, Tang Q, Wang Z, Zhao Y, Zhang K. Cyclic polymers based on UV-induced strain promoted azide–alkyne cycloaddition reaction. Polym Chem 2015;6:4096–101.
[98] Diels O, Alder K. Synthesen in der hydroaromatischen Reihe. Justus Liebigs Annalen der Chemie 1928;460:98–122.
[99] Pellissier H. Asymmetric hetero-Diels–Alder reactions of carbonyl compounds. Tetrahedron 2009;65:2839–77.
[100] Diels–Alder reaction facilitated by special physical and chemical methods. The Diels–Alder Reaction2001. p. 143-204.
[101] Mizawa T, Takenaka K, Shiomi T. Synthesis of α-maleimide-ω-dienyl heterotelechelic poly(methyl methacrylate) and its cyclization by the intramolecular Diels–Alder reaction. J Polym Sci A: Polym Chem 2000;38:237–46.
[102] Durmaz H, Dag A, Hizal G, Tunca U. Cyclic homo and block copolymers through sequential double click reactions. J Polym Sci A: Polym Chem 2010;48:5083–91.
[103] Iha RK, Wooley KL, Nyström AM, Burke DJ, Kade MJ, Hawker CJ. Applications of orthogonal "click" chemistries in the synthesis of functional soft materials. Chem Rev 2009;109:5620–86.
[104] Glassner M, Blinco JP, Barner-Kowollik C. Diels–Alder reactions as an efficient route to high purity cyclic polymers. Macromol Rapid Commun 2011;32:724–8.
[105] Josse T, Altintas O, Oehlenschlaeger KK, Dubois P, Gerbaux P, Coulembier O, et al. Ambient temperature catalyst-free light-induced preparation of macrocyclic aliphatic polyesters. Chem Comm 2014;50:2024–6.
[106] Josse T, De Winter J, Altintas O, Dubois P, Barner-Kowollik C, Gerbaux P, et al. A sunlight-induced click reaction as an efficient route to cyclic aliphatic polyesters. Macromol Chem Phys 2015;216:1227–34.
[107] Tang Q, Wu Y, Sun P, Chen Y, Zhang K. Powerful ring-closure method for preparing varied cyclic polymers. Macromolecules 2014;47:3775–81.
[108] Sun P, Ja L, Zhang Z, Zhang K. Scalable preparation of cyclic polymers by the ring-closure method assisted by the continuous-flow technique. Polym Chem 2016;7:2239–44.
[109] Tang Q, Zhang W, Yuan J, Zhao Q. Templated synthesis of cyclic poly(ionic liquid)s. React Funct Polym 2019;138:1–8.
[110] Lu D, Jia Z, Monteiro MJ. Synthesis of alkyne functional cyclic polymers by one-pot thiol–ene cyclization. Polym Chem 2013;4:2080–9.
[111] Liu B, Wang H, Zhang L, Yang G, Liu X, Kim I. A facile approach for the synthesis of cyclic poly(N-isopropylacrylamide) based on an anthracene–thiol click reaction. Polym Chem 2013;4:2428–31.
[112] Long S, Tang Q, Wu Y, Wang L, Zhang K, Chen Y. A method for preparing water soluble cyclic polymers. React Funct Polym 2014;80:15–20.
[113] Zhao J, Zhou Y, Zhou Y, Zhou N, Pan X, Zhang Z, et al. A straightforward approach for the one-pot synthesis of cyclic polymers from RAFT polymers via thiol–Michael addition. Polym Chem 2016;7:1782–91.
[114] Liu W, Zhang S, Liu S, Wu Z, Chen H. Efficient heterodifunctional unimolecular ring-closure method for cyclic polymers by combining RAFT and SuFEx click reactions. Macromol Rapid Commun 2019;40:1900310.
[115] Konomoto T, Nakamura K, Yamamoto T, Tezuka Y. Synthesis and unimolecular ESA-CF polymer cyclization of zwitterionic telechelic precursors. Macromolecules 2019;52:9208–19.
[116] Zhao Y, Zhu S, Liao C, Wang Y, Lam JWY, Zhou X, et al. Cobalt-mediated switchable catalysis for the one-pot synthesis of cyclic polymers. Angew Chem Int Ed 2021;60:16974–9.
[117] Dong J, Krasnova L, Finn MG, Sharpless KB. Sulfur(VI) fluoride exchange (SuFEx): another good reaction for click chemistry. Angew Chem Int Ed 2014;53:9430–48.
[118] Tezuka Y. Electrostatic self-assembly and covalent fixation (ESA-CF) process. Topological polymer chemistry. p. 49-70.
[119] Geiser D, Höcker H. Synthesis and investigation of macrocyclic polystyrene. Macromolecules 1980;13:653–6.
[120] Hild G, Kohler A, Rempp P. Synthesis of ring-shaped macromolecules. Eur Polym J 1980;16:525–7.
[121] Roovers J, Toporowski PM. Synthesis of high molecular weight ring polystyrenes. Macromolecules 1983;16:843–9.
[122] Roovers J, Toporowski PM. Synthesis and characterization of ring polybutadienes. J Polym Sci B Polym Phys 1988;26:1251–9.
[123] Hogen-Esch TE, Sundararajan J, Toreki W. Synthesis and characterization of topologically interesting vinyl polymers. Makromol Chem Macromol Symp 1991;47:23–42.
[124] Madani AE, Favier J-C, Hémery P, Sigwalt P. Synthesis of ring-shaped polyisoprene. Polym Int 1992;27:353–7.
[125] Ishizu K, Kanno H. Novel synthesis and characterization of cyclic polystyrenes. Polymer 1996;37:1487–92.
[126] Ishizu K, Ichimura A. Synthesis of cyclic diblock copolymers by interfacial condensation. Polymer 1998;39:6555–8.
[127] Yan Z-G, Yang Z, Price C, Booth C. Cyclisation of poly(ethylene glycol)s and related block copolymers. Makromol Chem, Rapid Commun 1993;14:725–32.
[128] Yu G-E, Sinnathamby P, Price C, Booth C. Preparation of large cyclic poly(oxyethylene)s. Chem Commun 1996:31–2.
[129] Sun T, Yu G-E, Price C, Booth C, Cooke J, Ryan AJ. Cyclic polyethers. Polymer 1995;36:3775–8.
[130] Hövelmann CH, Gooßen S, Allgaier J. Scale-up procedure for the efficient synthesis of highly pure cyclic poly(ethylene glycol). Macromolecules 2017;50:4169–79.
[131] Sharma S, Ntetsikas K, Ladelta V, Bhaumik S, Hadjichristidis N. Well-defined cyclic polymer synthesis via an efficient etherification-based bimolecular ring-closure strategy. Polym Chem 2021;12:6616–25.
[132] Oike H, Imaizumi H, Mouri T, Yoshioka Y, Uchibori A, Tezuka Y. Designing unusual polymer topologies by electrostatic self-assembly and covalent fixation. J Am Chem Soc 2000;122:9592–9.
[133] Oike H, Hamada M, Eguchi S, Danda Y, Tezuka Y. Novel synthesis of single- and double-cyclic polystyrenes by electrostatic self-assembly and covalent fixation with telechelics having cyclic ammonium salt groups. Macromolecules 2001;34:2776–82.
[134] Tezuka Y, Mori K, Oike H. Efficient synthesis of cyclic poly(oxyethylene) by electrostatic self-assembly and covalent fixation with telechelic precursor having cyclic ammonium salt groups. Macromolecules 2002;35:5707–11.
[135] Tezuka Y. Topological polymer chemistry designing complex macromolecular graph constructions. Acc Chem Res 2017;50:2661–72.
[136] Stanford MJ, Pflughaupt RL, Dove AP. Synthesis of stereoregular cyclic poly(lactide)s via "thiol−ene" click chemistry. Macromolecules 2010;43:6538–41.
[137] Sun P, Chen J, Ja L, Zhang K. Self-accelerating click reaction for cyclic polymer. Macromolecules 2017;50:1463–72.
[138] Sun P, Zhu W, Chen J, Ja L, Wu Y, Zhang K. Synthesis of well-defined cyclic polyesters via self-accelerating click reaction. Polymer 2017;121:196–203.
[139] Zhang M, Wu Y, Liu Z, Li J, Huang L, Zhang K. An efficient ring-closure method for preparing well-defined cyclic polynorbornenes. Macromol Rapid Commun 2020;41:1900598.
[140] Qu L, Sun P, Wu Y, Zhang K, Liu Z. Efficient homodifunctional bimolecular ring-closure method for cyclic polymers by combining RAFT and self-accelerating click reaction. Macromol Rapid Commun 2017;38:1700121.
[141] Li Z, Qu L, Zhu W, Ja L, Chen J-Q, Sun P, et al. Self-accelerating click reaction for preparing cyclic polymers from unconjugated vinyl monomers. Polymer 2018;137:54–62.
[142] Liu X, Chen J-Q, Zhang M, Wu Y, Yang M, Zhang K. A versatile method for cyclic polymers from conjugated and unconjugated vinyl monomers. J Polym Sci A: Polym Chem 2019;57:1811–20.
[143] Zhang H-L, Xu W, Liu C, Hong C-Y. Synthesis of a bead-like multicyclic polymer by UV-induced coupling of an anthracene-telechelic monocyclic precursor and its reversible topological conversion. Polym Chem 2021;12:5357–63.
[144] Hosoi Y, Takasu A, Matsuoka S-I, Hayashi M. N-Heterocyclic carbene initiated anionic polymerization of (E,E)-methyl sorbate and subsequent ring-closing to cyclic poly(alkyl sorbate). J Am Chem Soc 2017;139:15005–12.
[145] Oga Y, Hosoi Y, Takasu A. Synthesis of cyclic Poly(methyl methacrylate) via N-Heterocyclic carbene (NHC) initiated-anionic polymerization and subsequent ring-closing without need of highly dilute conditions. Polymer 2020;186:122019.
[146] McGraw ML, Reilly LT, Clarke RW, Cavallo L, Falivene L, Chen EY-X. Mechanism of spatial and temporal control in precision cyclic vinyl polymer synthesis by Lewis pair polymerization. Angew Chem Int Ed 2022;61:e202116303.
[147] Kricheldorf HR. Biodegradable polymers with variable architectures via ring–expansion polymerization. J Polym Sci A: Polym Chem 2004;42:4723–42.
[148] Kricheldorf HR, Lee S-R. Polylactones. 35. Macrocyclic and stereoselective polymerization of b-D,L-butyrolactone with cyclic dibutyltin initiators. Macromolecules 1995;28:6718–25.
[149] Kricheldorf HR, Lee S-R, Schittenhelm N. Macrocycles, 1. Macrocyclic polymerizations of (thio)lactones – stepwise ring expansion and ring contraction. Macromol Chem Phys 1998;199:273–82.
[150] Kricheldorf HR, Langanke D. Macrocycles, 7. Cyclization of oligo- and poly(ethylene glycol)s with dibutyltin dimethoxide – a new approach to (super)macrocycles. Macromol Chem Phys 1999;200:1174–82.
[151] Kricheldorf HR, Langanke D. Macrocycles, 8. Multiblock copoly(ether-esters) of poly(THF) and ϵ-caprolactone via macrocyclic polymerization. Macromol Chem Phys 1999;200:1183–90.
[152] Kricheldorf HR, Langanke D. Polylactones, 56. ABA Triblock Copolymers Derived from ε-Caprolactone or L-Lactide and a Central Polysiloxane Block. Macromol Biosci 2001;1:364–9.
[153] Kricheldorf HR, Lee S-R, Bush S. Polylactones 36. Macrocyclic polymerization of lactides with cyclic Bu_2Sn initiators derived from 1,2-ethanediol, 2-mercaptoethanol, and 1,2-dimercaptoethane. Macromolecules 1996;29:1375–81.
[154] Kricheldorf HR, Weidner SM, Scheliga F. Cyclic poly(l-lactide)s via ring-expansion polymerizations catalysed by 2,2-dibutyl-2-stanna-1,3-dithiolane. Polym Chem 2017;8:1589–96.
[155] Kricheldorf HR, Al-Masri M, Schwarz G. Macrocycles. 20. Cyclic poly(ethylene glycol) phthalates via ring-exchange substitution. Macromolecules 2002;35:8936–42.

[156] Kricheldorf HR, Weidner SM. High molar mass cyclic poly(l-lactide) via ring–expansion polymerization with cyclic dibutyltin bisphenoxides. Eur Polym J 2018;105:158–66.
[157] Kricheldorf HR, Weidner SM. High molar mass cyclic poly(l-lactide) obtained by means of neat tin(ii) 2-ethylhexanoate. Polym Chem 2020;11:5249–60.
[158] Kricheldorf HR, Weidner SM. Syntheses of polylactides by means of tin catalysts. Polym Chem 2022.
[159] Weil J, Mathers RT, Getzler YDYL. Lactide cyclopolymerization by an alumatrane-inspired catalyst. Macromolecules 2012;45:1118–21.
[160] Reisberg SH, Hurley HJ, Mathers RT, Tanski JM, Getzler YDYL. Lactide cyclopolymerization kinetics, X-ray structure, and solution dynamics of (tBu-SalAmEE)Al and a cautionary tale of polymetalate formation. Macromolecules 2013;46:3273–9.
[161] Wongmahasirikun P, Prom-on P, Sangtrirutnugul P, Kongsaeree P, Phomphrai K. Synthesis of cyclic polyesters: effects of alkoxy side chains in salicylaldiminato tin(ii) complexes. Dalton Trans 2015;44:12357–64.
[162] Ungpittagul T, Wongmahasirikun P, Phomphrai K. Synthesis and characterization of guanidinate tin(ii) complexes for ring-opening polymerization of cyclic esters. Dalton Trans 2020;49:8460–71.
[163] Bonnet F, Stoffelbach F, Fontaine G, Bourbigot S. Continuous cyclo-polymerisation of l-lactide by reactive extrusion using atoxic metal-based catalysts: easy access to well-defined polylactide macrocycles. RSC Adv 2015;5:31303–10.
[164] Zhu J-B, Watson EM, Tang J, Chen EY-X. A synthetic polymer system with repeatable chemical recyclability. Science 2018;360:398–403.
[165] Hong M, Chen EYX. Completely recyclable biopolymers with linear and cyclic topologies via ring-opening polymerization of γ-butyrolactone. Nat Chem 2016;8:42–9.
[166] Tang X, Chen EYX. Toward infinitely recyclable plastics derived from renewable cyclic esters. Chem 2019;5:284–312.
[167] Impemba S, Della Monica F, Grassi A, Capacchione C, Milione S. Cyclic Polyester Formation with an [OSSO]-Type Iron(III) Catalyst. ChemSusChem 2020;13:141–5.
[168] Li H, Ollivier J, Guillaume SM, Carpentier J-F. Tacticity control of cyclic poly(3-thiobutyrate) prepared by ring-opening polymerization of racemic β-thiobutyrolactone. Angew Chem Int Ed 2022;61:e202202386.
[169] Shea KJ, Walker JW, Zhu H, Paz M, Greaves J. Polyhomologation. A living polymethylene synthesis. J Am Chem Soc 1997;119:9049–50.
[170] Shea KJ, Lee SY, Busch BB. A new strategy for the synthesis of macrocycles. The polyhomologation of boracyclanes. J Org Chem 1998;63:5746–7.
[171] Kudo H, Makino S, Kameyama A, Nishikubo T. Synthesis of cyclic polymers: ring-expansion reaction of cyclic S-dithioester with thiiranes. Macromolecules 2005;38:5964–9.
[172] Kudo H, Sato M, Wakai R, Iwamoto T, Nishikubo T. A novel approach to cyclic polysulfides via the controlled ring-expansion polymerization of cyclic thiourethane with thiiranes. Macromolecules 2008;41:521–3.
[173] Takahashi A, Yuzaki R, Ishida Y, Kameyama A. Controlled ring-expansion polymerization of thiiranes based on cyclic aromatic thiourethane initiator. J Polym Sci A: Polym Chem 2019;57:2442–9.
[174] Takahashi A, Tsunoda S, Yuzaki R, Kameyama A. Thioacyl-transfer ring-expansion polymerization of thiiranes based on a cyclic dithiocarbamate initiator. Macromolecules 2020;53:5227–36.
[175] Bielawski CW, Benitez D, Grubbs RH. An "endless" route to cyclic polymers. Science 2002;297:2041–4.
[176] Bielawski CW, Benitez D, Grubbs RH. Synthesis of cyclic polybutadiene via ring-opening metathesis polymerization: the importance of removing trace linear contaminants. J Am Chem Soc 2003;125:8424–5.
[177] Wang T-W, Huang P-R, Chow JL, Kaminsky W, Golder MR. A Cyclic Ruthenium Benzylidene Initiator Platform Enhances Reactivity for Ring-Expansion Metathesis Polymerization. J Am Chem Soc 2021;143:7314–19.
[178] Gonsales SA, Kubo T, Flint MK, Abboud KA, Sumerlin BS, Veige AS. Highly tactic cyclic polynorbornene: stereoselective ring expansion metathesis polymerization of norbornene catalyzed by a new tethered tungsten-alkylidene catalyst. J Am Chem Soc 2016;138:4996–9.
[179] Nadif SS, Kubo T, Gonsales SA, VenkatRamani S, Ghiviriga I, Sumerlin BS, et al. Introducing “ynene” metathesis: ring-expansion metathesis polymerization leads to highly cis and syndiotactic cyclic polymers of norbornene. J Am Chem Soc 2016;138:6408–11.
[180] Roland CD, Li H, Abboud KA, Wagener KB, Veige AS. Cyclic polymers from alkynes. Nat Chem 2016;8:791–6.
[181] Miao Z, Gonsales SA, Ehm C, Mentink-Vigier F, Bowers CR, Sumerlin BS, et al. Cyclic polyacetylene. Nat Chem 2021;13:792–9.
[182] Jakhar V, Pal D, Ghiviriga I, Abboud KA, Lester DW, Sumerlin BS, et al. Tethered tungsten-alkylidenes for the synthesis of cyclic polynorbornene via ring expansion metathesis: unprecedented stereoselectivity and trapping of key catalytic intermediates. J Am Chem Soc 2021;143:1235–46.
[183] Mandal U, Ghiviriga I, Abboud KA, Lester DW, Veige AS. Double tethered metallacyclobutane catalyst for cyclic polymer synthesis. J Am Chem Soc 2021;143:17276–83.
[184] Miao Z, Kubo T, Pal D, Sumerlin BS, Veige AS. pH-Responsive water-soluble cyclic polymer. Macromolecules 2019;52:6260–5.
[185] Miao Z, Pal D, Niu W, Kubo T, Sumerlin BS, Veige AS. Cyclic poly(4-methyl-1-pentene): efficient catalytic synthesis of a transparent cyclic polymer. Macromolecules 2020;53:7774–82.
[186] Niu W, Gonsales SA, Kubo T, Bentz KC, Pal D, Savin DA, et al. Polypropylene: now available without chain ends. Chem 2019;5:237–44.
[187] Pal D, Miao Z, Garrison JB, Veige AS, Sumerlin BS. Ultra-high-molecular-weight macrocyclic bottlebrushes via post-polymerization modification of a cyclic polymer. Macromolecules 2020;53:9717–24.
[188] Miao Z, Konar D, Sumerlin BS, Veige AS. Soluble polymer precursors via ring–expansion metathesis polymerization for the synthesis of cyclic polyacetylene. Macromolecules 2021;54:7840–8.
[189] Sueyoshi S, Taniguchi T, Tanaka S, Asakawa H, Nishimura T, Maeda K. Understanding the polymerization of diphenylacetylenes with tantalum(V) chloride and cocatalysts: production of cyclic poly(diphenylacetylene)s by low-valent tantalum species generated in situ. J Am Chem Soc 2021;143:16136–46.
[190] Morrison CM, Golder MR. Ring-expansion metathesis polymerization initiator design for the synthesis of cyclic polymers. Synlett 2022;33 A-F.
[191] Kubo T, Yadav R, Veige AS. Ring-expansion polymerization of cycloalkenes and linear alkynes by transition metal catalysts. In: Tezuka Y, Deguchi T, editors. Topological Polymer Chemistry: Concepts and Practices. Singapore: Springer Singapore; 2022. p. 261–75.
[192] Johnston DS. Macrozwitterion polymerization. Berlin, Heidelberg: Springer Berlin Heidelberg; 1982. p. 51–106.
[193] Szwarg M. Some aspects of anionic polymerization. Makromol Chem 1960;35:132–58.
[194] Culkin DA, Jeong W, Csihony S, Gomez ED, Balsara NP, Hedrick JL, et al. Zwitterionic polymerization of lactide to cyclic poly(lactide) by using N-heterocyclic carbene organocatalysts. Angew Chem Int Ed 2007;46:2627–30.
[195] Jeong W, Shin EJ, Culkin DA, Hedrick JL, Waymouth RM. Zwitterionic polymerization: a kinetic strategy for the controlled synthesis of cyclic polylactide. J Am Chem Soc 2009;131:4884–91.
[196] Shin EJ, Brown HA, Gonzalez S, Jeong W, Hedrick JL, Waymouth RM. Zwitterionic copolymerization: synthesis of cyclic gradient copolymers. Angew Chem Int Ed 2011;50:6388–91.
[197] Shin EJ, Jeong W, Brown HA, Koo BJ, Hedrick JL, Waymouth RM. Crystallization of cyclic polymers: synthesis and crystallization behavior of high molecular weight cyclic poly(ε-caprolactone)s. Macromolecules 2011;44:2773–9.
[198] Brown HA, Xiong S, Medvedev GA, Chang YA, Abu-Omar MM, Caruthers JM, et al. Zwitterionic ring-opening polymerization: models for kinetics of cyclic poly(caprolactone) synthesis. Macromolecules 2014;47:2955–63.
[199] Brown HA, De Crisci AG, Hedrick JL, Waymouth RM. Amidine-mediated zwitterionic polymerization of lactide. ACS Macro Lett 2012;1:1113–15.
[200] Brown HA, Chang YA, Waymouth RM. Zwitterionic polymerization to generate high molecular weight cyclic poly(carbosiloxane)s. J Am Chem Soc 2013;135:18738–41.
[201] Acharya AK, Chang YA, Jones GO, Rice JE, Hedrick JL, Horn HW, et al. Experimental and computational studies on the mechanism of zwitterionic ring-opening polymerization of δ-valerolactone with N-heterocyclic carbenes. J Phys Chem B 2014;118:6553–60.
[202] Stukenbroeker TS, Solis-Ibarra D, Waymouth RM. Synthesis and topological trapping of cyclic poly(alkylene phosphates). Macromolecules 2014;47:8224–30.
[203] Zhang X, Waymouth RM. Zwitterionic ring opening polymerization with isothioureas. ACS Macro Lett 2014;3:1024–8.
[204] Chang YA, Rudenko AE, Waymouth RM. Zwitterionic ring-opening polymerization of N-substituted eight-membered cyclic carbonates to generate cyclic poly(carbonate)s. ACS Macro Lett 2016;5:1162–6.
[205] Kerr RWF, Ewing PMDA, Raman SK, Smith AD, Williams CK, Arnold PL. Ultrarapid cerium(III)–NHC catalysts for high molar mass cyclic polylactide. ACS Catal 2021;11:1563–9.
[206] Asenjo-Sanz I, Veloso A, Miranda JI, Pomposo JA, Barroso-Bujans F. Zwitterionic polymerization of glycidyl monomers to cyclic polyethers with $B(C_6F_5)_3$. Polym Chem 2014;5:6905–8.
[207] Asenjo-Sanz I, Veloso A, Miranda JI, Alegría A, Pomposo JA, Barroso-Bujans F. Zwitterionic ring-opening copolymerization of tetrahydrofuran and glycidyl phenyl ether with B(C6F5)3. Macromolecules 2015;48:1664–72.
[208] Childers MI, Longo JM, Van Zee NJ, LaPointe AM, Coates GW. Stereoselective epoxide polymerization and copolymerization. Chem Rev 2014;114:8129–52.
[209] Haque FM, Schexnayder CM, Matxain JM, Barroso-Bujans F, Grayson SM. MALDI-ToF MS study of macrocyclic polyethers generated by electrophilic zwitterionic ring expansion polymerization of monosubstituted epoxides with B(C6F5)3. Macromolecules 2019;52:6369–81.
[210] Haque FM, Alegria A, Grayson SM, Barroso-Bujans F. Detection, quantification, and “click-scavenging” of impurities in cyclic poly(glycidyl phenyl ether) obtained by zwitterionic ring-expansion polymerization with B(C6F5)3. Macromolecules 2017;50:1870–81.
[211] Kim SE, Yang HJ, Choi S, Hwang E, Kim M, Paik H-J, et al. A recyclable metal-free catalytic system for the cationic ring-opening polymerization of glycidol under ambient conditions. Green Chem 2022;24:251–8.
[212] Al Assiri MA, Gómez Urreizti E, Pagnacco CA, Gónzalez de San Román E, Barroso-Bujans F. Reactivity of B(C6F5)3 towards glycidol: the formation of branched cyclic polyglycidol structures. Eur Polym J 2022;171:111194.
[213] Tokar R, Kubisa P, Penczek S, Dworak A. Cationic polymerization of glycidol: coexistence of the activated monomer and active chain end mechanism. Macromolecules 1994;27:320–2.
[214] Kammiyada H, Konishi A, Ouchi M, Sawamoto M. Ring-expansion living cationic polymerization via reversible activation of a hemiacetal ester bond. ACS Macro Lett 2013;2:531–4.
[215] Kammiyada H, Ouchi M, Sawamoto M. A convergent approach to ring polymers with narrow molecular weight distributions through post dilution in ring expansion cationic polymerization. Polym Chem 2016;7:6911–17.

[216] Engler A, Kohl PA. Kinetic investigation on the cationic polymerization of o-phthalaldehyde: understanding ring-expansion polymerization. Macromolecules 2020;53:1543–9.
[217] Chen Y, Shen J, Liu S, Zhao J, Wang Y, Zhang G. High efficiency organic Lewis pair catalyst for ring-opening polymerization of epoxides with chemoselectivity. Macromolecules 2018;51:8286–97.
[218] Wang Q, Zhao W, He J, Zhang Y, Chen EYX. Living ring-opening polymerization of lactones by N-heterocyclic olefin/Al(C6F5)3 Lewis pairs: structures of intermediates, kinetics, and mechanism. Macromolecules 2017; 50:123–36.
[219] Xu T, Chen EYX. Probing site cooperativity of frustrated phosphine/Borane Lewis pairs by a polymerization study. J Am Chem Soc 2014; 136:1774–7.
[220] Zhang Y, Miyake GM, Chen EY-X. Alane-based classical and frustrated lewis pairs in polymer synthesis: rapid polymerization of MMA and naturally renewable methylene butyrolactones into high-molecular-weight polymers. Angew Chem Int Ed 2010;49:10158–62.
[221] Piedra-Arroni E, Ladavière C, Amgoune A, Bourissou D. Ring-opening polymerization with Zn(C6F5)2-based lewis pairs: original and efficient approach to cyclic polyesters. J Am Chem Soc 2013;135:13306–9.
[222] Li X-Q, Wang B, Ji H-Y, Li Y-S. Insights into the mechanism for ring-opening polymerization of lactide catalyzed by Zn(C6F5)2/organic superbase Lewis pairs. Catal Sci Technol 2016;6:7763–72.
[223] Luo Z, Chaemchuen S, Zhou K, Verpoort F. Ring-opening polymerization of l-lactide to cyclic poly(lactide) by zeolitic imidazole framework ZIF-8 catalyst. ChemSusChem 2017;10:4135–9.
[224] Shaik M, Peterson J, Du G. Cyclic and linear polyhydroxylbutyrates from ring-opening polymerization of β-butyrolactone with amido-oxazolinate zinc catalysts. Macromolecules 2019;52:157–66.
[225] Kim SE, Lee Y-R, Kim M, Seo E, Paik H-J, Kim JC, et al. Highly tunable metal-free ring opening polymerization of glycidol into various controlled topologies catalyzed by frustrated lewis pairs. Polym Chem 2022; 13:1243–52.
[226] Kammiyada H, Ouchi M, Sawamoto M. Ring-expansion living cationic polymerization of vinyl ethers: optimized ring propagation. Macromol Symp 2015;350:105–16.
[227] Daito Y, Kojima R, Kusuyama N, Kohsaka Y, Ouchi M. Magnesium bromide (MgBr2) as a catalyst for living cationic polymerization and ring-expansion cationic polymerization. Polym Chem 2021;12:702–10.
[228] Kaitz JA, Diesendruck CE, Moore JS. End group characterization of poly(phthalaldehyde): surprising discovery of a reversible, cationic macrocyclization mechanism. J Am Chem Soc 2013;135:12755–61.
[229] Zhang Z, Nie X, Wang F, Chen G, Huang W-Q, Xia L, et al. Rhodanine-based Knoevenagel reaction and ring-opening polymerization for efficiently constructing multicyclic polymers. Nat Commun 2020;11:3654.
[230] He T, Zheng G-H, Pan C-Y. Synthesis of cyclic polymers and block copolymers by monomer insertion into cyclic initiator by a radical mechanism. Macromolecules 2003;36:5960–6.
[231] Bunha A, Cao P-F, Mangadlao JD, Advincula RC. Cyclic poly(vinylcarbazole) via ring-expansion polymerization-RAFT (REP-RAFT). React Funct Polym 2014;80:33–9.
[232] Narumi A, Zeidler S, Barqawi H, Enders C, Binder WH. Cyclic alkoxyamine-initiator tethered by azide/alkyne-"click"-chemistry enabling ring-expansion vinyl polymerization providing macrocyclic polymers. J Polym Sci A: Polym Chem 2010;48:3402–16.
[233] Narumi A, Hasegawa S, Yanagisawa R, Tomiyama M, Yamada M, Binder WH, et al. Ring expansion-controlled radical polymerization: synthesis of cyclic polymers and ring component quantification based on SEC–MALS analysis. React Funct Polym 2016;104:1–8.
[234] Narumi A, Yamada M, Unno Y, Kumaki J, Binder WH, Enomoto K, et al. Evaluation of ring expansion-controlled radical polymerization system by AFM observation. ACS Macro Lett 2019;8:634–8.
[235] Kricheldorf HR, Von Lossow C, Schwarz G. Tertiary amine catalyzed polymerizations of α-amino acid N-carboxyanhydrides: the role of cyclization. J Polym Sci, Part A: Polym Chem 2006;44:4680–95.
[236] Kricheldorf HR, Lossow C V, Schwarz G. Primary amine and solvent-induced polymerizations of L- or D,L-phenylalanine N-carboxyanhydride. Macromol Chem Phys 2005;206:282–90.
[237] Guo L, Zhang D. Cyclic poly(α-peptoid)s and their block copolymers from N-heterocyclic carbene-mediated ring-opening polymerizations of N-substituted N-carboxylanhydrides. J Am Chem Soc 2009;131:18072–4.
[238] Li A, Lu L, Li X, He L, Do C, Garno JC, et al. Amidine-mediated zwitterionic ring-opening polymerization of N-alkyl N-carboxyanhydride: mechanism, kinetics, and architecture elucidation. Macromolecules 2016;49:1163–71.
[239] Guo L, Lahasky SH, Ghale K, Zhang D. N-Heterocyclic carbene-mediated zwitterionic polymerization of N-substituted N-carboxyanhydrides toward poly(α-peptoid)s: kinetic, mechanism, and architectural control. J Am Chem Soc 2012;134:9163–71.
[240] Lee C-U, Smart TP, Guo L, Epps TH, Zhang D. Synthesis and characterization of amphiphilic cyclic diblock copolypeptoids from N-heterocyclic carbene–mediated zwitterionic polymerization of N-substituted N-carboxyanhydride. Macromolecules 2011;44:9574–85.
[241] Lahasky SH, Serem WK, Guo L, Garno JC, Zhang D. Synthesis and characterization of cyclic brush-like polymers by N-heterocyclic carbene-mediated zwitterionic polymerization of N-propargyl N-carboxyanhydride and the grafting-to approach. Macromolecules 2011;44:9063–74.
[242] Salas-Ambrosio P, Tronnet A, Since M, Bourgeade-Delmas S, Stigliani J-L, Vax A, et al. Cyclic poly(α-peptoid)s by lithium bis(trimethylsilyl)amide (LiHMDS)-mediated ring-expansion polymerization: simple access to bioactive backbones. J Am Chem Soc 2021;143:3697–702.
[243] Fèvre M, Pinaud J, Leteneur A, Gnanou Y, Vignolle J, Taton D, et al. Imidazol(in)ium hydrogen carbonates as a genuine source of N-heterocyclic carbenes (NHCs): applications to the facile preparation of NHC metal complexes and to NHC-organocatalyzed molecular and macromolecular syntheses. J Am Chem Soc 2012;134:6776–84.
[244] Zhang Y, Liu R, Jin H, Song W, Augustine R, Kim I. Straightforward access to linear and cyclic polypeptides. Commun Chem 2018;1:40.
[245] White CJ, Yudin AK. Contemporary strategies for peptide macrocyclization. Nature Chem 2011;3:509–24.
[246] Rivera DG, Ojeda-Carralero GM, Reguera L, Van der Eycken EV. Peptide macrocyclization by transition metal catalysis. Chem Soc Rev 2020;49:2039–59.
[247] Adebomi V, Cohen RD, Wills R, Chavers HAH, Martin GE, Raj M. CyClick chemistry for the synthesis of cyclic peptides. Angew Chem Int Ed 2019;58:19073–80.
[248] Chow HY, Zhang Y, Matheson E, Li X. Ligation technologies for the synthesis of cyclic peptides. Chem Rev 2019;119:9971–10001.
[249] Lambert JN, Mitchell JP, Roberts KD. The synthesis of cyclic peptides. J Chem Soc, Perkin Trans 2001;1:471–84.
[250] Dolinnaya NG, Sokolova NI, Ashirbekova DT, Shabarova ZA. The use of BrCN for assembling modified DNA duplexes and DNA-RNA hybrids; comparison with water-soluble carbodiimide. Nucleic Acids Res 1991;19:3067–72.
[251] Nakamoto K, Abe N, Tsuji G, Kimura Y, Tomoike F, Shimizu Y, et al. Chemically synthesized circular RNAs with phosphoramidate linkages enable rolling circle translation. Chem Comm 2020;56:6217–20.
[252] De Mesmaeker A, Waldner A, Lebreton J, Hoffmann P, Fritsch V, Wolf RM, et al. Amides as a new type of backbone modification in oligonucleotides. Angew Chem Int Ed Engl 1994;33:226–9.
[253] El-Sagheer AH, Sanzone AP, Gao R, Tavassoli A, Brown T. Biocompatible artificial DNA linker that is read through by DNA polymerases and is functional in *Escherichia coli*. Proc Natl Acad Sci U S A 2011;108:11338–43.
[254] Kumar R, El-Sagheer A, Tumpane J, Lincoln P, Wilhelmsson LM, Brown T. Template-directed oligonucleotide strand ligation, covalent intramolecular DNA circularization and catenation using click chemistry. J Am Chem Soc 2007;129:6859–64.
[255] Obi P, Chen YG. The design and synthesis of circular RNAs. Methods 2021;196:85–103.
[256] Petkovic S, Müller S. Synthesis and engineering of circular RNAs. In: Dieterich C, Papantonis A, editors. Circular RNAs: Methods and Protocols. New York, NY: Springer New York; 2018. p. 167–80.
[257] Müller S, Appel B. In vitro circularization of RNA. RNA Biology 2017;14:1018–27.
[258] Petkovic S, Müller S. RNA circularization strategies in vivo and in vitro. Nucleic Acids Res 2015;43:2454–65.
[259] Gaglione M, Di Fabio G, Messere A. Current methods in synthesis of cyclic oligonucleotides and analogues. Curr Org Chem 2012;16:1371–89.
[260] Litke JL, Jaffrey SR. Trans ligation of RNAs to generate hybrid circular RNAs using highly efficient autocatalytic transcripts. Methods 2021;196:104–12.
[261] Liang X, Chen H, Li L, An R, Komiyama M. Ring-structured DNA and RNA as key players in vivo and in vitro. Bull Chem Soc Jpn 2021;94:141–57.
[262] El-Sagheer AH, Brown T. Click nucleic acid ligation: applications in biology and nanotechnology. Acc Chem Res 2012;45:1258–67.
[263] Jana S, Suresh V, Lepore SD. Synthesis of novel C-pivot lariat 18-crown-6 ethers and their efficient purification. Synlett 2015;26:1977–80.
[264] van Zon ADJF, Reinhoudt DN, Torny GJ, Onwezen Y. Chemistry of crown ethers XVIII. Isolation and purification of 18-crown-6 by selective complexation with non-ionic compounds. Recl Trav Chim Pays-Bas 1981; 100:453–9.
[265] Suzuki T, Yamamoto T, Tezuka Y. Constructing a macromolecular K3,3 graph through electrostatic self-assembly and covalent fixation with a dendritic polymer precursor. J Am Chem Soc 2014;136:10148–55.
[266] Tomikawa Y, Fukata H, Ko YS, Yamamoto T, Tezuka Y. Construction of double-eight and double-trefoil polymer topologies with core-clickable kyklo-telechelic precursors. Macromolecules 2014;47:8214–23.
[267] Lee HC, Lee H, Lee W, Chang T, Roovers J. Fractionation of cyclic polystyrene from linear precursor by HPLC at the chromatographic critical condition. Macromolecules 2000;33:8119–21.
[268] Singla S, Zhao T, Beckham HW. Purification of cyclic polymers prepared from linear precursors by inclusion complexation of linear byproducts with cyclodextrins. Macromolecules 2003;36:6945–8.
[269] Urbani CN, Bell CA, Lonsdale DE, Whittaker MR, Monteiro MJ. Reactive alkyne and azide solid supports to increase purity of novel polymeric stars and dendrimers via the "click" reaction. Macromolecules 2007;40:7056–9.
[270] Barroso-Bujans F, Alegria A. Kinetic differences in the intercalation of linear and cyclic penta(ethylene oxide)s into graphite oxide leading to separation by topology. Phys Chem Chem Phys 2017;19:18366–71.
[271] Ruiz D, Alegria A, Barroso-Bujans F. Isolation of cyclic penta(ethylene oxide) from mixtures with its linear analog by combining selective intercalation into graphite oxide and solvent approaches. Sep Purif Technol 2019;213:142–50.
[272] Barroso-Bujans F, Allgaier J, Alegria A. Poly(ethylene oxide) melt intercalation in graphite oxide: sensitivity to topology, cyclic versus linear chains. Macromolecules 2020;53:406–16.

[273] Barroso-Bujans F, Cerveny S, Alegría Á, Colmenero J. Chain length effects on the dynamics of poly(ethylene oxide) confined in graphite oxide: a broadband dielectric spectroscopy study. Macromolecules 2013;46:7932–9.
[274] Sawayama T, Wang Y, Watanabe T, Takayanagi M, Yamamoto T, Hosono N, et al. Metal-organic frameworks for practical separation of cyclic and linear polymers. Angew Chem Int Ed 2021;60:11830–4.
[275] Arrighi V, Higgins JS. Local effects of ring topology observed in polymer conformation and dynamics by neutron scattering—a review. Polymers 2020;12:1884.
[276] Clarson SJ, Dodgson K, Semlyen JA. Studies of cyclic and linear poly(dimethylsiloxanes): 19. Glass transition temperatures and crystallization behaviour. Polymer 1985;26:930–4.
[277] Di Marzio EA, Guttman CM. The glass temperature of polymer rings. Macromolecules 1987;20:1403–7.
[278] Hogen-Esch TE. Synthesis and characterization of macrocyclic vinyl aromatic polymers. J Polym Sci, Part A: Polym Chem 2006;44:2139–55.
[279] Clarson SJ, Semlyen JA, Dodgson K. Cyclic polysiloxanes: 4. Glass transition temperatures of poly(phenylmethylsiloxanes). Polymer 1991;32:2823–7.
[280] Gambino T, Martínez de Ilarduya A, Alegría A, Barroso-Bujans F. Dielectric relaxations in poly(glycidyl phenyl ether): effects of microstructure and cyclic topology. Macromolecules 2016;49:1060–9.
[281] Gao L, Oh J, Tu Y, Chang T, Li CY. Glass transition temperature of cyclic polystyrene and the linear counterpart contamination effect. Polymer 2019;170:198–203.
[282] Gan Y, Dong D, Hogen-Esch TE. Effects of lithium bromide on the glass transition temperatures of linear and macrocyclic poly(2-vinylpyridine) and polystyrene. Macromolecules 1995;28:383–5.
[283] Pasquino R, Vasilakopoulos TC, Jeong YC, Lee H, Rogers S, Sakellariou G, et al. Viscosity of ring polymer melts. ACS Macro Lett 2013;2:874–8.
[284] Kapnistos M, Lang M, Vlassopoulos D, Pyckhout-Hintzen W, Richter D, Cho D, et al. Unexpected power-law stress relaxation of entangled ring polymers. Nat Mater 2008;7:997–1002.
[285] Brás AR, Pasquino R, Koukoulas T, Tsolou G, Holderer O, Radulescu A, et al. Structure and dynamics of polymer rings by neutron scattering: breakdown of the Rouse model. Soft Matter 2011;7:11169–76.
[286] Santangelo PG, Roland CM, Chang T, Cho D, Roovers J. Dynamics near the glass temperature of low molecular weight cyclic polystyrene. Macromolecules 2001;34:9002–5.
[287] Nam S, Leisen J, Breedveld V, Beckham HW. Dynamics of unentangled cyclic and linear poly(oxyethylene) melts. Polymer 2008;49:5467–73.
[288] Tsolou G, Stratikis N, Baig C, Stephanou PS, Mavrantzas VG. Melt structure and dynamics of unentangled polyethylene rings: rouse theory, atomistic molecular dynamics simulation, and comparison with the linear analogues. Macromolecules 2010;43:10692–713.
[289] Halverson JD, Lee WB, Grest GS, Grosberg AY, Kremer K. Molecular dynamics simulation study of nonconcatenated ring polymers in a melt. I. Statics. J Chem Phys 2011;134:204904.
[290] Martínez-Tong DE, Ochs J, Barroso-Bujans F, Alegria A. Broadband dielectric spectroscopy to validate architectural features in Type-A polymers: Revisiting the poly(glycidyl phenyl ether) case. Eur Phys J E 2019;42:93.
[291] Stockmayer WH. Dielectric dispersion in solutions of flexible polymers. Pure Appl Chem 1964;15:539–54.
[292] Tezuka Y, Ohtsuka T, Adachi K, Komiya R, Ohno N, Okui N. A defect-free ring polymer: size-controlled cyclic poly(tetrahydrofuran) consisting exclusively of the monomer unit. Macromol Rapid Commun 2008;29:1237–41.
[293] Córdova ME, Lorenzo AT, Müller AJ, Hoskins JN, Grayson SM. A comparative study on the crystallization behavior of analogous linear and cyclic poly(ε-caprolactones). Macromolecules 2011;44:1742–6.
[294] Lopez JV, Perez-Camargo RA, Zhang B, Grayson SM, Muller AJ. The influence of small amounts of linear polycaprolactone chains on the crystallization of cyclic analogue molecules. RSC Adv 2016;6:48049–63.
[295] Zardalidis G, Mars J, Allgaier J, Mezger M, Richter D, Floudas G. Influence of chain topology on polymer crystallization: poly(ethylene oxide) (PEO) rings vs. linear chains. Soft Matter 2016;12:8124–34.
[296] Chen B, Jerger K, Fréchet JMJ, Szoka FC Jr. The influence of polymer topology on pharmacokinetics: differences between cyclic and linear PEGylated poly(acrylic acid) comb polymers. J Control Release 2009;140:203–9.
[297] Nasongkla N, Chen B, Macaraeg N, Fox ME, Fréchet JMJ, Szoka FC. Dependence of pharmacokinetics and biodistribution on polymer architecture: effect of cyclic versus linear polymers. J Am Chem Soc 2009;131:3842–3.
[298] Rubinstein M. Dynamics of ring polymers in the presence of fixed obstacles. Phys Rev Lett 1986;57:3023–6.
[299] Vinograd J, Lebowitz J, Radloff R, Watson R, Laipis P. The twisted circular form of polyoma viral DNA. Proc Natl Acad Sci 1965;53:1104–11.
[300] Yu C-Y, Kuo H-C. The emerging roles and functions of circular RNAs and their generation. J Biomed Sci 2019;26:29.
[301] Freifelder D, Kleinschmidt AK, Sinsheimer RL. Electron microscopy of single-stranded DNA: circularity of DNA of bacteriophage φX174. Science 1964;146:254–5.
[302] Barrett SP, Salzman J. Circular RNAs: analysis, expression and potential functions. Development 2016;143:1838–47.
[303] Hansen TB, Jensen TI, Clausen BH, Bramsen JB, Finsen B, Damgaard CK, et al. Natural RNA circles function as efficient microRNA sponges. Nature 2013;495:384–8.
[304] Feinberg EC, Hernandez HL, Plantz CL, Mejia EB, Sottos NR, White SR, et al. Cyclic poly(phthalaldehyde): thermoforming a bulk transient material. ACS Macro Lett 2018;7:47–52.
[305] Ball M, Zhong Y, Fowler B, Zhang B, Li P, Etkin G, et al. Macrocyclization in the design of organic n-type electronic materials. J Am Chem Soc 2016;138:12861–7.
[306] Miao Z, Esper AM, Nadif SS, Gonsales SA, Sumerlin BS, Veige AS. Semiconducting cyclic copolymers of acetylene and propyne. React Funct Polym 2021;169:105088.
[307] Singh M, Dong M, Wu W, Nejat R, Tran DK, Pradhan N, et al. Enhanced dielectric strength and capacitive energy density of cyclic polystyrene films. ACS Polym Au 2022.
[308] Xu L, Gao B-R, Xu X-H, Zhou L, Liu N, Wu Z-Q. Controlled synthesis of cyclic-helical polymers with circularly polarized luminescence. Angew Chem Int Ed 2022;61:e202204966.
[309] Johnson JM, Chen R, Chen X, Moskun AC, Zhang X, Hogen-Esch TE, et al. Investigation of macrocyclic polymers as artificial light harvesters: subpicosecond energy transfer in poly(9,9-dimethyl-2-vinylfluorene). J Phys Chem B 2008;112:16367–81.
[310] Yamamoto T, Tezuka Y. Cyclic polymers revealing topology effects upon self-assemblies, dynamics and responses. Soft Matter 2015;11:7458–68.
[311] Wang CE, Wei H, Tan N, Boydston AJ, Pun SH. Sunflower polymers for folate–mediated drug delivery. Biomacromolecules 2016;17:69–75.
[312] Morgese G, Cavalli E, Rosenboom J-G, Zenobi-Wong M, Benetti EM. Cyclic polymer grafts that lubricate and protect damaged cartilage. Angew Chem Int Ed 2018;57:1621–6.
[313] Morgese G, Shirmardi Shaghasemi B, Causin V, Zenobi-Wong M, Ramakrishna SN, Reimhult E, et al. Next-generation polymer shells for inorganic nanoparticles are highly compact, ultra-dense, and long-lasting cyclic brushes. Angew Chem Int Ed 2017;56:4507–11.
[314] Morgese G, Trachsel L, Romio M, Divandari M, Ramakrishna SN, Benetti EM. Topological polymer chemistry enters surface science: linear versus cyclic polymer brushes. Angew Chem Int Ed 2016;55:15583–8.
[315] Divandari M, Morgese G, Ramakrishna SN, Benetti EM. Surface-grafted assemblies of cyclic polymers: shifting between high friction and extreme lubricity. Eur Polym J 2019;110:301–6.
[316] Divandari M, Morgese G, Trachsel L, Romio M, Dehghani ES, Rosenboom J-G, et al. Topology effects on the structural and physicochemical properties of polymer brushes. Macromolecules 2017;50:7760–9.
[317] Divandari M, Trachsel L, Yan W, Rosenboom J-G, Spencer ND, Zenobi–Wong M, et al. Surface density variation within cyclic polymer brushes reveals topology effects on their nanotribological and biopassive properties. ACS Macro Lett 2018;7:1455–60.
[318] Yan W, Divandari M, Rosenboom J-G, Ramakrishna SN, Trachsel L, Spencer ND, et al. Design and characterization of ultrastable, biopassive and lubricious cyclic poly(2-alkyl-2-oxazoline) brushes. Polym Chem 2018;9:2580–9.
[319] Pei H-W, Liu X-L, Liu H, Zhu Y-L, Lu Z-Y. Enhancement of surface nonwettability by grafting loops. Phys Chem Chem Phys 2017;19:4710–18.
[320] Aboudzadeh MA, Kruse J, Sanromán Iglesias M, Cangialosi D, Alegria A, Grzelczak M, et al. Gold nanoparticles endowed with low-temperature colloidal stability by cyclic polyethylene glycol in ethanol. Soft Matter 2021;17:7792–801.
[321] Wang Y, Quinsaat JEQ, Ono T, Maeki M, Tokeshi M, Isono T, et al. Enhanced dispersion stability of gold nanoparticles by the physisorption of cyclic poly(ethylene glycol). Nat Commun 2020;11:6089.
[322] Wang Y, Qin W, Qiu D. Small-angle neutron scattering study of cyclic poly(ethylene glycol) adsorption on colloidal particles. Langmuir 2014;30:5170–5.
[323] Gu Y, Zhao J, Johnson JA. Polymer networks: from plastics and gels to porous frameworks. Angew Chem Int Ed 2020;59:5022–49.
[324] Lee C-U, Lu L, Chen J, Garno JC, Zhang D. Crystallization-driven thermoreversible gelation of coil-crystalline cyclic and linear diblock copolypeptoids. ACS Macro Lett 2013;2:436–40.
[325] Yu J, Li K, Li L, Liu L, zhou Y, Zhang Z, et al. Photo-responsive gels based on cyclic/linear polymers: efficient synthesis and properties. Polym Chem 2019;10:2872–80.
[326] Porel M, Thornlow DN, Phan NN, Alabi CA. Sequence-defined bioactive macrocycles via an acid-catalysed cascade reaction. Nature Chem 2016;8:590–6.